NEW ALGORITHMS FOR ATMOSPHERIC WIND PROFILER RADAR SIGNAL PROCESSING AND TARGET CLASSIFICATION

A THESIS

Submitted in partial fulfilment

of the requirements for the degree of

DOCTOR OF PHILOSOPHY

by

SWATI SINHA

ID. No.2013PHXF004U

Under the Supervision of

Dr. Mary Lourde R.

&

Dr. T. V. C. Sarma

BITS Pilani

Pilani | Dubai | Goa | Hyderabad

BIRLA INSTITUTE OF TECHNOLOGY AND SCIENCE, PILANI

2017

BIRLA INSTITUTE OF TECHNOLOGY AND SCIENCE, PILANI

CERTIFICATE

This is to certify that the thesis entitled **New Algorithms for Atmospheric Wind Profiler Radar Signal Processing and Target Classification** and submitted by **Swati Sinha** ID No **2013PHXF004U** for award of Ph.D. of the Institute embodies original work done by ~~him/~~her under my supervision.

Signature of the Supervisor:

Name in capital letters: **Dr. MARY LOURDE R.**

Designation: **Associate Professor, EEE Dept.**
BITS PILANI DUBAI CAMPUS, Dubai
Date:

Signature of the Co-Supervisor:

Name in capital letters: **Dr. T. V. CHANDRASEKHAR SARMA**

Designation: **Scientist/ Engineer SG;**
National Atmospheric Research Laboratory
Dept. of Space, Govt. of India, GADANKI
Date:

Acknowledgement

I would like to acknowledge my thanks to Prof. R. N. Saha, Director, BPDC, and Dr. Neeru Sood, Dean ARD, for all their support and timely guidance.

I also express my sincere gratitude to my co-supervisor, Dr. T. V. C. Sarma for teaching the technicalities of atmospheric radars and providing a large amount of data.

I would like to express my sincere gratitude to my supervisor Dr. Mary Lourde R. for the continuous support of my Ph.D study and research, for her patience, motivation, enthusiasm and immense knowledge. Her guidance helped me in all the time of research and writing of this thesis. I could not have imagined having a better advisor and mentor for my Ph.D study.

I would also like to thank my DAC committee members Dr. Abdul Razak and Dr. T. G. Thomas, for their encouragement, insightful comments.

My sincere thanks also goes to all the faculty members of EEE department of BITS Pilani Dubai campus for providing patronage and free research environment.

I also owe the credit of the work done to my friends and colleagues for their help at different stages of the study.

Lastly, I would like to state that the effort towards the doctoral study was the result of the blessings of the elders and cooperation of my family members.

Abstract

Wind Profiler is a generic term for ground based remote probing instrument used to study the dynamics of the earth's atmosphere. These atmospheric radars are coherent pulsed Doppler radars operating in VHF or UHF bands. They transmit radio frequency pulses in *vertical* and *off-vertical* directions. Backscatter from atmospheric and other targets is received by sensitive receivers. These echoes are digitized. Subsequently, echoes from the targets in the same region are combined and subjected for Doppler analysis to get a Doppler Power Spectrum for each range-bin. On this processing, the primary products such as *Signal Power*, *Doppler Shift* and *Spectral Width* for each range bin are generated. From these primary products, atmospheric parameters like *target density, wind speed and turbulence intensity* etc., can be derived. These parameters are very useful for atmospheric modeling and predictions. The *Doppler Power Spectra* is conventionally considered as the basic form of data from which all products and weather parameters are derived. However, obtaining backscattered signal from atmospheric target is very difficult as the echoes are too weak (power around -140dBm). Also, the signal could be contaminated with clutter, echoes from non-atmospheric targets, precipitation and radio frequency interference (RFI) and so on. Discontinuous coverage in range and time is also observed occasionally. Consistent and reliable extraction of atmospheric parameters is possible by applying appropriate post processing methodology to analyze the Doppler power spectra.

This doctoral research has been carried out with the intention of developing initial understanding of the Radio Frequency (RF) scattering process and getting a mathematical estimation of the backscattered power. Subsequently, an understanding is being developed on the signal processing operation of wind profiler radars and the standard data formats. Algorithms are developed for the following:

1. Modeling and Simulation of the wind profiler Doppler Power spectra: This involved mathematical formulation of the backscattered signal as output from the RF receiver of the radar, performing mathematical operations of digital signal processing and creating Doppler power spectra. By this process one can make spectral data with user defined features. This data could be used as a test bench to evaluate the performance of various processing techniques and algorithms.

2. Preprocessing of the Doppler Power Spectra: This activity involves estimation of noise power and identification of the echoes from non-atmospheric targets and removal of all the *unwanted* signals. This way the data is made suitable for the next stage of *profile extraction*.

3. Estimation of the Doppler profile: This activity mainly deals with Doppler profile tracing. The algorithm developed can be used for most type of data without change of parameters. Such an algorithm is expected to be used for automated processing of huge data generated by WP radars.

4. Target classification from Doppler Power Spectra: Automated processing of the radar data also require the data to be classified based on the atmospheric targets.

All the algorithms have been implemented on the data of Indian MST radar at Gadanki, India. The functionality of the algorithm has been tested repeatedly and found consistent. The performances of algorithms are compared with some of the established methods currently in being used for the same purpose. It is observed that the newly developed algorithms show improvement over the existing methods in Clutter and RFI removal and profile tracing. The algorithms show consistent results in classification of the spectral data along with less computational complexity.

In summary, the algorithms presented in the thesis can be effectively used in the following

1. To generate Doppler power spectral data corresponding to various weather conditions. This data is used to evaluate wind profiler data processing algorithms.
2. Preprocessing of the Doppler Power Spectra.
3. Automated Doppler profile tracing.
4. Algorithm development for automated classification of the Doppler power spectra

Key Words

Wind profiler, Doppler Spectra, Spectral Moment, RFI and Clutter removal, Modeling and simulation, Doppler profile tracing, target classification.

Contents

List of Figures

List of Tables

List of Acronyms

CDR	:	Clear-air Doppler radar
DBS	:	Doppler Beam Swinging
DSP	:	Digital Signal Processing/ Processor
DWR	:	Doppler Weather Radar
WP	:	Wind Profiler
FDI	:	Frequency Domain Interferometry
FMCW:		Frequency Modulated Continuous Wave
FOM	:	Figure of Merit
IPP	:	Inter-Pulse Period
MAP	:	Maximum APosteriori (Method)
MSE	:	Mean squared error
PRF	:	Pulse Repetition Frequency
RIM	:	Range Imaging
RCS	:	Radar Cross Section
RR	:	Range Resolution
RSP	:	Relative spectral power
SMM	:	Stochastic Mixing Model
SML	:	Stochastic Maximum Likelihood
Sodar	:	Sound Detection And Ranging
WGN	:	White Gaussian Noise

List of Symbols

η	:	Noise in time domain (MAP)
λ	:	Wavelength
σ	:	Reflectivity (radars), Standard deviation of noise term (MAP)
θ	:	Beam tilt angle (radar)
ψ	:	Wavelet Basis function
$\mathbf{C}$	:	Covariance matrix
$\mathbf{H}$	:	Spatial response matrix (MAP)
$\mathbf{S}$	:	Spectral response matrix (MAP)
r	:	Range (radars)
u	:	Radial wind velocity component obtained by the east beam of radar
U	:	Easterly component of the wind
v	:	Radial wind velocity component obtained by the north beam of radar
V	:	Northerly component of the wind
w	:	Radial wind velocity component obtained by the zenith beam of radar
W	:	Vertical component of the wind (updraft)
$\mathbf{y}$	:	Low resolution spectral component vector (MAP), observed variable
$\mathbf{z}$	:	A vector consisting of spectral components of the high resolution spectra
Z	:	Rayleigh scattering factor for spherical Scatterers
n	:	Radar Refractive index

.

Chapter 1

Introduction

Atmospheric studies leading to weather prediction have always assumed cardinal importance in the history of human civilisation. The well-being and even existence of human civilisation depends on the atmospheric conditions. This is especially true for a predominantly agricultural country like India. It is also known that climatic changes in one part of the world bring about corresponding changes in distant part of the globe. Understanding this, the meteorologists and oceanic scientists all over the world study and monitor the environment by regular observations. They also exchange data for correlation of studies. The collaborative processing of the data leads to better observations and understanding of these natural processes. On the basis of these observations *weather forecast and prediction models* are made.

Most of the modern observational tools of lower and middle atmospheric terrestrial dynamics are Doppler radars. They transmit radio-frequency (RF) pulses and observe the back scattered signal from different atmospheric and oceanic targets. The received signal is analysed to find the time delay of the echo and RF frequency shift. The information is represented on *Range-Doppler* plane, from which the location and the velocity of the target can be determined.

Meteorologists need to take regular atmospheric observations for weather modeling and predictions. Continuous up-gradation in the instrumentation and innovative methods to obtain remote atmospheric parameters has always been in demand of researchers. The information is mainly in the form of wind velocity, temperature and humidity. Occasionally, other parameters like pressure, ion content, solar radiation etc. are also observed. In early days, these observations were taken vide in-situ measurements using balloon flights. This was the main method of monitoring the atmosphere. The most important parameter amongst these is the wind velocity profile. Modern studies depend strongly on the wind velocity profile obtained from atmospheric radar observations. A brief account of development of various radar data processing techniques is given below.

1.1 Radar Meteorology

In 1960's radar technology became available for non-military operations. The technological advancement has been in following major stages.

- The receiver sensitivity started getting better (upto -90 dBm or picowatt). Due to this it became possible to process echoes from air targets. This capability facilitated the determination of scatterers range.
- Measurement of Doppler frequency shift became possible and the velocity of air/wind was determined. This determination of wind velocity became a great boost to weather prediction.
- Generation and steering of narrow radar beam added the capability of perceiving the structure of the target. The internal movement of larger clouds and atmospheric layers led to greater understanding and analytical capability of wind dynamics.

As a result of this, different types of weather radars were developed and are commercially available. Later regular observations using radars became a standard practice.

1.2 Need for Automated Processing and Classification

With the advent of these radar technologies, *radar meteorology* has assumed greater importance and radar data is being used more often by atmospheric scientists. The practice of collectively taking the radar data has become very common and regular benchmark methods for atmospheric observations were developed. Modern radars operate round the clock taking the observations. Due to these long operating hours, large amount of data are generated. The interpretation of the data and extraction of meteorological information in term of parameters like Scatterers Reflectivity, 3-D wind speed, and wind turbulence at all ranges are the immediate tasks. This basic process of getting atmospheric parameter is often referred as *product generation*. Conventionally, this task was done by professional experts. These professionals used to take decisions based on their experience and the knowledge of similar events occurred before. Considering the volume of data from modern radars, it is very difficult to analyze this large amount of data manually. Due to this reason, an automated processing algorithm functioning without manual supervision and to deal effectively with the spectral contaminations and discontinuities are highly desirable.

Identification and tracing the Doppler profile corresponding to the echoes from wind and air turbulence is the main challenge. As mentioned earlier, the signal is not easily seen due to lower strength compared to the noise and contamination due to other non-atmospheric targets such as RFI and clutter. The allied sub-tasks would be as follows:

a) To develop a versatile simulation tool to create Doppler Power spectral data for a wide variety of atmospheric conditions. An elaborate collection of such data sets will enable the researchers to test the profile extraction algorithms on most types of atmospheric conditions. This would provide an objective method to evaluate the efficacy of the Doppler profile extraction algorithms.

b) To develop algorithms to eliminate the unwanted signals. Identifying and eliminating the echoes of non-atmospheric targets would clean the data and make tracing of the Doppler profile much easier. Clutter and Radio Frequency Interference (RFI) are the major unwanted signals. This task is included in the Pre-processing of the Doppler power spectra.

c) To develop Doppler Profile Extraction algorithm. This main task needs to be achieved by an objective algorithm which would not need parameter changes for different atmospheric conditions. The new algorithm needs to work in low Signal to Noise Ratio (SNR) condition and offer a performance *imitating human expert.*

d) The wind profilers are also capable of detecting characteristic Doppler profiles of Ionospheric echoes, Meteoric echoes, Precipitation echoes and so on. These atmospheric conditions result into much stronger echoes compared to clear air winds. It is not probable to extract wind echoes in the presence of such signals. It would be worthwhile to develop a sorting algorithm capable of classifying the *Doppler power spectral data* into these phenomena along with the clear air echoes.

1.3 Motivation and research gap

Many researchers have come up with very effective algorithms for Doppler profiling. However, most of them need meticulous parameter selection depending on atmospheric conditions and radar system specifications. For the best results expertise of professional analysts are also required. This is a lengthy process and often the decisions were subjective in the sense that they were dependent on human expert's perception. Such approach may not be feasible on large amount of data generated by the wind profiling radars. Therefore, there is a need of an

objective profile extraction method which would perform well in most of the conditions. The requirement can be stated as follows:

Modern radars are operated continuously for long durations and generate large amount of data. In order to process this data in real time the profile tracing must be fast. Therefore the computational complexity of the method needs to be moderate so as to handle large data throughput of modern radars. Taking motivation from this, the research was directed towards developing new algorithm for profile tracing. There is also a need to perform automated classification of the data for its appropriate archival. In this research, an effective Doppler profile tracing algorithm is developed. And a strategy for the real time classification of the WP Doppler spectra is also developed.

1.4 Objective of the Research

The research has been carried out with the motivation of developing automated tools for processing the data of wind profiling radars. The main challenge of this research towards automated processing was large data volume and limited time for processing. With typical operating parameters, the radar generates a data set of Doppler Power Spectra, approximately every 16 seconds or 32 seconds. Typical observation session of the Indian MST radar session generates 120 data sets in 30 minutes. Other WP radars have data generation at similar rate depending on their operating parameters. A real-time automated computation scheme is expected to process the data as it is generated. Doppler Power Spectra is the standard product of wind profiler radars. Processing of this data involves three steps; namely, preprocessing or the removal of echo components from non-atmospheric targets, determining the wind velocity information and classification of the data into different atmospheric processes based on the observed prominent echo types.

Therefore the problem statement of the research is **to develop the algorithms for preprocessing, wind profile extraction and classification of the Doppler power spectra. Also, these algorithms must be implemented in time less than the data generation time.**

With this research aim, research objectives are detailed as follows

A. **Background development**

1. *Understanding the wind profiler radar operation and associated mathematics to generate the Doppler power spectra*: Information on the data generation process provides insight of the radar signal processing.

2. *Understanding the scattering of the radio waves from atmospheric targets and the mathematical expression to compute and describe the echo signal:* The knowledge of the scattering phenomenon provides requisite help in the mathematical description of the backscattered signal. In other words it gives the descriptor features of the target signature.

3. *Learning effective technique to simulate the Doppler power spectral data for different atmospheric targets*: Simulation of the data requires good understanding of the process of radar backscatter. Accurate simulation capability is developed only after detailed correlation of the signal features with atmospheric phenomenon. This knowledge is useful to develop data classification criterion and for the removal of non-atmospheric signal components. The data sets corresponding to different atmospheric conditions can serve as a test bench for the wind profile extraction algorithms.

B. Pre-processing of the Wind Profiler data:

1. *Development of the algorithm for the preprocessing of Doppler power spectral data*: Wind profiler receives the echoes from Clear Air Turbulence (CAT) and other types of atmospheric targets. The echoes from these targets are very weak in power and the receiver often receives noise and unwanted signals. First step is to remove noise and signals from the non-atmospheric targets from Doppler power spectra. This is termed as pre-processing. After pre-processing, atmospheric echoes become prominent and further processing of Doppler power spectra becomes easy.

2. *Implementation of the algorithm with different operating parameters on the same radar and different radars:* This work involved understanding the relation between various radar parameters and its effect on the data. After this understanding, a strategy needs to be developed to translate the algorithm seamlessly to different radars. This exercise establishes the transportability of preprocessing algorithm

C. Development of automated Doppler Profile Tracing algorithm

1. *Development of computationally simple algorithm for the profile extraction*: Wind profiler radar receives echoes from radio refractive index change occurring due to CAT. Additionally, echoes from precipitation, meteoric echoes, mesospheric echoes and ionospheric activities are also observed. The analysis of CAT echoes leading to wind profile estimation is

main function of the wind profiler radars. Echoes from other types of atmospheric phenomenon could be used for specific studies.

CAT echoes are very weak in power and the receiver often receives noise and unwanted signals. The profile extraction algorithm initially removes noise and signals from the non-atmospheric targets. Once these signals are removed, atmospheric echoes become prominent and further processing becomes easier. Profile tracing algorithm identifies the wind echoes and connects the spectral points in the data to form a wind profile. The work needs to be directed towards development of a new algorithm capable of implementing the profile extraction to match the data generation speed.

2. *Performance comparison of the newly developed method with leading established methods available in the literature:* The performance of the newly developed Doppler profile tracing algorithm need to be tested with other established algorithm for the same purpose. The comparison must be done for the accuracy of the wind estimation and the implementation time.

3. *Performance validation of the Doppler profile tracing algorithm*: The performance of any method is considered validated when the results match with other independent method used for the same purpose. The performance of the newly developed algorithms needs to be tested with the wind estimation obtained by the GPS Sonde observations.

4. *Implementation of the algorithm with different operating parameters on the same radar and different radars:* The utility of the algorithm is established multiple times if it can be seamlessly implemented with different parameters as well as different radars. Work must be planned towards this ability to establish the effectiveness of the profile extraction algorithm.

5. *Study the performance of the algorithm in low signal conditions and in presence of the interfering signals*: In atmospheric radars it is often observed that the processing algorithms perform differently in different noise conditions. The ruggedness of the algorithm is established when it works in most of the possible conditions. The tests for this are expected to be done on the real data of various conditions as well as the simulated data creating extreme conditions.

D. Development of Automatic classification algorithm for Wind Profiler data

Classification of the data is another important function of the data processing. It helps segregation of the data for the purpose of analysis and data archival.

1. *Development of wind profiler data classification algorithm*: After appropriate processing and information extraction from the echoes, the wind profiler data needs to be classified. An algorithm that performs automatic classification of WP data with the speed matching with the data generation is needed. This means that apart from successful classification, the algorithm must have computational simplicity. The implementation time of the algorithms must be such that the Doppler profile extraction and the classification can be implemented at the speed higher than the data generation.
2. *Performance testing of the algorithm in low signal and in presence of the interfering signal:* Wind profiling radar data is often contaminated with noise and interference. It is an advantage if the classification algorithm works in adverse signal conditions. The performance of the classification algorithm needs to be tested in low SNR and in presence of interference. The success rate may be compared with the classification done by human experts.

Thus, the research was carried out to achieve four main objectives divided into nine different tasks.

1.5 Literature Survey

After setting the research objective, thorough literature survey has been conducted. The efforts were focused towards understanding the reported research to develop insight in four different areas of this thesis work.

1.5.1. Historical development of radar meteorology

One of the early reports on radar meteorology was by Atlas [1] which introduced various possibilities of radar observations. In this chapter, Atlas reviewed various techniques of radar observation and presented the basis of radar reflection from atmospheric targets or scatterers. In early days the echoes from the atmospheric scatterers were analyzed only for the distance or the range from the radar. The technique of detecting relative velocity was not established. Later, in 1970s, experiments of estimating wind velocity by Doppler radars were carried out and many scientists, namely, Woodman[2], Zrnić[3], Röttger[4], Zrnić[5] ,Sato[6], Strauch[7], Doviac[8] Woodman[9], Ecklund[10], Clifford[11], Boyer[12], Dombrowsky[13] et al., presented observations

which established that the Doppler radars could be used to get reliable wind information. These experiments were conducted at different frequencies and the observations were taken at different heights. The efforts of many scientists have proven that by choosing appropriate frequency, it is possible to focus on a specific region of the atmosphere. As an example, frequencies between 800 MHz to 3 GHz give strong echoes from the targets in the lower troposphere (altitudes of 1 to 12 km). Whereas, lower UHF are used for the observations from the altitudes of 10 km to 20 km. VHF ranges of frequencies are used for stratosphere and mesospheric (altitudes of 15 to 60 km) echoes. The radars need to be designed considering the target reflectivity, required RF beam directivity etc. Scientists like Fukao [14][15], Rao[16] have published engineering details of the systems and its significance. Results on radio scattering properties were reported by Gossard [17], Bean [18], Tatarski [19] and so on. Good results are obtained only if the radar frequency power and the beam directions are appropriate for the intended targets. With appropriate radar instrumentation it became possible to observe specific phenomenon. Radar observation of specific atmospheric phenomenon like Kelvin-Helmholtz Billows has been reported by Chilson [20]. These are wavy structures repeating at regular intervals. Observation of vertical wind velocity profile with its 3 dimensional components has been the most important need for weather prediction and the study of wind dynamics. These radars are categorized depending on the height coverage; namely, boundary layer radars, tropospheric radars, Stratospheric- Tropospheric (ST) radars and the Mesospheric- Stratospheric- Tropospheric (MST) radars. The generic name for these radars is the Wind Profiler (WP) radars. Wind profiler radars are established as standard product and companies like Vaisala [21] market different models of radar profilers. Some results of second generation and newly refurbished radars were reported by Srinivasulu [22] and Hall [23].

1.5.2. Pre-processing of the wind profiler data

First step in the wind profiler data processing is the removal of noise and echoes of the non-atmospheric signals. This process is also known as pre-processing. First step is to estimate the noise level. Hildebrand [24] presented a method to estimate the noise. Though, proposed about 4 decades ago, this method still offers the best estimate of the noise in atmospheric signals. Mathematical characterization of noise was presented by Petitdidier [25] and Igor [26] [27].

Atmospheric signals are often contaminated with Clutter echoes. Clutter signals are the echoes received from terrestrial objects in the vicinity of radar. The terrestrial objects subtend a large solid angle at the radar. Therefore these signals are strong compared to the atmospheric signals. Jordan [28] presented a method of clutter removal by exploiting the properties of the signals like low Doppler frequency and large magnitude with sharp frequency peaks. Processing noisy data with discriminatory threshold has been presented by Riddle [29], Volker [30]. These techniques use dynamically moving threshold for the removal of noise.

Clutter removal is easier in the transform domain processing. Volker [30][31] showed that Gabor transform based methods were effective for the removal of clutter. Later, wavelet transform based methods were used for the clutter removal. DB 20 wavelets were found to be the more effective [32][33]**.** Wind profiler signals often get interference from electrical noise as well as terrestrial noise. These signals appear as sharp peaks present in multiple ranges. An autonomous interference filtering technique was presented by Anandan [34]. The interference detection and its removal problem is very similar in polarimetric and imaging radars. The techniques reported by Tian [35], Le [36] and Bradley [37] use similar signal processing techniques.

1.5.3. Wind profiler data processing techniques

Processing of the wind profiler data is the main research theme. Therefore, a detailed literature survey has been specifically directed to review the strengths and weaknesses of radar signal processing to the existing algorithms. With the use of radars, researchers have already established the direct relation between Doppler shift and wind velocities. After 1990s, the research has been directed towards identifying and enhancing the weather echo components. This was then followed by developing the technique to interpret the data. This effort amounts to assigning specific features of atmospheric targets to the signal components.

The calibration of the spectral components with atmospheric parameters is often an issue. The calibration often changes with the radar parameters and the beam directions. Tridon [38] addressed the issue of calibration. Technical application note of Vaisala [39] consolidates the practical aspects of the wind profiler radars. After appropriate calibration, the atmospheric feature extraction is possible by using appropriate techniques. The technique based on Kalman filtering has been presented by Tuckley [40]. Efforts of many researchers for the removal of unwanted signals are also established.

The main task, however, is to extract *Doppler profile* from the power spectral data. The Doppler profile is directly related to the wind velocity in the direction of the beam. Many methods were developed in last couple of decades. The methods which showed consistent results and have been established over the time are presented in the following literature.

Adaptive moment estimation (Anandan [41]) is an established approach with estimation of the moments based on criterion that is adapted at every range bin while tracing the Doppler profile from the lower ranges to the higher ranges. The Doppler profiling is best done by using soft computing techniques like Fuzzy logic (FL) methods and Artificial Intelligence (AI) techniques. Some of the techniques use combination of these methods. Following scientists have reported different Fuzzy logic and Neural Network methods. Clothiaux [42], Morse [43], Cornman [44], Bianco [45], Gaffard [46], Allabaksh [47] et al. These methods take the Doppler power spectra as the input. Individual spectral components are then examined for different properties like slope, curvature, spectral power and spectral spread. In addition to these standard parameters some techniques use parameters like spectral symmetry and skewness of the spectral components. They assign membership functions to each of these parameters. This gives function value for each of the attribute. A weighted sum of these values is then computed. The result of the weighted mean is subjected to a threshold to determine whether the spectral components are atmospheric echoes. This methodology is adapted with slight variations by the researchers mentioned above. The selection of membership function and decision of the threshold value is critical to these methods. In case of atmospheric signals, there is no established basis for such decisions. Therefore artificial intelligence (AI) technique is adapted for the selection of membership functions and thresholds. The AI technique involves learning by processing a large amount (approximately 200 data sets) data being analyzed in past. To understand these processing techniques, the knowledge of radar operation and configuration is necessary. Due to this, more discussions on processing techniques are presented in chapter 4 and chapter 5.

Though these methods claim very good results, they are computationally complex and often needs change of parameters according to Radar system specifications and climatic conditions. Intervention of technical experts is also often needed. Hence, it is required to have an automated processing of the Doppler Spectra using computationally simple algorithms.

1.5.4. Scattering of the radio waves from atmospheric targets

It is important to have knowledge of the radar backscatter process while developing the signal processing technique for wind profiler radar. The study of back scattering of the radio waves gives the idea of the expected received power and its nature in terms of frequency shift distribution and amplitudes. This knowledge is crucial for the radar design as well as the analysis of the echoes.

Atmospheric targets backscatter the signals depending on the relative size of the target compared to the radio wavelength. Battan[48] showed that when the wavelength and the target dimensions are comparable, the backscatter is Mie scattering. In such case, the received signal depends on the shape of the scatterer. When the diameter 'D' of the scatterers is less than 0.1 λ, the scattering mechanism is Rayleigh. The received signal power depends on the target particle diameter to the power six! This analysis is particularly dominant for the analysis of the precipitation echoes.

However, the wind profiling radars mainly receive echoes from the clear air targets. In such cases, the air particles are very small and the echo is mainly due to the change in the RF refractive index. Battan[48]. has also provided this analysis in his book *Radar Observation of the Atmosphere*.

Turbulence within the target volume of interest is defined as atmospheric structure. For radio waves, the quantitative estimation of received power is obtained by defining a volume reflectivity (η) for electromagnetic waves and the structural constant C_n^2.

Repetitive structures provide a large reflection of radio waves if the wavelength is double the repetition scale in the atmospheric targets. This is known a Bragg criterion. Detection of micro-structures is possible with the help of enhanced echoes due to this phenomenon.

Chapter 3 of this thesis discusses these aspects in details.

1.5.5. Radar target classification techniques

Radar target classification has been a very well-studied topic and a good amount of literature is available for various types of radars. The target classification is often decided by the atmospheric parameters and their relative positions, sometimes referred as structures [43][49]. The accuracy of the classification or the correct determination of the target echoes is often an

increased multifactor consideration [50]. These methods are categorized as signature matching techniques. Such techniques are used in other types of radars like surface surveillance radars [51] [52] and acoustic ranging and detection systems [53][54]. Ground Penetrating radars (GPR) also use these techniques of signature matching [55]. Very few literatures are available on the classification of wind profiler targets. However, the techniques used in other radars offer good guideline and prompts towards the innovative techniques for the wind profiler targets classification.

Chandrasekhar [56] presented a consolidated report of classification techniques on dual polarized weather targets. Hurricanes and water carrying targets have been more important targets for socio economic reasons. Various techniques have been used for identification, classification and resolving different types of targets from radar data. Luke presented a technique to separate drizzle and precipitation [57] and Harasti used similar technique for resolving different types of hurricanes [58]. Neural network methods are popular for bulk meteoric classification using polarimetric radar [59][60]. Some of the observations of meteor types have been presented by Wannberg [61] and Krishna [62]. Following sections present a new spectral feature based technique to classify different types of wind profiler targets.

Chapter 7 discusses some of these techniques. It also presents a new technique developed for the wind profiler spectral data, by appropriate consolidation of the concepts used by various classification techniques available.

1.6. Problem Definition

Develop algorithms to process Doppler power spectra of wind profiling radars. This involves; preprocessing, Doppler profile extraction and classification according to the target types. Signal modeling technique is also allied capability for this research problem. All the above algorithms should be optimized for implementation in minimum time, such that they can be used for automated processing. The echo signals from atmospheric targets are a distribution of many weak signals and they appear as cluster of barely perceptible signals. Another problem with atmospheric signals is that the received signal to noise ratio (SNR) is often very poor. The characteristics of atmospheric echoes strongly depend on the weather conditions and the nature of the scatterers. In short, due to bad SNR and the distributed nature of the target, the estimation of *position and velocity* of the target is difficult. Better interpretation of the atmospheric signals could be evolved by a study of atmospheric processes and formulating statistical representation

for the atmospheric echoes. As the air is a continuous media, the wind or turbulence does not show abrupt spatial variations. This apriori knowledge is used to develop signal processing algorithms for the Doppler power spectra.

1.7. Organization of the Thesis

This thesis presents the signal processing techniques for the estimation of Doppler profile from Power Spectral data. The understanding of the problem and research contribution is presented in the following chapters as below.

Chapter 2 gives the theory on Wind Profiling radars and estimation of 3D winds.

Chapter 3 presents the information on radio wave backscatter due to atmospheric structures. This information along with the data give estimation of received power.

These two chapters give the background knowledge of the wind profiler systems.

Chapter 4 explains the need and technique for modeling the Doppler power spectra corresponding to different atmospheric conditions. It also gives the results of Matlab simulation and its comparison with the real radar data.

Chapter 5 explains Pre-processing of the radar data. This includes the procedure to read the Power spectral data in standard formats used by Indian MST radars. This chapter also presents the estimation of noise and noise removal. The techniques of Clutter and RFI removal is also described and is illustrated with the help of Matlab simulation.

Chapter 6 In this chapter step by step description on wind profiling, using newly developed Doppler profile estimation algorithm is presented. This is the major contribution of the thesis. It also presents the performance comparison with other established methods and validation of this technique with other independent methods.

Chapter 7 explains mathematical approach for the target classification. The Spectral Feature Based Atmospheric Target Classification algorithm is explained in this chapter. The flow chart, Matlab programs, and its results are also included.

Chapter 8 summarizes the contribution of the thesis and its significance in practical applications.

Chapter 9 concludes the thesis with future scope of the study

Chapter 2

Wind Profiling Radars and Estimation of 3-D Winds

Wind profilers are a special category of ground based radar instruments used to obtain three dimensional profile of wind velocity along the altitude in atmosphere. Studies of atmospheric dynamics, weather prediction and climate change require wind information at various heights above the ground, on a regular basis. Radar wind profilers (WP) can provide continuous three dimensional wind data with a high temporal resolution.

The atmospheric targets are weak reflectors of radio frequency radiations. Also, the different parts of the targets are in different state of motion. As a result, the echoes received by the radar are a vector sum of many weak signals. It is described as an ensemble of statistically distributed signals. Therefore these targets are known as distributed targets. This situation is different from that in the conventional aircraft tracking radars. The surveillance radars and the strategic radars are predominantly being used as the aircraft tracking radars have finite number of distinct targets. These are generally fast moving targets whose echoes are received with good Signal to Noise Ratio (SNR). On the other hand, weather targets are often slow moving continua with very poor SNR. Therefore, the strategy of analysis of weather signals is different from the method used for surveillance radars. Surveillance radars use fast tracking and detection algorithms, whereas weather radars use computationally intensive methods to improve the SNR and feature extraction. This processing determines the value of atmospheric parameters from the echoes. This chapter describes various types of atmospheric radars followed by the description of wind profiler signal processing and presentation of the data.

2.1 Types of atmospheric radars

There are two classes of atmospheric radars. The radars radiating in the horizontal direction seeking the terrestrial wind velocities are generally referred as *Doppler Weather Radars (DWR)*. The radars transmitting pulses in vertical direction are known as *Wind Profilers (WP)*. The DWRs are mainly used for prediction of terrestrial wind patterns like cyclone, monsoon; whereas the WPs give three dimensional wind profiles up to large heights and generally used for weather monitoring. The current research is focused on the WP data processing and extraction of weather parameters. Wind profilers offer wind speed and directions

up to desired heights. This information is used for weather modeling and predictions. Such information is useful for the agricultural estimation, water resources planning and has a great impact on socio-economic aspects of society. The wind information is also useful for avionic navigation and to determine the landing conditions of airplanes. Air pollution monitoring and estimating wind potential of a particular region are amongst other uses of the wind data.

2.2 Theory of Wind Profilers

Wind Profiler is a class of ground based remote probing radar instrument operating in VHF and UHF frequency bands. These are Coherent Pulsed Doppler radars transmitting pulses in vertical and off-vertical directions (in three or more non-planar directions, typically in zenith, tilted eastwards and tilted northwards as shown in Fig.2.1). Depending on the operating frequency and power, the range coverage of WP could vary from a few kilometres to about a few hundred kilometres. Table 2.1 shows the typical frequency, power and coverage. The WP radar receives echoes and has a very sensitive super heterodyne receiver with ultra-high frequency stability. This receiver down converts the signal to base band giving the Doppler shift in the transmit frequency. This signal is digitally processed. The delay time of the echo gives the range of the target and the Doppler shift determines the radial velocity component of the target in each beam direction. The echoes received in a particular time interval are segregated together as they correspond to a limited section in the air-column above. In other words, signals from a *slice* of air at particular height (referred as range-bin) are processed together for Doppler analysis. The base band signal is digitized using *Analog to Digital Converter* (ADC) at regular intervals. A sequence of these *digitized samples* forms the *time series* of the down converted signal. This series is subjected to *Fast Fourier Transform (FFT).* This discrete frequency domain representation is called Doppler spectrum of that range-bin. In this way a Doppler spectrum for each range-bin is obtained. The set is referred as *Doppler Power Spectra.* This gives observed radar parameters, namely; Signal power, Doppler shift and Spectral Width. From these parameters, target reflectivity, wind speed and turbulence could be derived. Data from at least three beams are collected. Conventionally, beam is pointed towards Zenith, tilted towards east (called East beam) and, tilted towards north (called North beam). This approach of estimating the wind profile is called Doppler Beam Swinging (DBS) method. The data from three beams are combined and the target locations and their radial velocities are resolved in

terms of orthogonal Cartesian velocity components at all the range-bins (as shown in equations 2.1 to 2.4). Thus a three-dimensional (3-D) wind profile is obtained.

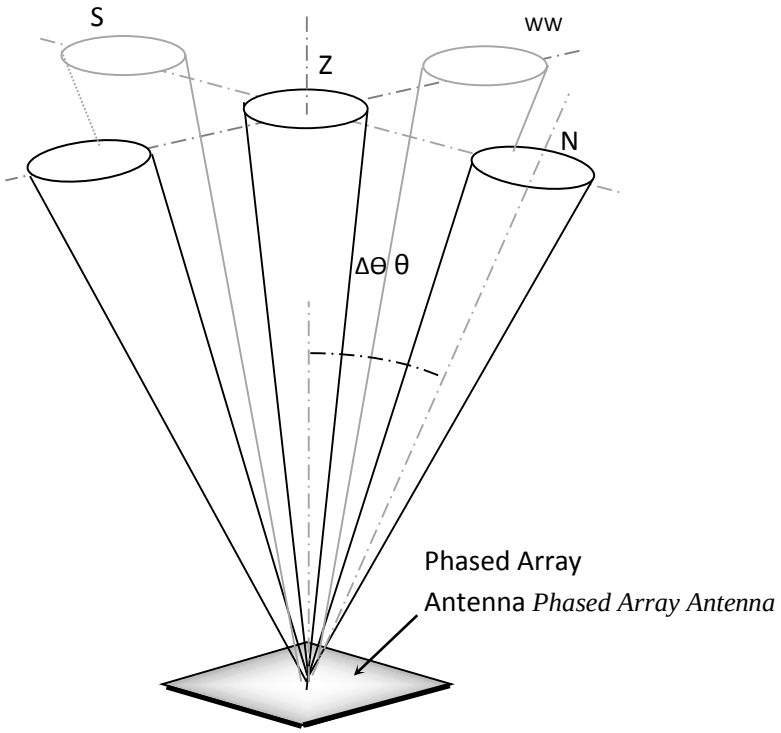

Fig 2.1 *Wind profiling by Doppler Beam Swinging (DBS) method.*

Table 2.1: Type of Wind Profiling Radar Instruments

Type of WP	Frequency of operation	Transmitter Peak Power	Maximum Height Coverage (Approximate)
Boundary Layer	900-3500 MHz	3-5 KW	1.5- 3.5 km
Tropospheric Profilers (T-radar)	400-490 MHz	8-20KW	7-16 km
Stratosphere - tropospheric Radar (ST Radars)	150-250 MHz	50 to 800 KW	12-30 km.
Mesosphere-Stratosphere-Tropospheric Radar (MST-Radar)	40-60 MHz	1000-3000 KW	25-250 km
Doppler mini SODAR*	3-4 KHz	300-800 Watts	0.3-1 km
Doppler SODAR*	0.1-1.5 KHz	0.5-2 KW	1.0-3.5 km

** SODARs are acoustic instruments working on Doppler radar Principle.*

$$f_{doppler} = \frac{2v_{air}}{v_{carrier}} f_{carrier} \quad (2.1)$$

$$\boldsymbol{w} = W \quad (2.2)$$

$$\boldsymbol{u} = \boldsymbol{W}\, Cos\ \theta + \boldsymbol{U}\, sin\ \theta \quad (2.3)$$

$$\boldsymbol{v} = \boldsymbol{W}\, Cos\ \theta + \boldsymbol{V}\, sin\ \theta \quad (2.4)$$

Where, ***u, v, w*** – radial wind velocity in the direction of beams (east, north,& zenith).

$\boldsymbol{\theta}$ - Off-zenith beam tilt direction

U, V, W -orthogonal wind velocity components (easterly, northerly and updraft)

2.3 Initial processing of time domain data

The systems working on the same principle but using sound waves as carriers are known as Sound Detection and Ranging (SODAR) systems. The principle of operation of all types of wind profilers and SODAR is the same. However, weather targets are very different from normal radar targets. Strategic radars and surveillance radars seek the echoes from *flying objects* like airplanes. These objects or targets reflect back the transmitted signal, showing frequency shift due to the *Doppler effect*. However, the weather target is an *air-mass* with all its particles having slightly different velocities. Such targets are known as *Distributed targets.* The echoes from such targets occurs as a *collection of faint replicas* of the transmitted signal showing frequency shifts which in turn corresponds to the Doppler shift around the mean velocity. As a result the Doppler spectra show a distribution of multiple frequency components. The WP signal processing involves Doppler spectrum from individual range bin. Fig. 2.2 shows typical Doppler spectra of a range bin. The diagram shows Doppler shifts received from all the targets in that particular range bin. In normal cases the envelope of the Doppler component is of Gaussian shape. It is seen that it is a spectrum which presents positive as well as negative Doppler components. Most of the components are noisy. The *prominent* or *higher magnitude* component represents the Doppler frequency of the target. The power (P_r) represents the target reflectivity. The frequency value (f_D) represents the mean wind velocity at the range. The spectral width (W_f) represents the *wind-turbulence* in that range bin.

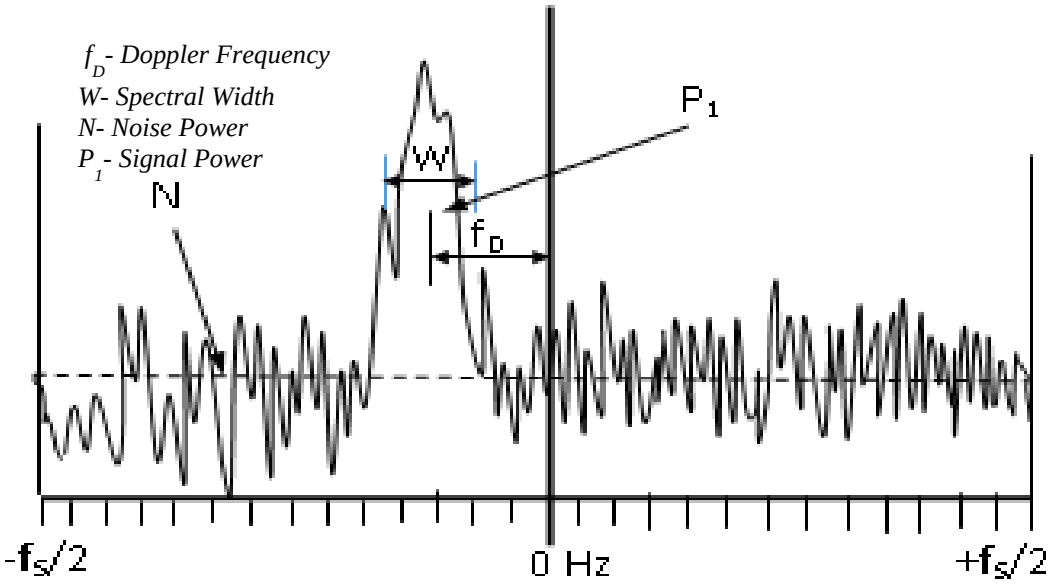

Fig.2.2 *Typical Doppler Spectrum of a range-bin.*

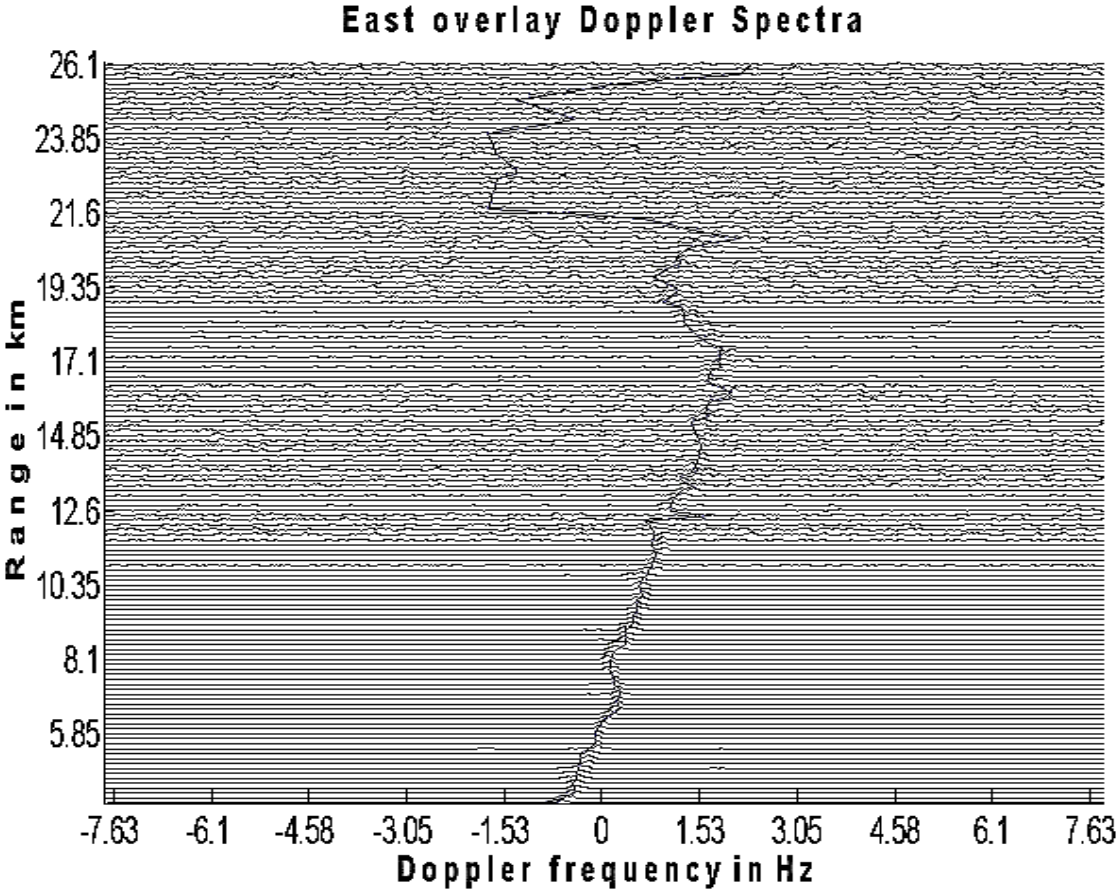

Fig.2.3 *Typical MST radar Doppler spectra of Beam Direction: East beam 10^0*
(Obtained by stacking individual range-bin spectra)

The Doppler spectrum is the basic data unit. All the spectra of the range-bins are stacked one above other in increasing range. This stack is called a *Doppler Power Spectra.* A line connecting the wind components in all the range bins is called the Doppler Profile. Fig 2.3 shows typical Doppler power spectra. The Doppler profile gives the wind speed at all the heights. The data from the Doppler profiles of three beams (conventionally, Zenith, East, and North) could be combined to get 3-D data. However, meteorologists are more interested in the winds in 2D plane. This data is represented in the form of wind speed (WS) and wind direction (WD). In a way similar to the polar coordinates. Fig.2.4 shows representation of horizontal winds as WS-WD data.

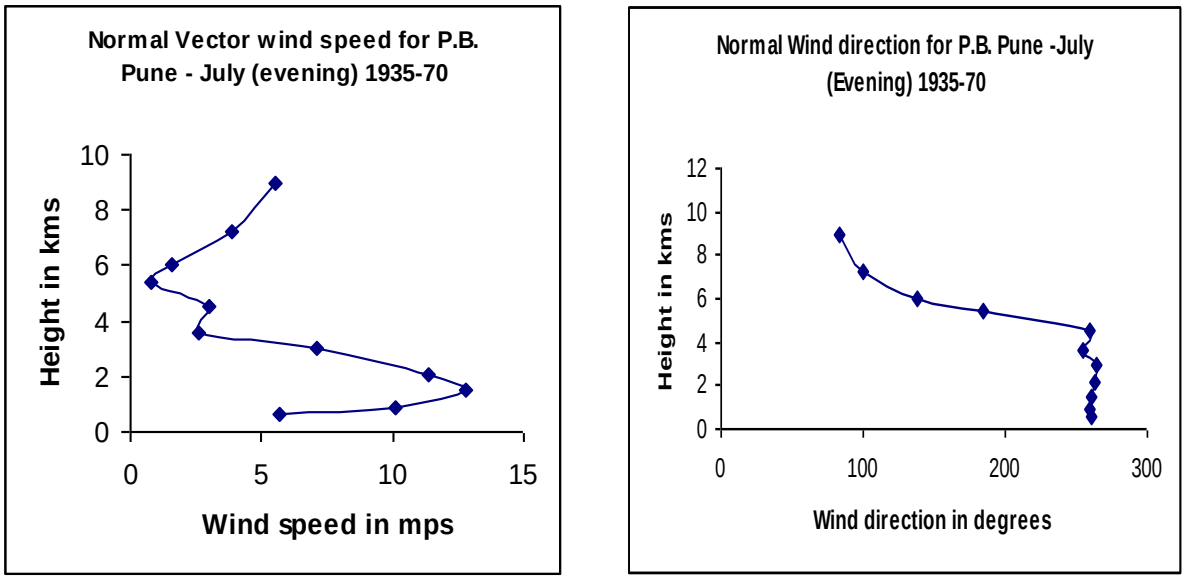

Fig. 2.4 *Typical WS-WD data of a 400 MHz wind profiler. (Source: IMD Pune, India)*

Long term (24 Hours, say) behaviour of the wind is represented as shown in Fig. 2.5. The figure illustrates that it is possible to identify the weather phenomenon at a glance using these representations. A picture of Indian MST radar is shown in Fig. 2.6.

2.4 Estimation of wind Profile

It is evident from the above discussion that the Doppler power spectra is the basic form of data and determining the Doppler profile is the most critical activity in wind profiler data processing. This is because all the wind parameters are derived from the Doppler profile data. However, obtaining the wind parameters from the radar is not an easy task as the radars echoes

are very weak (received power varies around -120 dBm to-140 dBm). They could be contaminated with clutter and interference. Echoes from clear air could also be contaminated with echoes from precipitation, insect swarm etc. Discontinuous coverage in range and time is also another problem. Due to these reasons getting a continuous profile or getting wind velocity values at all heights become difficult if not impossible. Therefore the scientists use the property of *continuity* and other estimation techniques to get Doppler frequency values at maximum possible ranges.

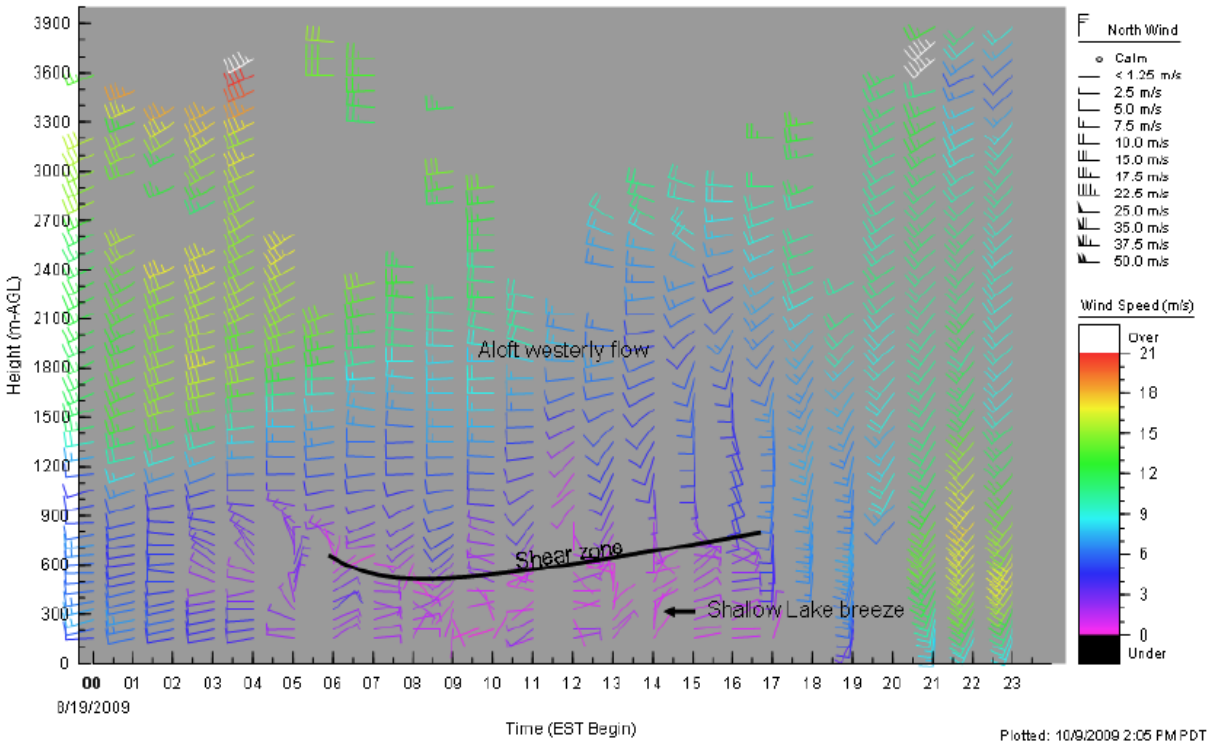

WP wind data from Cleveland-Newburgh Heights, Ohio on August 20, 2009.
Source: U.S. Environmental Protection Agency

***Fig. 2.5** A typical format of representing 'long term horizontal WS-WD' data*

Evolving strategy of identifying the atmospheric targets and estimating the speed is difficult as these targets are spread over a large volume and have pockets showing variation in scattering properties. The signal backscattered from such targets is the vector sum of all the individual echoes of smaller local scattering structures present in the radar pulse volume. Therefore the echoes received by the radar can be considered as an ensemble of many signals that are reflected from different parts of the target. Mathematically, these echoes are represented

as statistically distributed signals on the *time-frequency plane*. In the case of air defense and surveillance radars, the echoes are localized and are finite in number. Therefore they appear as prominent localized signal components on the received signal representation. On the other hand, the echo signals from atmospheric targets are a distribution of many weak signals and they appear as cluster of barely perceptible signals. The strategy to analyze these echoes is different from that used in conventional *air-defense* or *surveillance radars*.

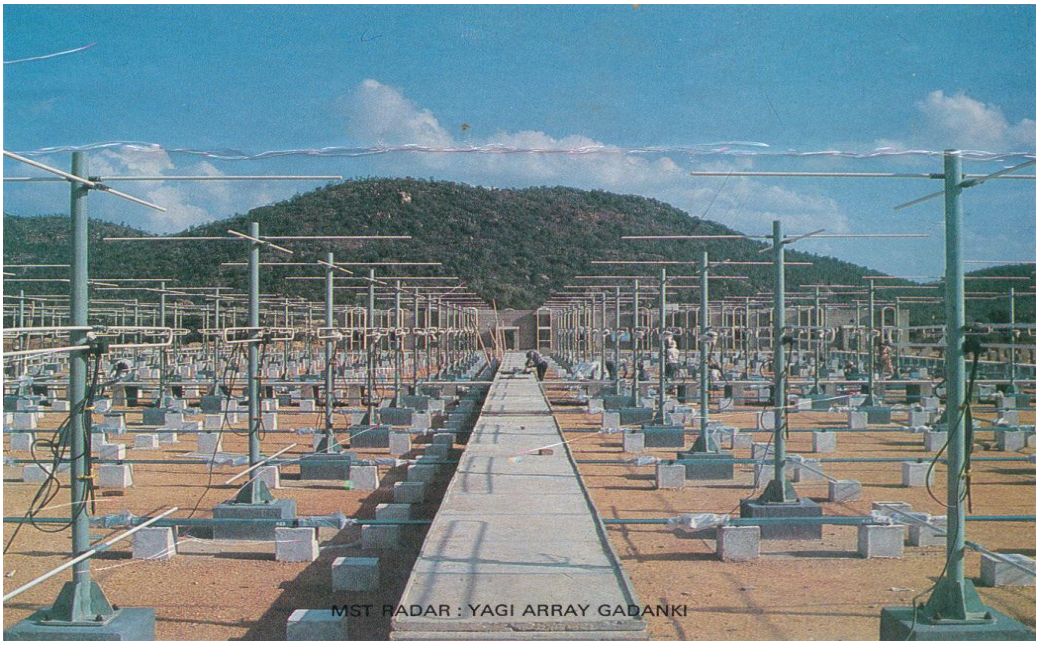

Fig 2.6 *Mesospheric Stratospheric Tropospheric (MST) radar at National Atmospheric Research laboratory (NARL), Gadanki, India*

2.5 Summary: In chapter 2 various types of atmospheric radars and the theory of wind profilers are presented. The initial processing of wind profiling data and estimation of wind profile is explained. The radio scattering mechanism on the atmospheric targets and dependence of the echo parameters on target characteristics are presented in chapter 3.

Chapter 3

Theory of Radar Backscatter and RF Reflectivity

Wind Profilers (WP) and Doppler Weather Radars (DWR) transmit RF pulses and analyse the backscattered echoes from the atmospheric scatterers. In this chapter the fundamentals of the wave scattering principles and the systems from which the data is obtained is described. Fig. 3.1(a) shows a concept diagram of a pulsed radar operation. The Doppler Weather Radars (DWR) transmits the pulses in horizontal directions; whereas; the wind profilers transmit the beam in vertical and off-vertical directions. Figure also shows volume occupied by the radar pulse, known as pulse volume or scattering volume. The signal received in a particular time interval corresponds to this specific volume. During the *echo-interval* radar receives the scattered echoes from all the scatterers present in the corresponding pulse volume. The expression for the received power by mono-static pulsed radar with Gaussian beam shape is derived as given below.

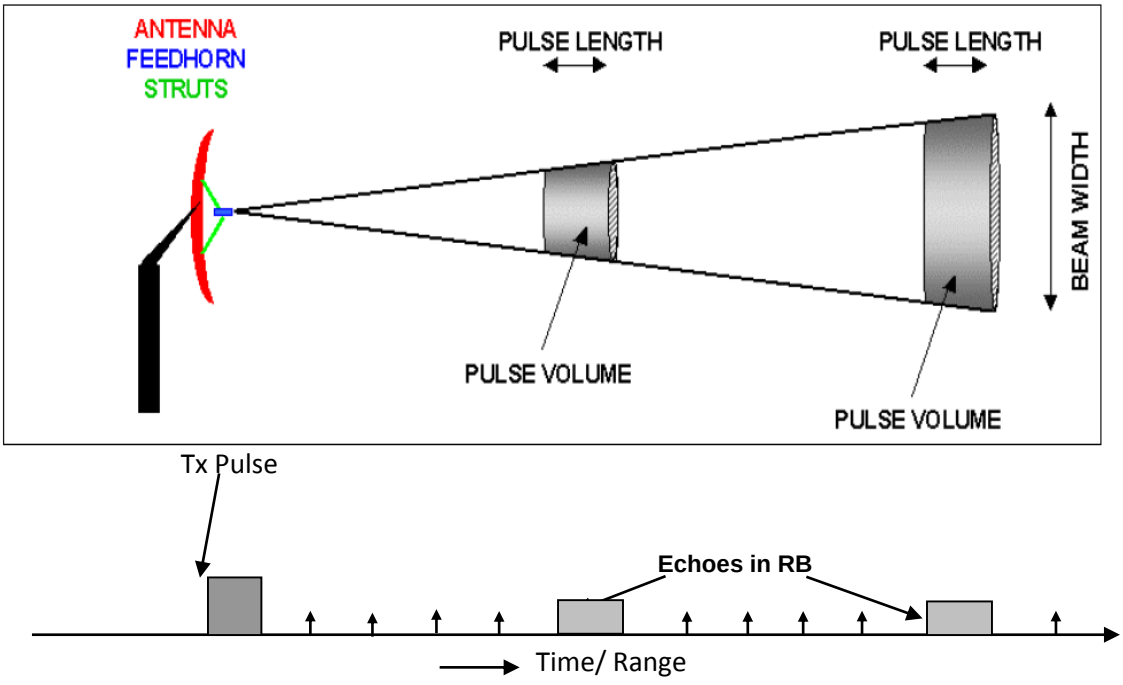

Fig. 3.1(a) *Schematic diagram showing the pulse volume and echo interval*

The basic form of radar equation[63] is given below in equation (3.1)

$$P_r = \frac{P_t G}{4\pi R^2} \cdot A_e \frac{\sigma_i}{4\pi R^2} \tag{3.1}$$

Where P_r is the received signal power in watts., P_t is the transmitted power by an isotropic antenna, in watts, G is the gain of antenna, A_e is an effective area in m^2, σ_i is the radar cross section in m^2 and $4\pi R^2$ is the surface area in m^2 of an isotropic antenna.

Fig. 3.1 (b) shows the radar beam shape. Incorporating the radar beam shape, the equation 3.1 becomes,

$$P_r = \frac{P_t G}{4\pi R^2} \cdot (Beamspotarea) \sum_{RBvol} \sigma_i \cdot \frac{A_e}{4\pi R^2} = \frac{P_t G}{4\pi R^2} \cdot \left(\frac{\pi R^2 \phi\theta}{4} \right) \sum_{RBvol} \sigma_i \cdot \frac{1}{4\pi R^2} \cdot \frac{G\lambda^2}{4\pi} \tag{3.2}$$

Where, $(Beamspotarea) \sum_{RBvol} \sigma_i$ is the radar cross section due to all scattering particles present in the pulse volume. For homogeneous target, it can be expressed as

$$P_r = \frac{P_t G}{4\pi R^2} \cdot (Vol.\text{Re}\ fl) \times (RBvol) \cdot \frac{A_e}{4\pi R^2} = \frac{P_t G}{4\pi R^2} \cdot \eta \left(\frac{c\tau}{2} \right) \left(\frac{\pi R^2 \phi\theta}{4} \right) \cdot \frac{1}{4\pi R^2} \cdot \frac{G\lambda^2}{4\pi} \cdot l^2(P) l_r(R) \tag{3.3}$$

Where, *Vol,Refl* (η) is volume reflectivity and *RB vol* is range bin volume [8]

The Summation term $\sum_{RBvol} \sigma_i$ in equation 3.2 is replaced by Vol, Refl × Pulse Volume in Equation 3.3.

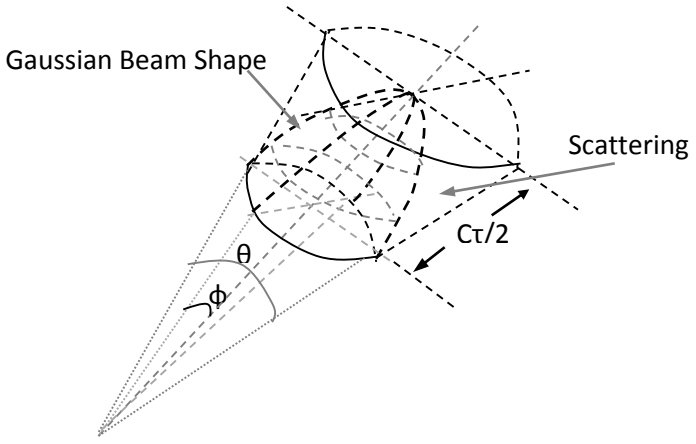

Fig. 3.1(b) *The radar beam: Scattering volume and Beam widths in azimuth and Elevation are φ and θ*

Rearranging the terms of Equation 3.3, the received power then simplifies to equation (3.4) given below. [8]

$$P_r = \frac{P_t G^2 \lambda^2 \eta}{(4\pi)^3 R^2} \cdot \left(\frac{c\tau}{2}\right)\left(\frac{\pi\phi\theta}{4}\right) \cdot l^2(P) l_r(R) \tag{3.4}$$

Where the two *l(P), l(R)* terms are the propagation loss and receiver loss respectively. Now, if Gaussian beam is assumed, then the volume changes. The factor 4 in the expression ($\pi\phi\theta/4$) in equation (3.4) is then replaced by 8 ln2 [8].

$$P_r = \frac{P_t G^2 \lambda^2 \eta}{(4\pi)^3 R^2} \cdot \left(\frac{c\tau}{2}\right)\left(\frac{\pi\phi\theta}{8\ln 2}\right) \cdot l^2(P) l_r(R) \tag{3.5}$$

When the target is not homogeneous, the volume reflectivity term η is being replaced by the generalized summation of reflectivity term, $\Sigma_{(RB\ vol)}\ \sigma_i$. Omitting the loss terms and replacing the value $\Sigma_{(RB\ vol)}\ \sigma_i$ in equation (3.5) , equation for power received is derived, as shown below[8]

$$p_r = \frac{P_t G^2 \lambda^2 \Delta\phi \Delta\theta}{8 \times (2\ln 2) \times 4^3 \pi^2 R^2} \sum_{RBvol} \sigma_i \tag{3.6}$$

Where, P_t and P_r are the transmitted and the received power respectively.

G is the gain of antenna, R is the range, λ is the wavelength, σ is the reflectivity,

θ and ϕ are the zonal and meridional beam widths of the radar beam.

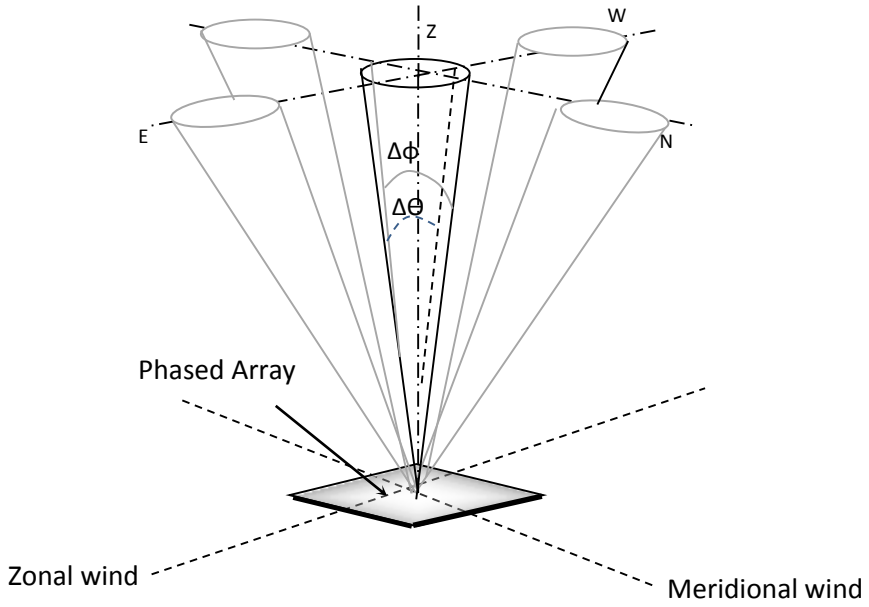

Fig. 3.2 *Schematic diagram showing Zonal and Meridional wind Directions*

Fig. 3.2 gives the Zonal and Meridional wind directions. The magnitude and the phase of the backscattered signal are strongly dependent on the size of the target, the RF wavelength used and the refractive index in the scattering volume. The number of targets and their relative position within the scanned volume is also a factor. The following sections describe different backscattering mechanisms and mathematical expressions quantifying the backscattered signal.

3.1 Factors Affecting Reflection and back scattering of RF Waves

RF waves are scattered by two types of targets. They are (i) particle-like or *particulate* scatterers and (ii) atmosphere layers with sharp change or gradient in refractive index. Various types of particulate scatterers like water droplets, dust, pollutants, insects, etc. are responsible for scattering of the RF waves. These scatterers are present in troposphere at heights up to about 12 km and the scattering occurs in microwave frequency bands, typically, at the frequencies more than 3 GHz. However, change in RF refractive index is observed up to altitudes of about 100 km and the backscatter is observed in UHF and VHF bands. Therefore, the dominant scatterers for the DWRs radars are the particulate scatterers. On the other hand, the Wind Profilers get scattered power mainly due to the atmospheric refractive index gradient. This type of backscatter is also referred as *clear air echoes*. The work presented in this thesis focus more on the wind profiler radars. However, for completeness, basic expressions of particulate scattering are also presented. Sections 3.1.1 and 3.1.2 discuss particulate scattering and sections 3.1.3 and 3.1.4 present the mathematical expressions for the scattering due to the refractive index gradient.

3.1.1 Particulate Scattering due to Relative Size of the Scatterers

It is well-known that the size of the scatterer relative to the RF wavelength determines the scattering mechanism. For atmospheric radars the mechanisms are broadly classified into two, namely Rayleigh scattering and Mie scattering. As an example, the cloud detecting radars operating at 30 to 60 GHz have the RF wavelength of 5 to 10 mm. The scatterers of interest for this radar are the rain-drops, hail, icicles etc. The size of these scatterers is comparable to the RF wavelength. Therefore the Mie scattering will be predominant in this case. Equation 3.7 gives the expression for the reflection coefficient of Mie scattering [48].

$$\sigma = \frac{\pi a^2}{\alpha^2}\left|\sum_{n=1}^{\infty}(-1)^n(2n+1)(a_n - b_n)\right|^2 \tag{3.7}$$

Where, a is the radius of the scatterer and α is a shape factor, $=2\pi a/\lambda$ for spherical objects. a_n

and b_n are constants which describe the effects of magnetic and electric dipoles, (and quadruples) in the scattering volume.[48]

When the diameter '*D'* of the scatterers is less than 0.1 λ, the scattering mechanism is Rayleigh. The reflection coefficient for Rayleigh scattering is given by the following expression in equation (3.8) [48].

$$\sigma = \frac{\pi^5}{\lambda^4}\left|\frac{m^2-1}{m^2+2}\right|^2 \sum_{i=1}^{n} D_i^6 = \frac{\pi^5}{\lambda^4}|K|^2 \sum_{i=1}^{n} D_i^6 \qquad (3.8)$$

Where, m is the complex index of refraction,

D is the target diameter and K= (m^2-1)/ (m^2+2).

Substituting the value of σ in equation (3.6), the received power is obtained as [48]

$$P_r = \frac{\pi^3 P_t G^2 \theta\phi |K^2|}{8\times 4^3 \times (2\ln 2)\lambda^2 r^2} \sum_{RBvol} D_i^6 = \frac{C|K^2|Z}{r^2} \qquad (3.9)$$

Where, C represents the constants and radar system parameters, *K* is the factor dependent on the refractive index of the scatterers and Z (= Σ D_i^6) is the Rayleigh scattering factor due to the spherical objects. Conventionally, Z is represented in logarithmic scale as dBZ (10 log Z).

Particles (which include smoke, dust and large pollen grains etc.) scatter RF energy in much the same way as rain drops. Since backscatter power is proportional to the diameter to the power six, the backscatter from a particle of less than 0.1 mm in diameter is very small [48]. However, a large number of airborne particulates are enough to produce significant return from weather radars and Sodars operating with smaller wavelengths. The observations of the particle backscatter provide the information about the distribution of the scatterers.

3.1.2 Effect of the Orientation of Scatterers

Clear-air echoes are often attributed to backscatter from biota, particularly insects. However, there is fairly conclusive evidence that at short wavelengths (e.g. K-Band) insects are the primary contributors to clear-air radar returns. Since most biota are not spherical, the magnitude of the return is strongly dependent on the biota orientation. This idea of orientation is represented using the differential radar reflectivity, Z_{DR}. It is defined as:

$$z_{DR} = 10\log\left[\frac{z_h}{z_v}\right](dB) \qquad (3.10)$$

Where, Z_h and Z_v are the horizontal and vertical co-polarized reflectivity factors. The schematic in Fig. 3.3 is a sketch showing the variation in backscattering cross section due to the orientation of the biota. The backscatter from the precipitation with large drop size also exhibit a similar difference in the amplitudes of backscatter from vertical and horizontal polarization. This is due to the fact that the drops get flattened in the vertical direction making the diameter in the vertical direction smaller. Typically, a drop of 3 mm size would show Z_{DR} of 1.5 dB and a 4.5 mm drop would show Z_{DR} of 3 dB [48].

The presence of a large differential reflectivity factor is a good indicator that the scatterers may be biota

Fig. 3.3 *Different orientation of the biota with respect to Radar beam*

3.1.3 Back Scattering due to Refractive Index Gradient

Radar power is scattered back with sharp inhomogeneities in the refractive index of the atmosphere that generally occur at air mass boundaries [48]. Such refractive index discontinuities also occur in turbulent air. This phenomenon is often called Bragg scattering. Most of the echoes of the vertical looking WPs are by Bragg scatter. The mechanisms resulting in Bragg scattering have coherence time of only a few seconds and are transitory. In other words the backscatter signal is sustained only for a short time.

Under special circumstances, gradients in refractive index may lead to specular reflections. Such reflections contribute significantly to clear-air returns. Partial specular reflection is observed as a result of layered structures in the refractive index field [48]. These layers are common in the stratosphere but may also exist within tropospheric inversions. Specular reflection of radar power is most important for radars of longer wavelengths (from tens of centimetres to a few metres). The reason for this is that such echoes provide information about the layered structure of the atmosphere. The atmosphere is primarily horizontally

stratified. The stratified layers with very high refractive index gradients at their interfaces reflect some of the radar power directly back to vertically pointing radar [64]. The effect is enhanced with altitude when the layers appear concave to the radar due to the earth's curvature. This focuses the reflected signal[1]. MST (mesosphere-stratosphere-troposphere) radars are particularly likely to observe some return due to specular reflection. These radars are used to probe the upper reaches of the atmosphere, and are usually operated within a few degrees of the vertical. The returns resulting from specular reflection tend to be coherent, often lasting for several minutes. Specular reflections are rarely seen by Doppler weather radars as they are configured to operate at higher frequencies. Also DWRs usually employ a steerable dish antenna and are normally operated at elevation angles less than 60 degrees.

Physical properties of the medium, determines its Refractive index: For air, the refractive index is a function of atmospheric density at radio frequencies It is also known as the radio or radar refractive index, *n*. This reflective index is very close to unity and varies very minimally due to atmospheric layers [18]. To address these minor variations, radar meteorologists use the term *N*, given by $(n - 1) \times 10^6$. The refractive index of radar combines three important meteorological parameters. These parameters are sensitive to, temperature, pressure and humidity, Equation (3.11) gives expression of *N* in terms of atmospheric parameters [18].

$$N = \frac{77.6}{T}\left[P + \frac{4810e}{T}\right] \tag{3.11}$$

Where, *T* is temperature in Kelvin, *P* is atmospheric pressure in milli bar and *e* is the vapour pressure in milli bar.

Spatial refractive index gradients bring about the refraction and reflections of the radar beam. The refractive index gradient ∇N, is usually denoted with the symbol *M*. The changes in refractive index are caused by dry parameters (pressure and temperature) as well as the wet parameters (vapour-pressure and temperature). As a result, the refractive index gradient M has two contributory terms: the dry term is given by 77.6 P/T (the first term of eq. 3.11) and the wet term is given by 373256 e/T^2 (the second term of Equation 3.11). Dry term typically contributes up to 60% of N [18]. Usually the variation in T and P is not abrupt on the micro-scale, so this term is not as significant in creating large fluctuations of N. On a few occasions large

gradients of temperature may exist on the boundaries of atmospheric layers, at higher altitudes where the air is dry and also close to the ground.

Humidity variations in the atmosphere may be abrupt. Therefore, the wet term contributions can have dramatic variations, and that depends on the temperature and vapour pressure. Significant gradients of *N* can be produced by moisture and temperature gradients found at air mass boundaries. As an example, the boundary between warm dry continental air and cooler moist maritime air show large value of M. Such situations exist at a sea breeze front. With height, the moisture content of atmosphere decreases and hence wet term contributions also diminishes with height. The wet contribution becomes less significant in the upper troposphere and above. Thus, refractive index is more sensitive to humidity in lower atmosphere, while at higher ranges, a significant contribution to M is made by gradients of temperature, where water vapour pressure is small.

3.1.4 Turbulence Structure and Back Scattering of the Radio Waves

Turbulence within the volume of interest is defined for every atmospheric structure by the use of quantities known as *structure parameters*. They represent the root mean square difference between an atmospheric variable at two points located a unit distance apart. Structure parameters can be practically defined for any atmospheric variable. Refractive index structure constant, C_n^2 is of particular interest for the radar observers. The radar volume reflectivity (η) **[19]** for electromagnetic waves are related to the refractive index structure constant C_n^2 by the relation shown in equation 3.12. It is expressed as cross section (m^2) for unit volume (m^3). Therefore volume reflectivity unit is m^2/m^3 or m^{-1}.

$$\eta \approx 0.38\, C_n^2 \lambda^{-1/3} \tag{3.12}$$

This relationship assumes that the radar wavelength and the physical dimensions of the turbulence are of comparable dimensions. In such cases, the radar wavelength is said to fall in the *inertial sub-range*. It also assumes that for all clear air targets, the measured reflectivity is due to the effects of refractive index gradients. If other types of scatterers are present, their effect must be considered separately. It is also assumed that the turbulence producing the inhomogeneity is isotropic and fills the entire radar resolution volume.

The spatial dimension of the turbulence is defined by *inertial sub-range*. At a particular temperature and pressure, the atmospheric turbulence of a specific spatial dimension is sustained. The turbulence (eddies) of smaller dimensions diminish transferring most of the energy to the adjacent layers. On the other hand, the larger eddies are not isotropic and are very short lived. Thus there is lower and upper limit on the radar wavelength and upper limit for sustained turbulence. This range of spatial turbulence dimensions is known as the *inertial sub-range* (also known as limiting micro-scale). The lower limit of inertial sub-range is determined by the viscous dissipation of energy and the upper limit by the buoyant forces in the air mass. Within the inertial sub-range, turbulent eddies do not lose much energy to viscous processes. However, often, there is transfer of energy from the larger scale eddies to smaller scale eddies (large eddies slowly get converted into smaller ones going down to viscosity region). Fig. 3.4 shows the inertial sub-range at different heights.

Much of the Bragg theory related to the radar echoes, was developed by, Tatarski [19]. He showed that the radar reflectivity can be expressed as,

$$\eta = \frac{\pi^2}{2}(k)^4 F_n^*(k) \tag{3.13}$$

Where, k is the radar wave number given as $k=4\pi/\lambda$, F_n^* is a three-dimensional representation of the refractive index field.

It is also established that the RF radiation having the half wavelength ($\lambda/2$) comparable to the spatial variations of the refractive index field shows significant reflectivity. This is known as the Bragg or the Fourier mode reflection. This is why the radar $\lambda/2$ must be within the inertial sub-range. If this condition is not satisfied, very small reflected power is observed.

If the scatterers are homogeneously distributed, the expression of the received power reflected from clear-air targets uses the volume reflectivity term η. Neglecting the loss terms in equation 3.5 we get equation 3.14. This equation is used for estimating received power in wind profiler radars.

$$P_r = \frac{P_t G^2 \lambda^2 \eta}{(4\pi)^3 R^2} \cdot \left(\frac{c\tau}{2}\right)\left(\frac{\pi\phi\theta}{8\ln 2}\right). \tag{3.14}$$

The *lower dimensional limit of the spatial turbulence* is known as limiting micro-scale. This dimensional limit increases with height. Generally, the limiting micro-scale is of the order

of 1 to 2 cm at ground level. This limit increases to about 10 metres, at heights of 80 km as shown in Fig. 3.4 [65][66]. It is also reported that limiting micro-scale at the ground level is of the order of a few millimetres.

In view of the above, when the values of limiting micro-scales are very low, the radars employing K-band (and perhaps even X-band, if the limiting micro-scale is approximately 2 cm)will not be able to detect refractive index inhomogeneity at higher heights. If clear-air echoes are detected by such radars, it is due to other origins like particle scattering.

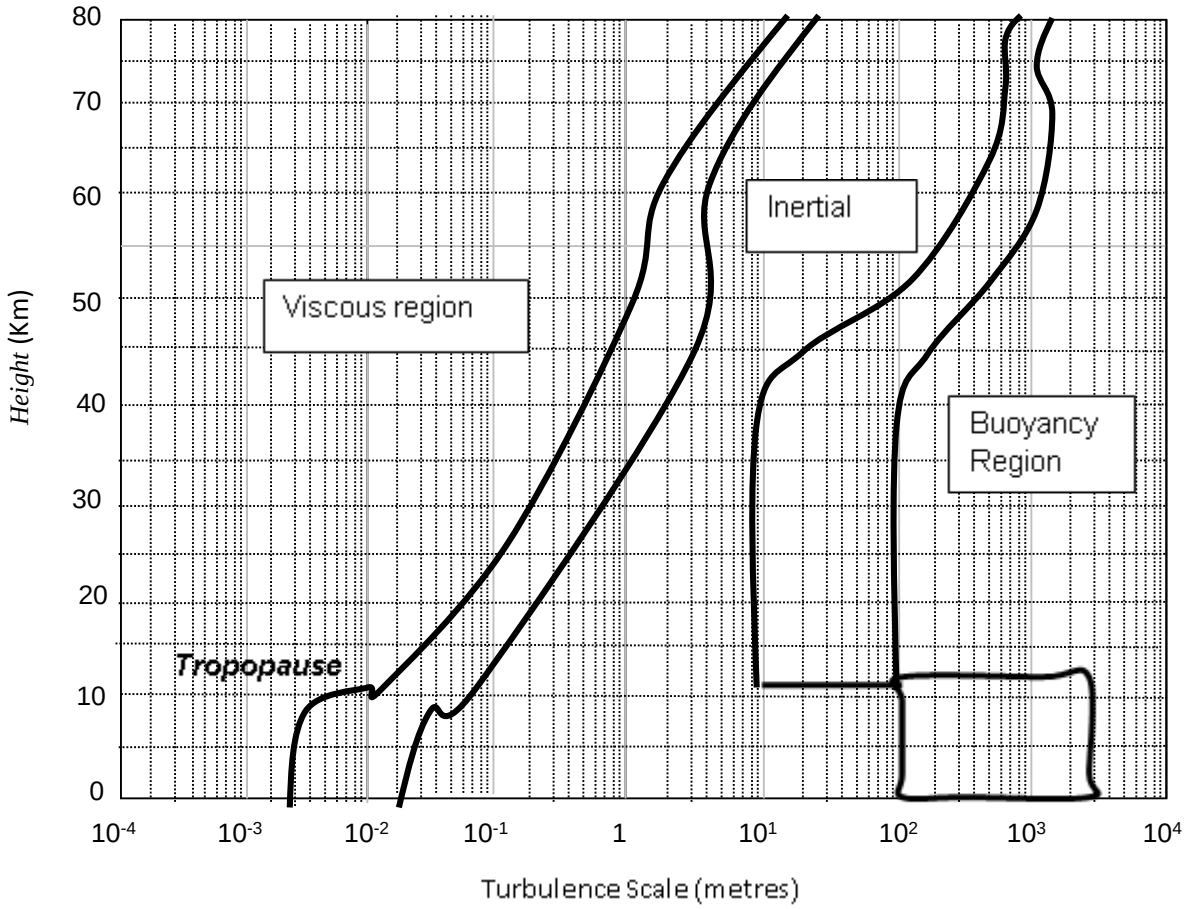

Fig 3.4 *Turbulent scale size versus altitude (Source: [40])*

The upper limit of the inertial sub-range is usually quite large. It is generally several hundred meters in convective conditions [65][66]. However, the upper limit may be less than 1m for thin and stable layers. In such cases, expected received power presented by equation (3.14) may not be met by HF (High Frequency) radars. From this discussion it is seen that the radar frequency

is selected depending on the region of observations and the size of the scatterers. Table 3.1 gives broad classifications of atmospheric radars and their operating frequencies.

The relation between the radar received power and the atmospheric parameters is established through C_n^2. To the radar designer and observer, C_n^2 is an extremely useful indicator. This quantity depends on three parameters. These parameters are pressure, temperature and humidity. The value of C_n^2 can be expressed as a linear combination of the structure constants for temperature, absolute humidity and the pressure with appropriate weights to each term.

From the radar observations and the measurement of received power, the value of C_n^2 can be calculated. Using this value of C_n^2, the atmospheric structure is analysed.

Table 3.1 Different atmospheric radars and their operating frequencies

	Frequency (λ)	**Typical Application**	**Scatterers**
Cloud radar (K/Ka band)	30/ 52 GHz (10 – 6 mm)	Vertical / horizontal looking radars for pollution dispersion and cloud monitoring	Pollutants, Nimbus cloud particles etc.
Doppler Weather radar	3-5 GHz (10 – 6 cm)	Horizontal viewing rain, cyclones, sea-breeze	Rain drops hail, sand and dust particles
Boundary layer radar	0.9- 1.5 GHz (0.3 – 2 m)	Vertical Beams, Wind profile at lower heights	Wind profiles up to 3 Km
Wind Profiler	400 MHz (0.75 m)	Vertical beams Tropospheric wind profile	Wind profiles up to 12 Km
ST radar	200 MHz (0.6 m)	Vertical beams Stratosphere tropospheric wind profile	Wind profiles up to 20 Km
MST radar	40-50 MHz (6 – 7 m)	Vertical beams, Mesospheric, stratospheric, Tropospheric wind profile	Wind profiles up to 30-90 Km
Sodar (Acoustic sounder)	3 KHz (0.1 m)	Vertical Looking, Surface wind profile	Wind profiles up to 1 Km

3.2 Back Scatter Measurements and Determination of the Atmospheric Parameters

Studies have been carried out which attempt to correlate observations of atmospheric parameters measured using traditional sensors. Wind profile or the wind velocities at different heights can be measured by conventional techniques using balloon. Fig. 3.5 shows the wind profile comparison between data obtained from three different systems namely, Radiosonde, precision wind sounding balloon (Jimsphere) and the radar (Altair). These readings show good correlations.

Gossard [17] reported that layer of dimension less than half the wavelength and having thermal stability, exhibit large refractive index gradient. In such cases partial specular reflections occur. In this case, the scattered echoes cannot be estimated by the Bragg theory. A mathematical approach to estimate the amplitude and the phase of the echo signal is presented in Section 3.4

With appropriate corrections, the experimental observations showed good correlations between the analysed *radar-data* and the in-situ observations However, this particular experiment proved that Bragg scattering was not the only agent of scattering. This was also not the principle agent of scattering. Such experiments more clearly define the effect of atmospheric structure on radar backscatter. It is also established that Doppler techniques provide the capability to study atmospheric dynamics. With Doppler radars, it is possible to carry out routine detailed analysis of the structure of clear air.

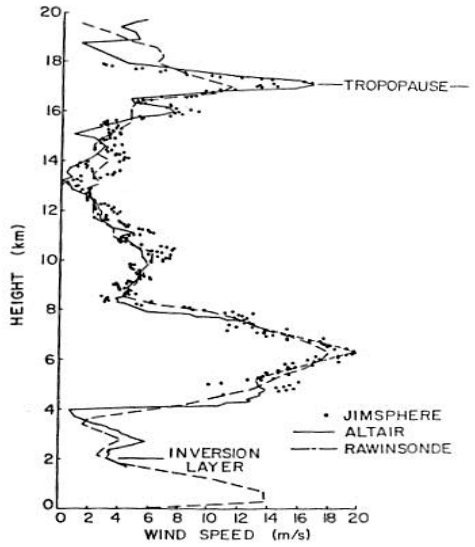

Fig. 3.5 *A comparison between the Doppler radar data and other observations*
(Source: Justin Sharp, "Clear-air Radar Observations and their Application in Analysis of Sea-breezes" http://www.atmos.washington.edu/~justin/radar_project/referenc.htm)

Scientists are interested in another phenomenon of thermal instability known as Kelvin-Helmholtz (K-H) billows. This turbulent situation is created due to the interaction of the two fluids of different density (mainly due to the temperature difference) moving relative to one another. Most common situation occurs in case of sea- breeze. The theory predicts K-H billows of twice the height of the main circulation. This is due to the temperature difference of about 3^0C (1% of the absolute temperature). When the wavelength is twice the periodicity of the K-H billows, they are distinctly observable by the radars [40]. The structure of K-H Billows is shown in Fig. 3.6 (a) and (b).

3.3 Experiments to Determine the Type of Scatter

It is very important to determine the nature of the scattering process using the radar echoes. In case of Doppler weather radars, determining the precipitation echoes is a relatively simple task. These radars operate at microwave frequencies and look for particulate echoes due to precipitation. The frequencies are generally around 3 GHz. Only a few types of scattering mechanisms prompt the echoes. After analyzing the echoes, detailed radar characteristics are known.

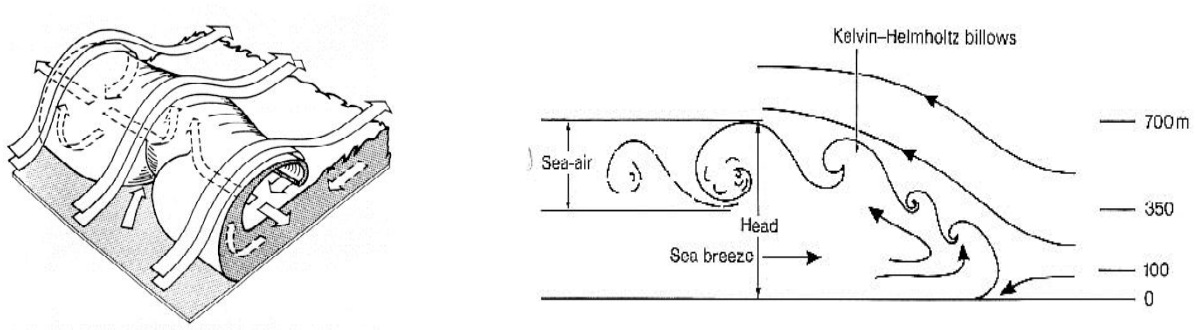

(a) K-H Billows, Artist's Impression. *(b) Eddies formed due to temperature difference*

Fig. 3.6 *Sketches of the Kelvin Helmholtz billows and the turbulent eddies formation.*

(Source: Justin Sharp, "Clear-air Radar Observations and their Application in Analysis of Sea-breezes" http://www.atmos.washington.edu/~justin/radar_project/referenc.htm)

However, in the case of clear-air echoes, the origin of the echoes is much more difficult to determine, as the received echoes may be due to the combination of several types of scattering mechanisms. Without knowledge of the scatterers responsible for the echo and the scattering mechanism it is not possible to analyse or estimate the extent of scattering. For this

reason, the scientists put a great deal of effort for developing ways of differentiating between different scatter mechanisms.

To use radar theory and equations to determine the size and number of distribution of scatterers, it is necessary to determine the type of scatter. For this one must determine whether scattering mechanism is Bragg scattering or particulate scattering. Also in case of particulate scattering, it is necessary to determine whether the scatterer, falls in Rayleigh region or the Mie region. Researchers have developed number of methods to determine the scattering mechanism. A brief description of some of these methods is given below.

(a) Simultaneous observations using radars of different wavelengths. It has been shown that there has been a difference in wavelength dependence of Bragg and particulate scattering processes ($\lambda^{-1/3}$ versus $\lambda^{-4,}$ as shown in eq.3.8 and 3.12). In order to resolve this issue, it is possible to use two wavelengths for observations. After the observations are over, the difference in results are taken to determine the type of scattering. It can be shown that the extent of two scattering can be resolved using the following expression for Bragg scattering [67]:

$$dBZ_{e1} - dBZ_{e2} = 10\log\left[\frac{\lambda_1}{\lambda_2}\right]^{-1/3} dB \qquad (3.15)$$

Where dBZ_{e1} and dBZ_{e2} are equivalent radar reflectivity factor for two different radar wavelength.

In this method, the change in reflectivity is predicted assuming that the scattering mechanism is Bragg scattering. If the observed signal strengths match, the scattering mechanism is likely to be Bragg scatter. When mismatch with the theoretical values is observed, it is concluded that the scatter is from particulates. Then it is possible to determine whether the *relative particle size* is in Rayleigh region or in the Mie region. A similar approach with different frequency radars is used to resolve this. Within the Rayleigh range, the effective reflectivity is inversely proportional to each wavelength used, whereas in the Mie region, the dependence is more complex. Using this fact, the reflected signal strengths for both the radars are compared and the mechanism for the scatter is determined. Though this method is relatively straightforward, it requires two or three radars. This kind of facility is available only at well-equipped research laboratories.

(b) Measurements of differential reflectivity, Z_{DR}. Biota, particularly insects are mostly responsible for most clear air particulate scatter. Most of these scatterers have the length to width ratios of around 1:3 and hence a random volume of such scatterers will produce significant differential reflectivity which then increases with magnitude if the scatterers become more elongated. Particularly for insects, the reflected magnitude changes as the insect population changes the path of movement.

Bragg scattering assumes that the inhomogeneities in refractive index responsible for scattering are due to isotropic turbulence on the scale of half a wavelength. The assumption that turbulence is isotropic is usually valid within the range of wavelengths typically used. Thus, differential reflectivity expected from Bragg scattering should be zero. In other words, the reflected signal strength due to the isotropic Bragg scatter does not fluctuate. Therefore if the measured signal strength shows differential reflectivity, it is likely to be particulate scattering.

(**c) Use of the K-Band radar**. As mentioned, when mill metric radar is used, it can usually be determined beyond doubt that no Bragg scattering will occur. Therefore, all echoes can be attributed to particulate scatter either in the Rayleigh region or Mie region.

(d) Apply findings of other experiments. The methods presented above have been used in research to understand the contribution of each scattering mechanism and the characteristics of the scatterers. They are often not practical to use with routine operational radar. Nonetheless, such research has provided valuable data which can serve as a baseline in routine radar analysis for carefully applying prudent assumptions to radar data.

In general, Bragg scatter is much more prevalent for longer wavelength radar sets (especially wavelengths greater than 20 cm) and typically does not yield reflectivity greater than about -10dBZ. Its intensity is proportional to the magnitude of the refractive index gradients. On the other hand, the magnitude of particulate scatter is dependent both on the scatterer number density and the scatterer size. The reflectivity is usually much higher, typically between -10dBZ to 20dBZ [68], with much higher values possible. Achtemeier [69] reported reflectivity values up to 40dBZ from an insect cloud. This difference will usually enable us to tell if particulate scattering is occurring, but this will not allow us to determine the possible additional contribution of Bragg scatter, if any.

3.4 Modeling of Clear air Doppler Radar Signals

Clear air Doppler radars normally operate in *monostatic mode.* In this configuration the transmitting and the receiving antenna is same. Phase coded RF energy is radiated. The echo signals are detected by correlating with the replica of the transmitted signal. After that the signal is subjected to the Fast Fourier Transform (FFT) to get the velocity information of the target. Fig. 3.7 shows the radar beam volume and the local volume.

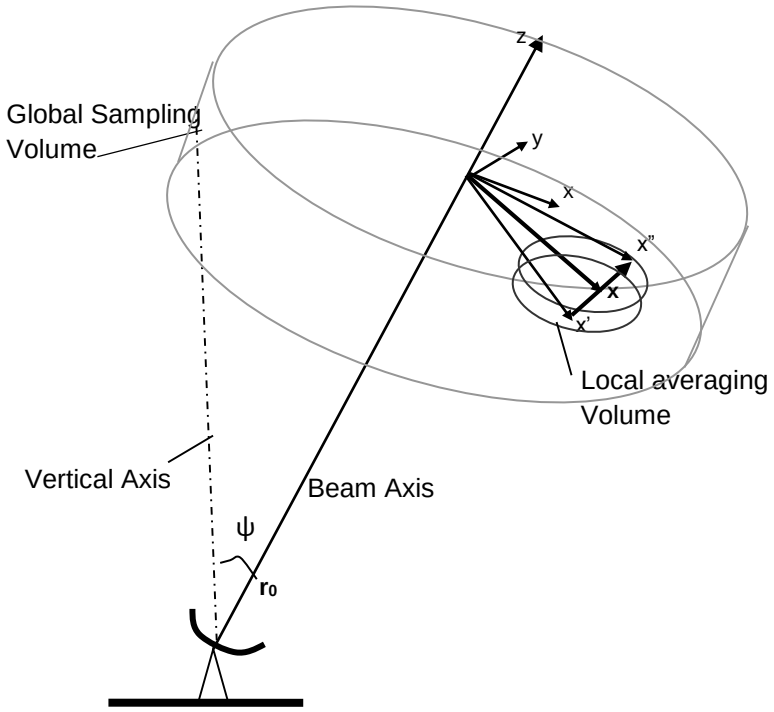

Fig. 3.7 *A sketch of sampling geometry for the CDR radar beam* ***(Source A. Muschinski [70])***

The echo signal is represented as a correlation function over the space filled by the beam.

$$\widetilde{C}_{12}^{(m)} = \iiint_{\mathbf{r}} \iiint_{x} G_{12}(\mathbf{x},\mathbf{r})\widetilde{R}_{12}^{(m)}(\mathbf{x},\mathbf{r},t)d^3xd^3r \tag{3.16}$$

Where, $\widetilde{C}_{12}^{(m)}$ is the mth *time-derivative* of the two-way correlation function, G_{12} is the two-way gain function of the radar beam and $\widetilde{R}_{12}^{(m)}$ is the auto-correlation function of the refractive index. The gain term is a product of the amplitude term A(x) and the phase term P(x). The phase term has a dependence of **r** and **x** given by the equation given below.

$$p(\mathbf{x}) = \exp\left[-ik_B(\mathbf{r}_0 + \mathbf{z} + \frac{x^2 + y^2}{2\mathbf{r}_o}) \right] \tag{3.17}$$

Where k_B is the wave number and r_0 is the range vector.

The first position dependent term of the quantity in the parenthesis (***z***) is due to the homogeneous Bragg scatter in the radar resolution volume. Analysis considering only the first term is known as *Fraunhofer approximation*. The second quadratic term in the above expression indicates location dependence in terms of coordinates x, y. This is the *Fresnel approximation*. With this approximation, for homogeneous scatter conditions, the echo from the scatterers in annular rings will have same phase. Also, the scattered power of the annular rings where value (x^2+y^2) for which the phase of G_{12} becomes π will add out of phase. This distance is called *Fresnel's radius* (*f*). Most of the scattered power is due to the volume within the Fresnel radius. The value of Fresnel radius for the two way gain function is

$$f = \sqrt{\frac{r_o \lambda}{2}} \tag{3.18}$$

Due to these effects the radar observations will show deviations in the backscattered echoes. The CDR backscatter is broadly classified into basically two different mechanisms: the scatter from Bragg-isotropic refractive index turbulence and the scatter from refractive index discontinuities in the form of sheets that are thin but extend beyond the radar beam in the transverse direction. The first type of scatter is known as the *Bragg-Scatter*. In this case, the target has the same texture of refractive index turbulence throughout the radar beam volume. Therefore it does not have any fluctuating effect or variations in the backscattered power. This phenomenon is mathematically represented by Fraunhofer approximation of the two way backscatter expression. The second type of backscatter is due to refractive index discontinuities. These discontinuities are often in form of layers of different refractive indices (also referred to as 'sheets'). The backscatter echoes in this case show specular reflections, aspect sensitivity (variation in backscatter amplitude with beam incident angle [71] and velocity biases in the wind measurements [72][73]. The mathematical analysis for this type requires Fresnel approximation or the inclusion of the quadratic term of the two way backscatter expressions.

3.5 Signal Processing Techniques to derive atmospheric parameters from The Backscattered Radar Signals

In the above sections a brief presentation of atmospheric scattering and the process of observation are presented. The radars are used to observe the back scattered signal from the atmospheric targets and facilitate to determine the structure and estimate the dynamics of the atmosphere. The backscattered signal is coherently sampled and FFT is computed for the Doppler analysis. Use of appropriate window on the time domain data helps in improving SNR[74]. With this background, the radar signals can be viewed as a discrete representation of the backscattered signal on the range-Doppler plane. This 2-D representation is subjected to spectral moment estimation followed by consensus averaging. This data is used to determine the structure of the target. For reliable and consistent determination of the target structure, it is important to estimate the error in the spectral parameters [75] and thereby the accuracy of the atmospheric parameters [68]. With the studies mentioned above, the statistical nature of the Doppler spectra is known in advance. This apriori knowledge can be used to optimize the signal processing strategy and determine the atmospheric parameters better. In subsequent chapters of the thesis three different approaches to analyze the radar signals are presented. These methods use the statistical nature of the scatterers along with the continuity and homogeneity of the atmospheric targets.

3.6 Summary: This chapter explain the concept of the radio wave scattering from atmospheric targets. The knowledge of scattering phenomenon helps in the mathematical description of the backscattered signal. With this understanding, it is possible to develop the spectral signature of atmospheric phenomenon and simulation of all types of weather phenomena, which is being described in chapter 4.

Chapter 4

Modeling of Doppler Spectra for Different Types of Weather Echoes

It is seen in the earlier chapters that the Doppler power spectra is the basic data set on which the further processing is done to extract the information of atmospheric parameters. Before developing any profile extraction technique, it is important to understand the signal processing of the classical wind profiler while operating in Doppler beam swinging method. We have seen that the wind profiler receives the backscatter from the atmosphere. This signal is amplified, filtered and down converted by a super heterodyne receiver to the base-band before subjecting to the digital processor (shown in Fig 4.1). It may be appreciated that a typical Doppler frequency is as small as approximately 10^{-8} to 10^{-7} times the carrier frequency. The Indian MST radar operating at 53 MHz expects Doppler frequencies of a few Hertz. This requires very high frequency stability in the receiver. Also, the expected signal strength is in the range of -140 to -110 dBm. This calls for a very *high-gain* or *sensitive* receiver.

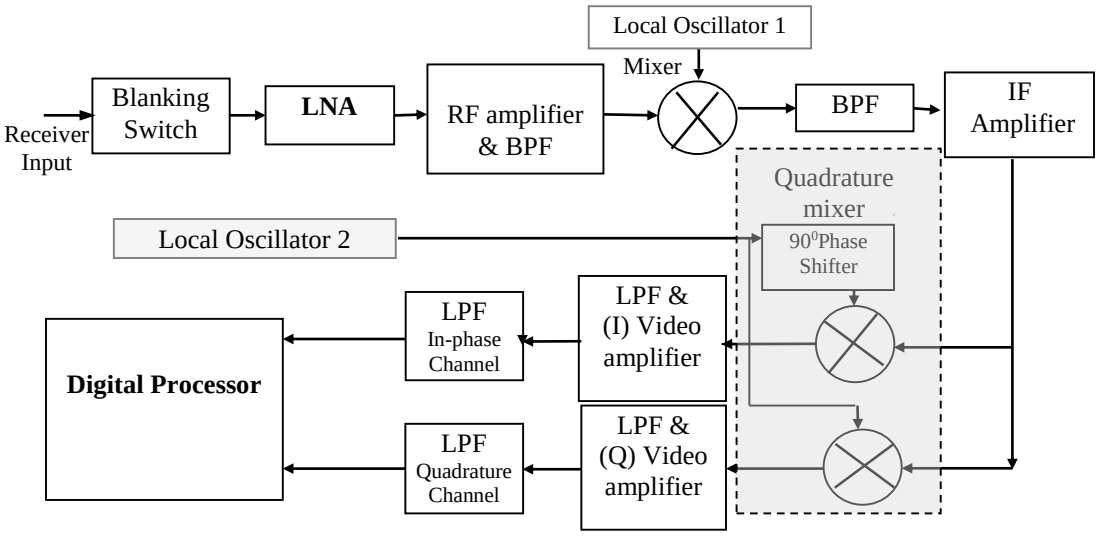

Fig. 4.1 *Schematic of the RF and analog part of a wind profiler receiver*

The receiver output is then subjected to a digital processor where the signal is digitized and then sequenced according to their time of arrival. Radars estimate the range of the target

from the *time of arrival* of the echo. The echoes from the same range are brought together. Signal samples are added coherently and then subjected to frequency estimation by calculating the Fast Fourier transform (FFT), as shown in Fig. 4.2.

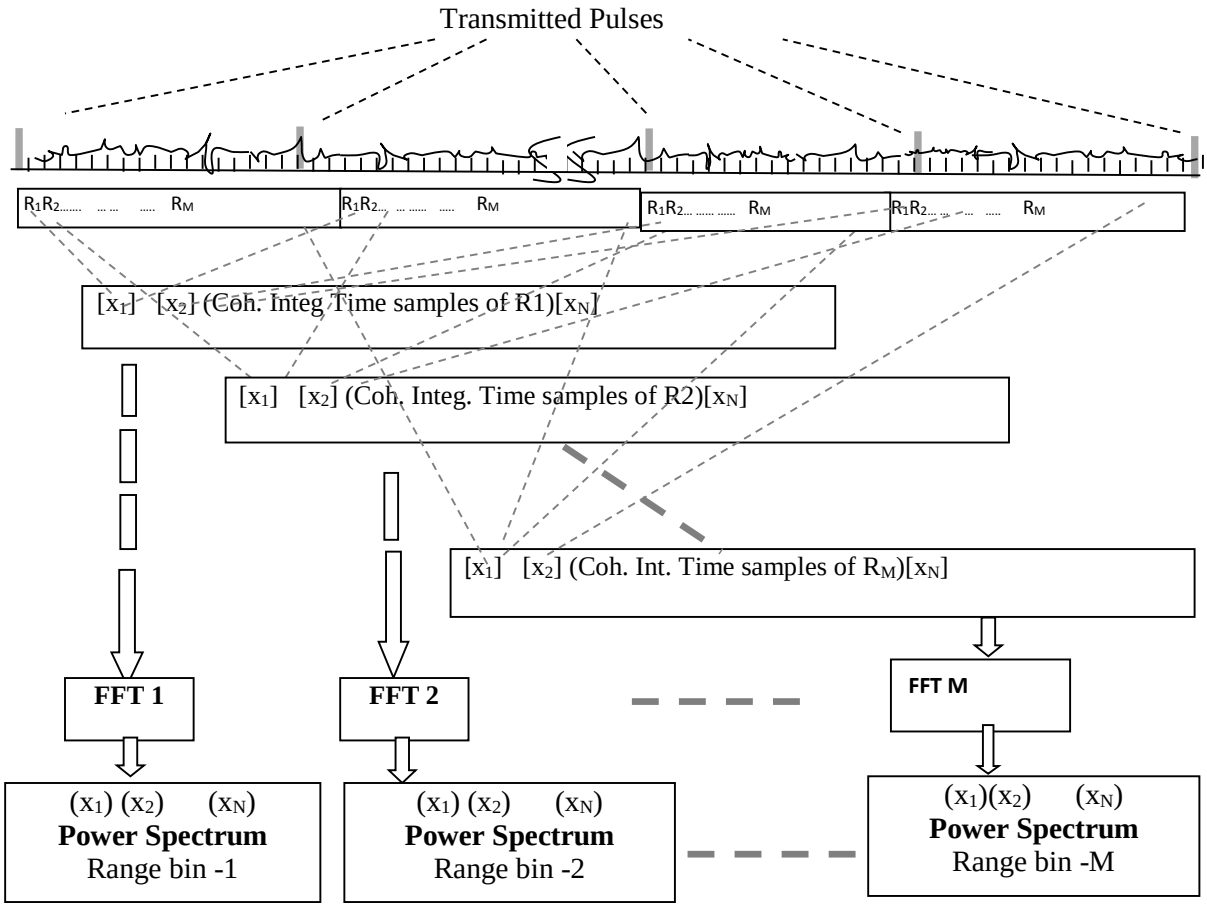

Fig 4.2 *Schematic representation of Signal processing in wind profiler radars.*

4.1 Need for Modeling

Before developing any post processing method it is important to understand the mathematical formulation of the input signal. This is best done by writing simulation program. This program should be done so as to imitate the exact mathematical operation of the digital processor. This way the correct mathematical representation of the Doppler power spectra could be formulated. Knowing the correct formulation of the signal would make it easier to develop the processing algorithms on the spectral data.

Modeling of the process provides correct understanding of the signal ingredients [66]. Another advantage of the modeling is that it gives the capability of creating *customized data*. In other words one can *create* Doppler power spectra corresponding to any type of weather condition! It is improbable that different atmospheric conditions occur at radar site. Also in operational radar it is not expected to have power spectral data of all possible weather conditions. However, one expects that the estimation algorithms to work in all possible conditions. The modeled data comes handy at such a situation and can be used as a test case.

In short, modeling provides insight into the input signal structure. And a set of simulation data corresponding to different atmospheric conditions serves as a benchmark test set with the help of which various processing algorithms could be evaluated.

4.2 Preprocessing of radar data

In this section we shall present the simulation steps that would imitate the wind profiler digital processor. The receiver gives two signals to the digital processor. These are the *In-phase* and *Quadrature* components of the Base-band signal (shown in Fig. 4.1.). They contain different frequency components depending on the target velocity variation. These signals are represented as *sum of sinusoids* with real and complex components. The digital samples are the numbers generated on complex sampling of these sinusoids or the Doppler components. Conventionally, the samples of the *In-phase channel* are represented by periodic digital values of cosine function. Similarly, the samples of the *quadrature -phase channel* are represented by periodic digital values of sine function. These values are the samples taken of the echoes, in the Inter Pulse Period (IPP) (shown in Fig. 4.2). It is known that the signals received early in the time are from the nearer ranges and the signals received in the later part of IPP are from the far ranges. The complete IPP time interval could be divided into many *time slots* corresponding to the range-bins. Fig. 4.2 shows name tags of 'R_1', 'R_2'… R_M to these time intervals.

It is obvious that the signals received in the corresponding *time slots* in subsequent IPP are also from the same range-bin. Such corresponding signals for a few (typically 40 to 60) consecutive IPPs are added. This operation is known as *coherent Integration*. The purpose of coherent integration is to enhance the *signal to Noise Ratio* (SNR). It can be seen that these addition equations (4.1) and (4.2) gives the mathematical expressions for the same.

The equation to compute the *in phase* component of Doppler spectra is as follows:

$$x(i,k) = \sum_{l=0}^{n_c-1} \sum_{m=-s}^{+s} a(k) G(m) \cos(2\pi(f_D + m \cdot \Delta f) \times IPP \times ((i \times n_c) + l)) \quad (4.1)$$

Similarly, the equation to compute the *quadrature* component is as follows:

$$y(i,k) = \sum_{l=0}^{n_c-1} \sum_{m=-s}^{+s} a(k) G(m) \sin(2\pi(f_D + m \cdot \Delta f) \times IPP \times ((i \times n_c) + l)) \quad (4.2)$$

In the equations (4.1) and (4.2), ***i*** is the index for time sample and ***k*** is the index for the range-bin and ***l*** is the number for coherent integrations. The simulation algorithm generates time sample ***x(i,k)*** this is **ith** in-phase sample of **kth** range bin; whereas, ***y(i,k)*** is **ith** quadrature-phase sample of **kth** range bin. The weather target echo in the Doppler power spectra is a collection of multiple frequencies (explanation is given in section 2.3). These signals are generated using the summation of multiple sinusoids with different frequencies around f_D. These frequency components are generated by the terms (f_D + mΔf) as shown in equations 4.1 and 4.2. The signal frequencies are modeled by **2s+1** components with frequencies (f_D-sΔf) to (f_D+sΔf). The index ***m*** is used for the frequency components. The index ***l*** is used for the number of coherent integration. Thus a time sample is formed by adding [(2s+1) × n_c] samples. This sample is computed by doing additions in two *For loops*. The terms *a(k)* is the amplitude of the signal from ***kth*** Range-bin. In reality, this value depends on the RF reflectivity of the scatterers. Clear air atmospheric target often has particles exhibiting Brownian motion. Therefore the amplitude envelope of the group of spectral components has Gaussian or the Bell shape. The term ***G(m)*** implements the Gaussian amplitude envelope. This is also generated by *'NORMPDF'* function in Matlab. At the frequency f_D , value of *G(m)* is 1 and will roll down for both positive and negative frequencies. By changing the variance parameter of the Gaussian envelope function, it is possible to choose slow roll down for high turbulence and fast roll down for more streamlined winds.

Though there is no limitation on value of the parameters, the user is expected to choose realistic values corresponding to the wind velocity. For the wind profiler, the wind velocity range is between 0 ms^{-1} to 24 ms^{-1}(86 Km/hr). This corresponds to Doppler frequency range 0 Hz to 7.8 Hz for the MST radar. However the cyclonic winds could take the wind values up to

100 ms^{-1} or Doppler frequency of 30 Hz approximately. Similarly, there is no limit on amplitude values. But most of the scientists prefer to use amplitude values normalized to 1.

The components *x(i, k)* and *y(i,k)* form the real and imaginary part of the complex *time sample*. It may be noted that the *Complex Sampling* of the received signal is required as +ve and –ve frequencies need to be measured. Complex sampling is possible with quadrature detection. In other words, the last down conversion need to be done with *Quadrature Mixer* (shown in Fig. 3.1) creating 2 –channel output; namely *in-phase* Channel and *quadrature phase* Channel.

4.3 Modeling and Simulation of Noise and Doppler Spectra

The received signal is always accompanied by noise. The wind profilers receive signals from open sky. Atmospheric backscatter signals from VHF/UHF bands generally have White Gaussian noise [1]. Therefore, under the normal circumstances, wind profiler signal encounters Additive *White Gaussian Noise* (AWGN). This inclusion of AWGN is simulated by simply adding complex random term ***n(k)*** as shown in equation (4.3). The additive WGN term ***n(k)*** is generated using the Matlab function (AWGN). However, the simulation algorithm allows the user to select noise of any probability distribution. Equation (4.4) shows the mathematical expression of complex FFT computation. ***Z (i,k)*** is the complex spectral component of the Doppler spectrum for the ***k^{th}*** range-bin. The power of the component is simply the squared addition of the real and imaginary parts of the component (given in equation 3.5).

$$z(i,k) = x(i,k) + jy(i,k) + n(k) \tag{4.3}$$

After addition of the noise, the signal is subjected to 'Fast Fourier Transform'

$$Z(i,j) = K\sum_{k=1}^{nDFT} z(i,k)e^{\left(\left(\frac{2\pi}{nDFT}\right)kxj\right)} \tag{4.4}$$

$$\mathbf{Z}(i,j) = \mathrm{Re}(Z(i,k))^2 + \mathrm{Im}(Z(i,k,))^2 \tag{4.5}$$

Fig.4.3a is an example showing the power spectra generation. It shows a sine wave power spectra demonstrating capability of generating *user defined* Doppler profile. Fig.4.3b shows customized Doppler profile imitating profiles obtained by radars.

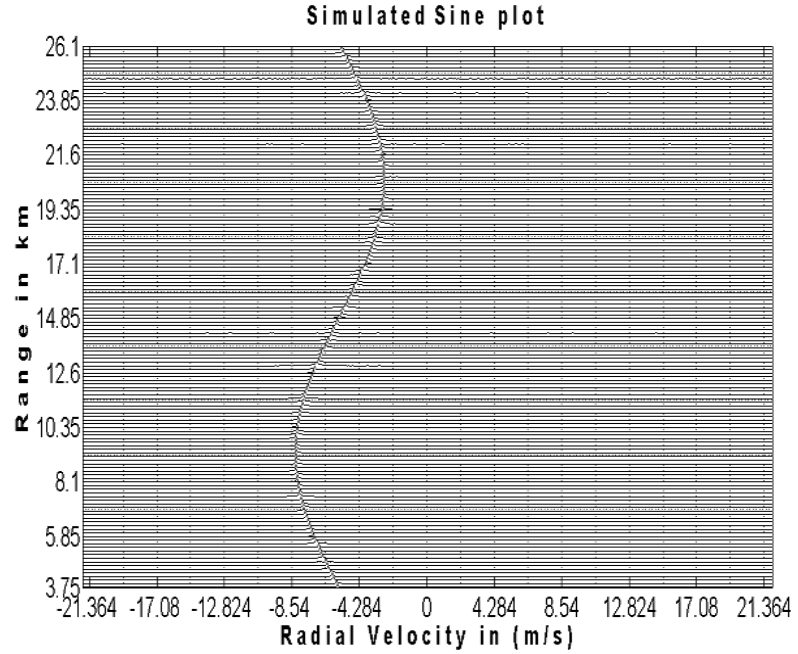

Fig. 4.3 (a) *Simulated Sine wave profile*

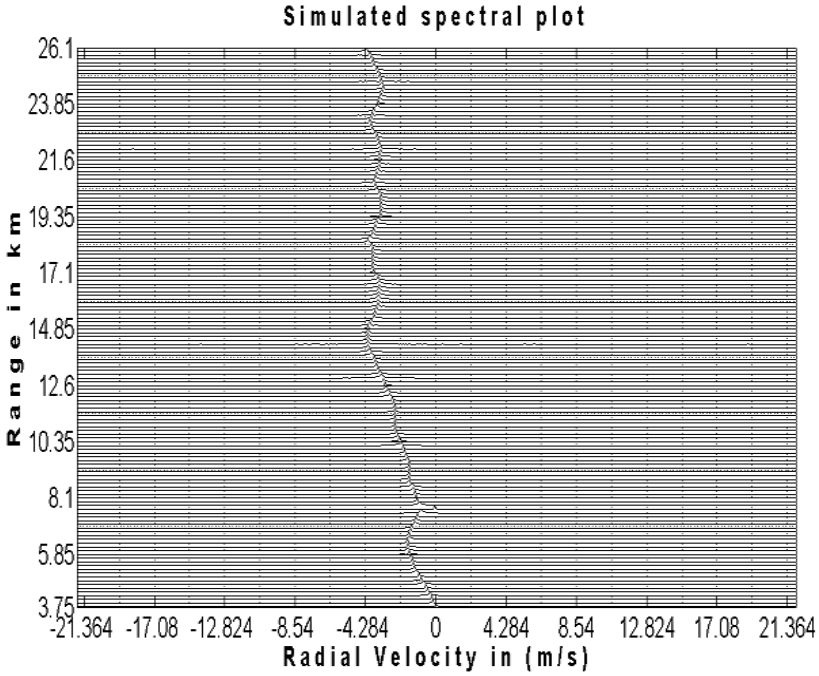

Fig. 4.3 (b) *Simulated Doppler power spectra*

Fig.4.4a shows the Doppler power spectra with noise. Different values of noise power could be programmed in different range bins. Fig.4.4b shows a real radar data. It may be seen that the simulated data and the radar data is practically indistinguishable.

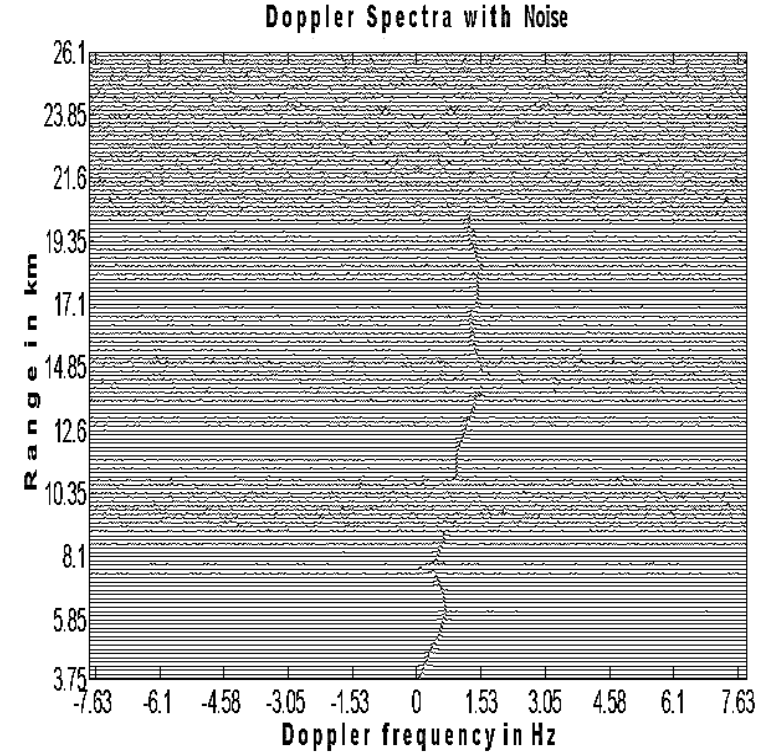

Fig 4.4(a) *Simulated Power spectra with noise at few range bins*

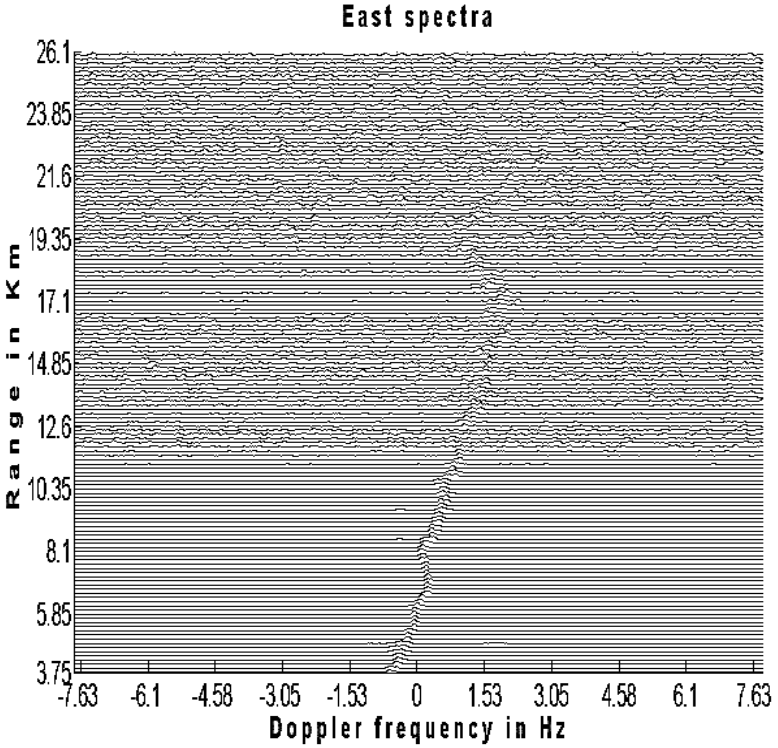

Fig. 4.4(b) *Representation of Radar Power Spectra (MST radar, Beam Direction: East 10^0)*

4.4 Modeling and Simulation of Clutter, RFI and other unwanted signals

It is often observed that the radar signal is occasionally contaminated by Clutter and *Radio Frequency Interference (RFI).* Clutter is the most common unwanted signal in the WPs. Clutter consists of echoes from nearby stationary and slowly moving objects like trees, hills, sea etc. On the Doppler power spectra, clutter appears as a low frequency spectral component symmetrically placed around 0 Hz. Since the clutter is signal from nearby terrestrial objects, it appears in the lower range-bins. These signals are simulated by adding extra components at low Doppler frequencies (corresponding to velocities below 2.5ms^{-1}) say f_{D1}. The mathematical expression for ***x(i,k)*** is the same as given in equation 3.6. Similar expression is used for ***y(i,k)*.** The notations of the variables are the same as described in section 4.2.

$$x(i,k) = \sum_{l=0}^{n_c-1} \sum_{m=-s}^{+s} a(k)G(m)(\cos(2\pi(f_D + m \cdot \Delta f) + a1(k)(\cos(2\pi f_{D1})) \times IPP \times ((i \times n_c) + l)) \quad (4.6)$$

System generated disturbances like electrical noise and power frequency leakage are occasionally observed in the power spectra. Power frequency disturbances and other interfering sources are categorized as RFI. RFI is generally a single frequency disturbance spanning over short time. This appears as a sharp spectral component in 8-10 or more range bins. RFI occurs at same Doppler bin at all the affected range bins. Hence this type of unwanted signal presents itself as a set of sharp peaks placed in a vertical line. This disturbance is simulated by adding another frequency component (say f_{D2}) in the expression of ***x(i,k)*** and ***y(i,k)*.**

In Matlab programming separate vectors of dimension (RB × 1) for frequency and amplitudes are created; where RB is the number of range bins. User can put any values of frequencies for each range bins. Fig. 4.5a shows simulated Doppler spectra with clutter contamination and Fig. 4.5b shows simulated Doppler spectra with RFI contamination.

Fig. 4.6a shows Simulated Doppler power spectra with Clutter and RFI contamination. Fig. 4.6b shows MST radar data having both clutter and RFI contamination. It is seen that the simulated data is perceived same as real radar data.

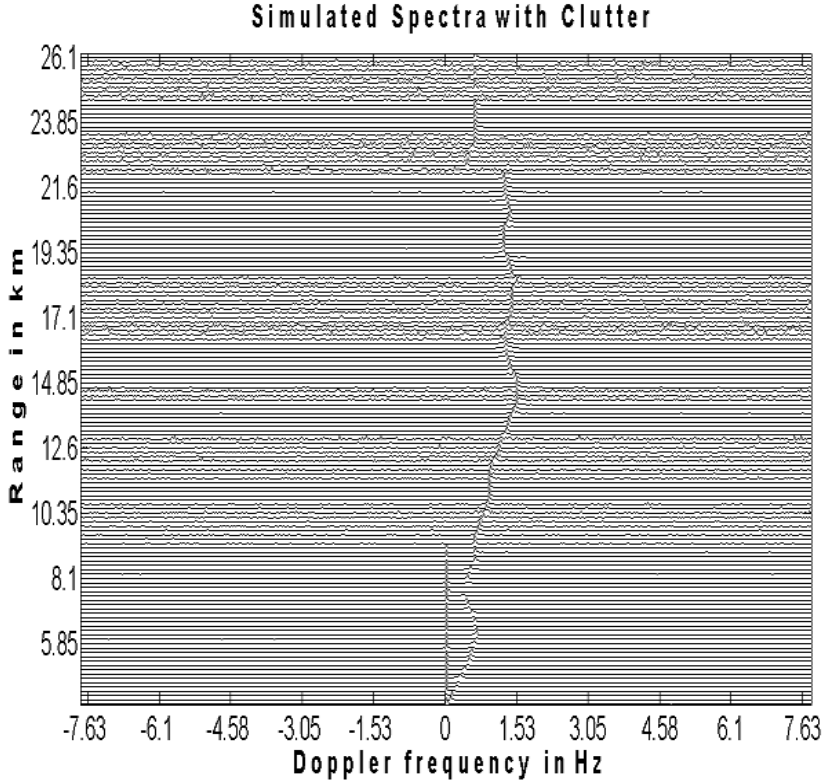

Fig. 4.5(a) *simulated Doppler spectra with clutter*

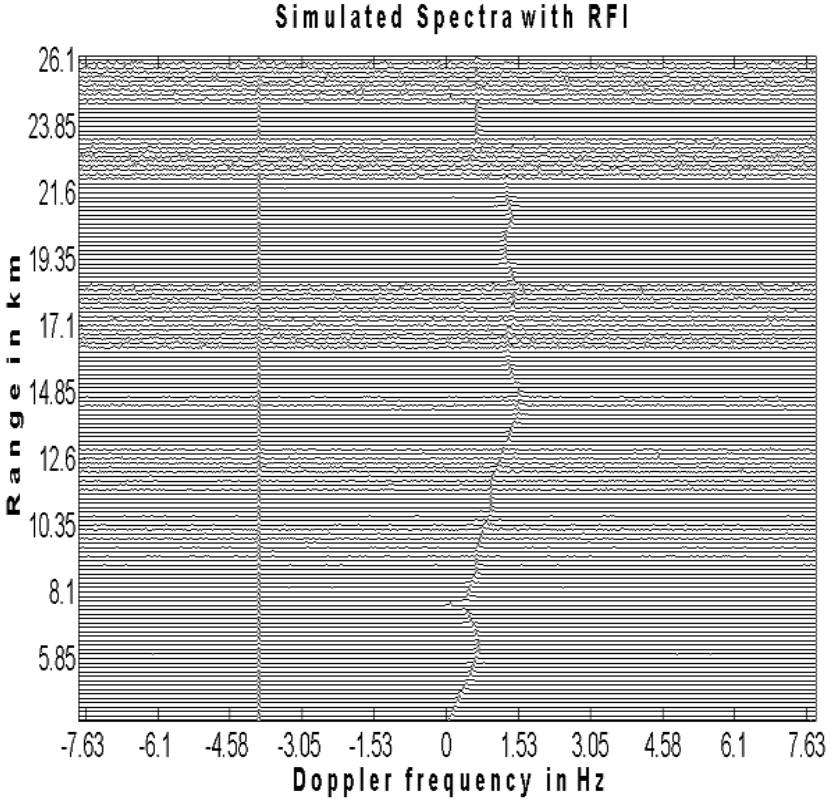

Fig. 4.5(b) *simulated Doppler spectra with RFI*

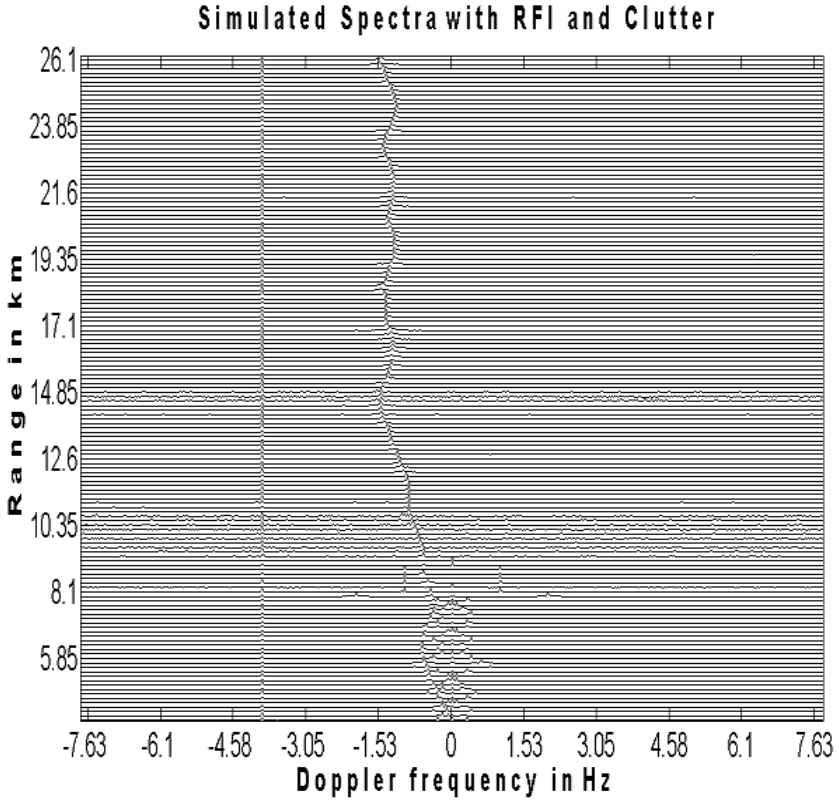

Fig 4.6(a) *simulated Doppler spectra with clutter & RFI.*

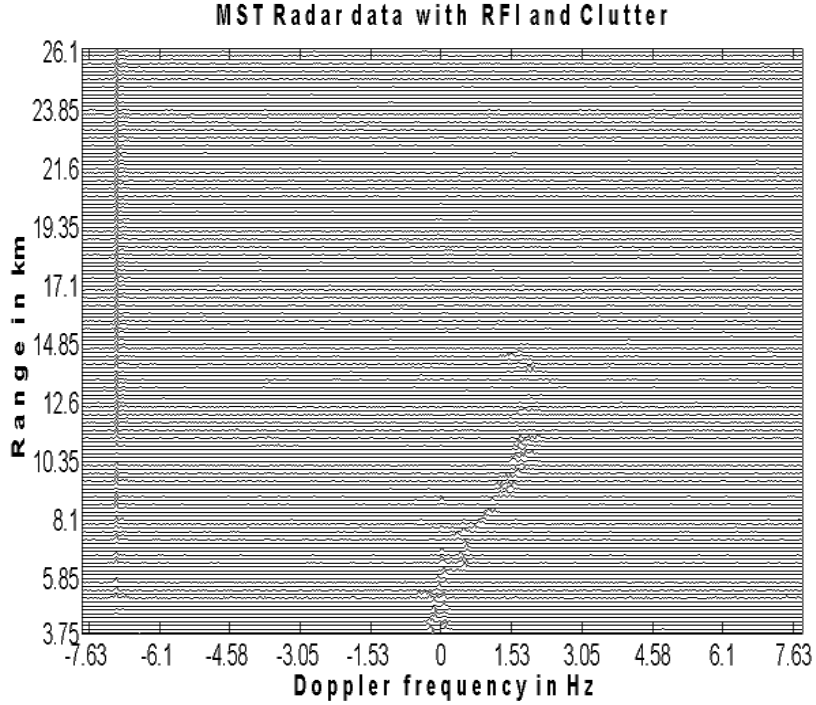

. ***Fig. 4.6(b)*** *Power spectra with RFI & Clutter (MST radar, Beam Direction: East 10^0)*

4.5 Modeling and Simulation of specific weather phenomenon

In this section, simulation of Doppler power spectra for *Precipitation* and *Ionospheric echoes* is presented. Precipitation echoes are created by adding additional components in the same form as equation (4.7) and equation (4.8). The only difference is the mean Doppler component is f_{pi} corresponding to the rain-drop velocity. The envelope function could $G_p(m)$ is generally a narrow Gaussian function (with standard deviation of approx. 1 Hz corresponding to 0.4 ms^{-1}, say). The precipitation echoes are generally observed for the range-bins below 8 km and with rain drop velocities in between $8ms^{-1}$ to $20ms^{-1}$ with range profile of a characteristic shape shown in Fig.4.8. Precipitation Doppler spectra corresponding obtained from radar is shown in Fig.4.7 for comparison. .

$$x(i,k) = \sum_{l=0}^{n_c-1} \sum_{m=-s}^{+s} a(i) G_p(m) \cos(2\pi(f_{pi} + m) \times IPP \times ((k \times n_c) + l)) \quad (4.7)$$

$$y(i,k) = \sum_{l=0}^{n_c-1} \sum_{m=-s}^{+s} a(i) G_p(m) \sin(2\pi(f_{pi} + m) \times IPP \times ((k \times n_c) + l)) \quad (4.8)$$

The ionospheric echoes could also be generated by adding frequency components in the same form as equation (4.7) and (4.8). The Doppler frequency values (to be indicated by f_{pi}) and envelope shape need to be chosen correspondingly. Ionospheric echoes are observed at heights above 80 km and typical radial winds are between 53 ms^{-1} and 140 ms^{-1}. This corresponds to) f_{pi} values of 19 Hz to 50 Hz for Indian MST radar operating at 53 MHz. Fig. 4.9 and Fig. 4.10 show simulated and radar ionospheric Doppler spectra respectively.

Similarly, Meteoric echoes are generally observed above 80 km. The Doppler frequency values (to be indicated by f_{pi}) are observed in between 28 Hz (77 ms^{-1}) to 222 Hz (623 ms^{-1}).

The envelope shape in all the cases can be decided using the variable $G_p(m)$ in equation (4.7) and equation (4.8) and the spread of the envelope can be decided using the variable m in equation (4.7) and equation (4.8). It can be seen that it is possible to create Doppler power spectra corresponding to any weather phenomenon whose spectra features are known.

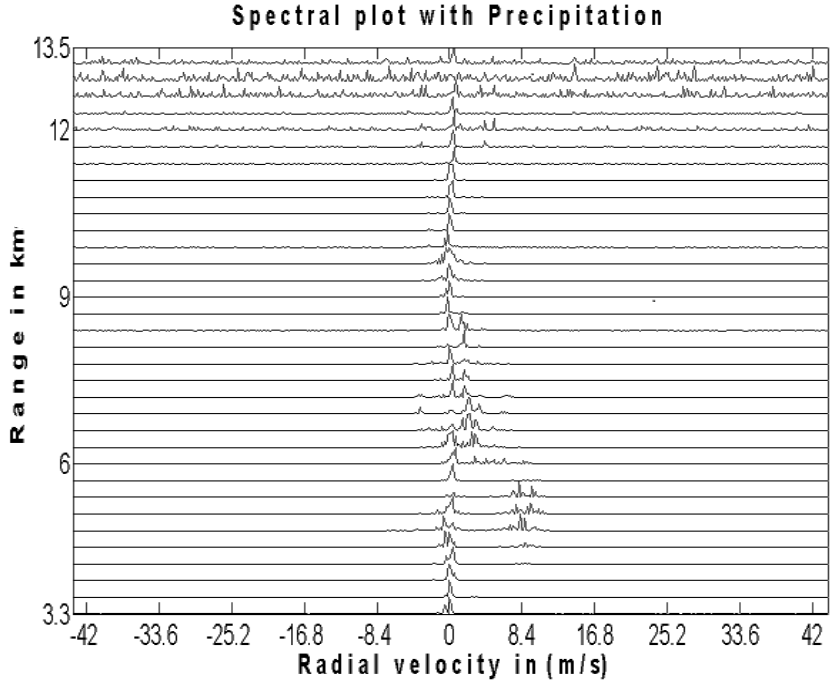

Fig. 4.7 *Precipitation plot (MST Radar, Beam Direction: South 10^0)*

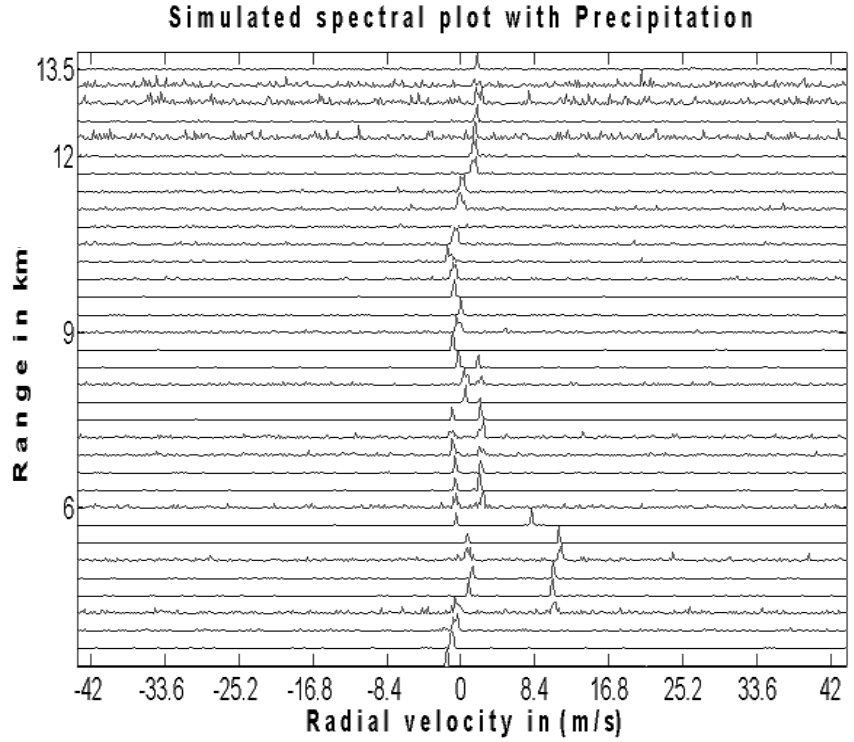

Fig. 4.8 *Simulated Precipitation plot*

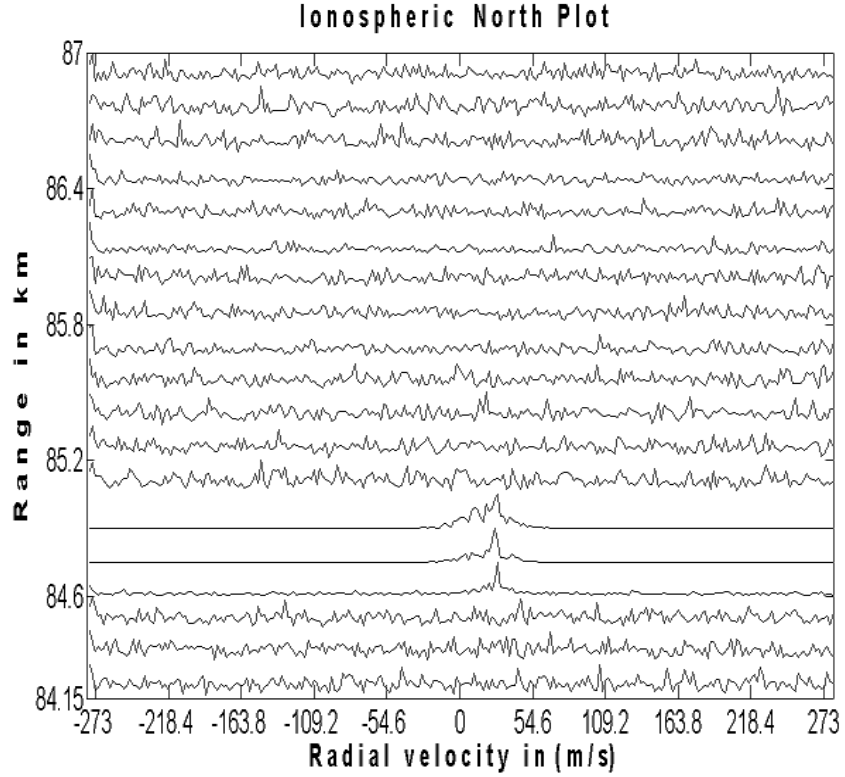

Fig. 4.9 *Ionospheric plot (MST Radar Data, Beam Direction: North 13^0)*

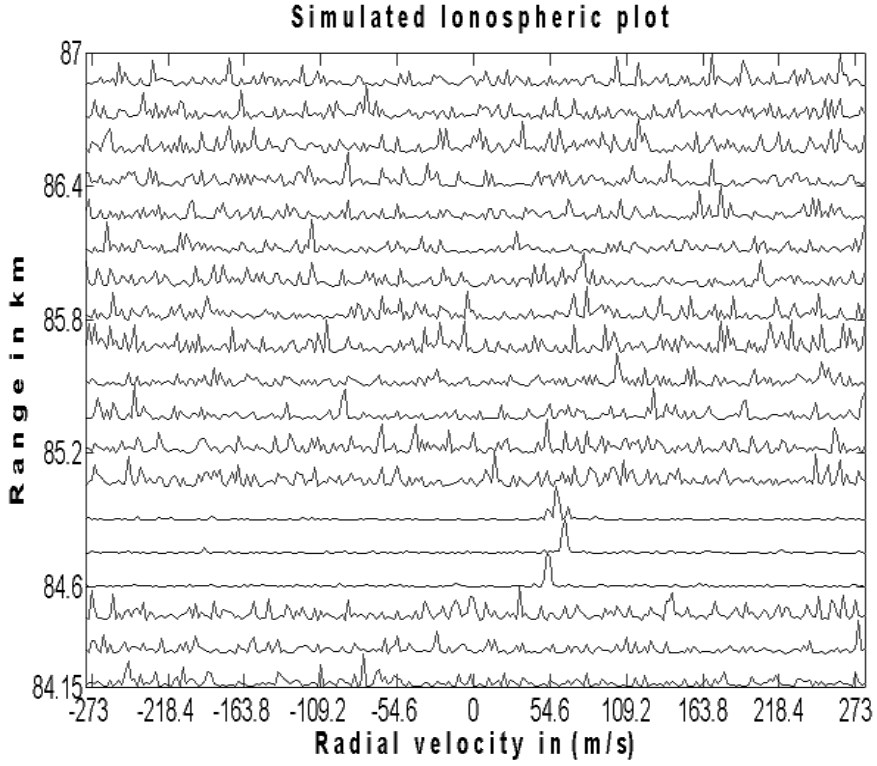

Fig.4.10 *Simulated Ionospheric plot*

4.6 Results

In the earlier sections we have seen that it is possible to simulate Doppler power spectra of all atmospheric condition. If the signature on *range- Doppler* plane is known, the spectra could be generated. Generally, the data of range-Doppler signature corresponding to most of the weather conditions is available as the atmospheric researchers have studied them and have found correlation and associated specific range-Doppler signature. In other words, the signal patterns appearing in the power spectra due to the backscattered echoes is known for almost all weather phenomenon. Using this information it is possible to prepare Doppler spectra of various atmospheric conditions and add disturbance of any kind.

The mathematical formulation described in the foregone sections is very versatile and can simulate any *range-Doppler* signature by appropriate choice of the variables and functions. It may be worthwhile to create data sets of all representative weather conditions and with disturbance signal of different levels. Such data set could be used as a *Benchmark platform* to evaluate the performance of post processing algorithms and also to compare the performance of multiple algorithms. This approach presented in this chapter may be seen as a *versatile* tool to simulate the power spectra of all weather conditions and different types of disturbances. This simulation tool is expected to pose itself as a generator of *benchmark platform* for testing and performance evaluation of post-processing algorithms.

4.7 Summary

Mathematical modeling of wind profiler power spectra is presented in this chapter. This method initially defines the spectral components and generates the *time samples* as generated by the radar ADC. Then it performs *wind profiler signal processing steps* as performed by the radar. This allows the user to generate *real weather-like* Doppler spectra by introducing realistic Doppler components at every range. It is also possible to include noise and other non- atmospheric components in the spectra. Similarly, atmospheric Doppler power spectra corresponding to specific atmospheric phenomenon could be generated by adding appropriate Doppler component. General strategy of algorithm is to include feature based Doppler components corresponding to physical parameters in the time domain samples. All programs were written in Matlab. The

modeled and simulated data sets are compared with radar spectral components of more than 100 observations from the Indian MST radar at NARL Gadanki, India.

This tool turns out to be a *versatile testing platform* for wind profiler radar data. This method can be effectively used to generate *'standardized data set'* of Doppler spectra to test the effectiveness of any newly developed profile tracing algorithm(s). The capability of adding specific spectral features could be used in ***reverse action*** for removal of specific spectral signatures from radar data. Hence developed algorithm also proves as an effective ***pre-processing tool*** as they are capable of removing the unwanted *non-atmospheric signals*.

The power spectral data modeling techniques presented in this chapter were used to generate the data where actual signals are not available and to create data sets corresponding to less probable situations like meteoric echo

Next chapter presents signal processing algorithm for the wind profiler Doppler power spectra. The implementation of all these algorithms are done on the real data of wind profiling radars.

Chapter 5

Pre-processing of Real Radar Doppler Spectra

It is seen that the wind profile data is very weak and often contaminated with the echoes from non-atmospheric sources. This makes it difficult to extract weather parameters from the radar data. Therefore it is advisable to perform pre-processing of the data set(s). The preprocessing involves following functions.

1. Noise estimation and removal.
2. Identification of the clutter and RFI components and the removal of these components.

This chapter presents the methodology and mathematical formulation of preprocessing. Real data from MST radar and the LAWP radar are used to apply preprocessing techniques as shown below. MST radar works at 53 MHZ radar with 2.5 MW, peak power. This radar is expected to estimate the wind profiles up to mesospheric heights (up to 60 km). LAWP is 1280 MHz, 10 KW power radar and expected to receive and process echoes from the targets up to altitude of about 5 km.

5.1 Reading the data from Binary Data file

The first step of the data processing is "reading the data format". Radars make the data available in a specific format. The data format for the Indian MST radar is given in Appendix-1. Initial part of the data format is the header which contains information of the operating radar parameters like *Pulse width, start and stop of observation window* etc. In general, MST radar can generate following data products.

a) Power Spectra: Received power in each Doppler frequency bin.
b) Raw data: Time samples data
c) Complex Power spectra: Complex values of the frequency components after FFT
d) Moments: Zeroth, First and Second central moments for each Range-bin.

e) UVW: U (Zonal), V (Meridional), W (vertical) winds computed by classical method[5].

These products are available to carryout research on different signal processing aspects of the radar. One of the objective of this thesis to develop a new Doppler Profile tracing algorithm. Therefore, only the Power spectral data will be relevant for this research. Considering this a detailed procedure is formed and the Matlab program is written for the same (explained in Appendix-2). Chau [76] attempted to extract information for Distance-Velocity Azimuth Display (DVAD) from the radar data. This new interpretation technique provides wind information at the locations substantially away from the radar. The data of Lower Atmospheric Wind profilers (LAWP) radars, with conventionally fed antenna array as well as active array are also processed in similar manner [77][78].

5.2 Noise Estimation in Each Range Bin

Estimation of noise in each range bin is done after the data acquisition and reading. The probability of estimation accuracy of wind in each range-bin depends on the signal to Noise Ratio (SNR). The processing strategy also changes with the value of SNR. Various noise estimation methods were studied [25][26][27]. However, the VHF/UHF radar noise is white Gaussian noise and classical method suggested by Hildebrand et. al.[24] is still found consistent. Hence, this thesis also used the same method and Matlab program is written for the noise estimation using Hildebrand method. Mathematical operations for the noise estimation with typical power spectral data set are as follows:

This algorithm is applicable for the noise estimation for atmospheric radar Doppler spectra. This algorithm is developed based on following reasonable assumptions.

1. Weather echo spectrum is Gaussian but colored. (non-uniform frequency contents)
2. The noise spectrum is Gaussian but white. (uniform frequency content)

The structure of the power spectra is as shown in Fig. 5.1.

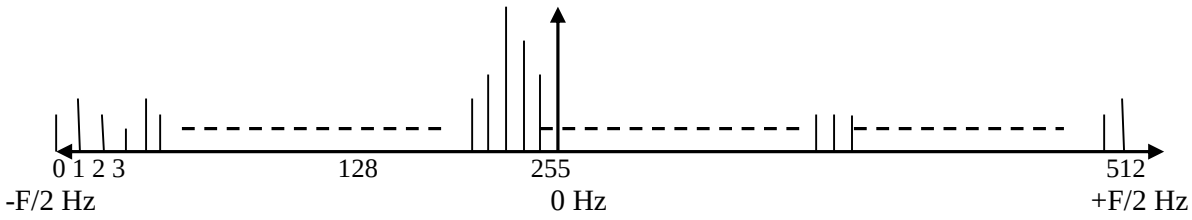

Fig. 5.1 *Typical Doppler Spectra of a range-bin*.

Mathematical implementation of noise estimation algorithm is as follows:

Total number of frequency components are indicated by N (N=512 in Fig 4.1). The index ***n*** is used to indicate individual frequency component. Spectral components are indicated by S_n and ***p*** is the number of spectra averaged (if more than 1). We compute the following quantities.

$$\sigma^2 = \left(\sum_{n-1}^{N} f_n^2 S_n / \sum_{n=1}^{N} S_n \right) - \left(\sum_{n=1}^{N} f_n S_n / \sum_{n=1}^{N} S_n \right)^2 \quad (5.1)$$

$$\sigma_N^2 = F^2 / 12 \quad (5.2)$$

$$P = \sum_{n-1}^{N} S_n / N \quad (5.3)$$

$$Q = \sum_{n-1}^{N} (S_n^2 / N) - P^2 \quad (5.4)$$

$$R_1 = \sigma_N^2 / \sigma^2 \quad (5.5)$$

$$R_2 = P^2 / p.Q \quad (5.5)$$

Where, σ^2 and σ_N^2 are spectral variances of the components and noise, ***P*** is average signal power, ***Q*** is the average noise power, $\mathbf{R_1}$ noise power threshold and $\mathbf{R_2}$ determines the signal power threshold. *F* is frequency spread of spectrum. *N* is the number of independent spectral densities. When all the spectral components belong to white noise the ratios R_1 and R_2 are unity. If any *non-random* component is present, then the value of R_1 is greater than 1 ($R_1>1$) and, the value of R_2 is less than 1 ($R_2<1$). The Noise estimation uses this property by following procedure.

It computes the ratios R_1 and R_2 for the complete spectra. Generally the ratios do not satisfy the condition for white noise. Then the largest spectral component is discarded and the value of N is decremented. The ratio is re-checked. This process continues till the ratios are equal to one (within some pre-decided tolerance). The corresponding value of ***P*** at that stage gives the noise power level.

5.2.1 Smoothing of Doppler Spectrum

The Doppler Spectrum of a range bin often show abrupt magnitude changes between adjacent Doppler Bins. This is removed by averaging a few spectra. *Three point averaging* is

done in this thesis. This procedure involves taking average of three consecutive Doppler components and replacing the central component. This procedure is widely adapted in spectral processing. The same practice is continued in this thesis.

5.2.2 Noise Removal

After the noise estimation in each range bin, the noise component is removed. This is done by subtracting the noise value through all the components. If the negative value is obtained after subtraction, it is replaced by zero or very small value, 0.1 × the noise level.

5.3 Identification of Clutter and RFI

The *signature* of the clutter and the RFI are presented in section 4.4. The word *signature* is used to describe the characteristics and the relative position of the spectral components. For identification of the Clutter and RFI the same ***apriori*** information is used. Here the occurrence of clutter and RFI is verified by observing the signature conditions for all the spectral points. The spectral points which satisfy these conditions are categorized, as clutter or RFI accordingly.

5.4 Removal of Clutter and RFI without affecting received atmospheric echoes

Once the clutter and RFI spectral points are identified it is easy to remove them. They are removed simply by replacing these components with calculated noise level value. This method shows better performance than other method. The advantage is mainly in terms of less *disturbance to other spectral components*. Most of the filter based methods show a small deviation (amplitude change of the adjacent components).

5.5 Computation of Moments for profiling

The definitions of the moments and their significance in this context are as follows:

$$m_0 = \int F(\omega) d\omega \qquad \text{Zeroth Moment (reflectivity)} \qquad (5.6)$$

$$m_1 = \int \omega F(\omega) d\omega \qquad \text{First moment (wind Velocity)} \qquad (5.7)$$

$$m_2 = \int (\omega - m_1)^2 F(\omega) d\omega \qquad \text{Second Central Moment (wind Turbulence)} \qquad (5.8)$$

Where, $F(\omega)$ is the power spectrum, m_0, m_1, m_2 are the zeroth, first and second moment respectively. However, in the remaining part of thesis, normal nomenclature for the power spectrum has been used as applicable in atmospheric science. Moment computations are very similar to those given in Equations (5.1) through (5.2).

The zeroth moment is the average of all the components and mathematically equal to the denominator term in equation (5.1) given by $\sum_{n=1}^{N} S_n$. The first moment is mathematically equal to the numerator of the second term of equation (5.1) given by $\sum_{n=1}^{N} f_n S_n$. The second central moment is the computed value of the equation (5.1) given by σ^2.

5.6 Results

Pre-processing of the Doppler spectra are done in following three steps.

(i) **Noise estimation and suppression:** Noise estimation has been done using classical Hildebrand algorithm. Hence the noise is partially suppressed.

(ii) **Identification of non-atmospheric spectral components and removal:** The algorithm developed to model the spectral features of the non-atmospheric components is used to identify them and subsequently to remove them.

This processing removes the unwanted signals and enhances the echoes of the atmospheric signals. This makes the data ready for its further processing and extracting the wind velocity information. The efficacy of preprocessing method was tested on simulated data as well as on various real data sets of the Indian MST radar and few results are presented below with the real MST radar data and simulated data. Fig 5.2(a) shows the unprocessed Doppler spectra of MST radar and Fig 5.2(b) Shows Doppler Power Spectra of the same data after noise removal using Hildebrand method.

Fig. 5.3 (a) and 5.3 (b) shows MST Radar Power Spectra before and after RFI and Clutter removal.

Fig. 5.4 (a) and (b) shows LAWP Power Spectra before and after clutter removal.

Fig. 5.5 (a) and (b) shows Simulated Power Spectra before and after RFI removal.

This knowledge of the Doppler signatures of RFI can be used to simulate wind profiler data contaminated with RFI. The RFI removal method is tested with the simulated data as well and the result is presented in Fig. 5.5(a) and 5.5 (b)

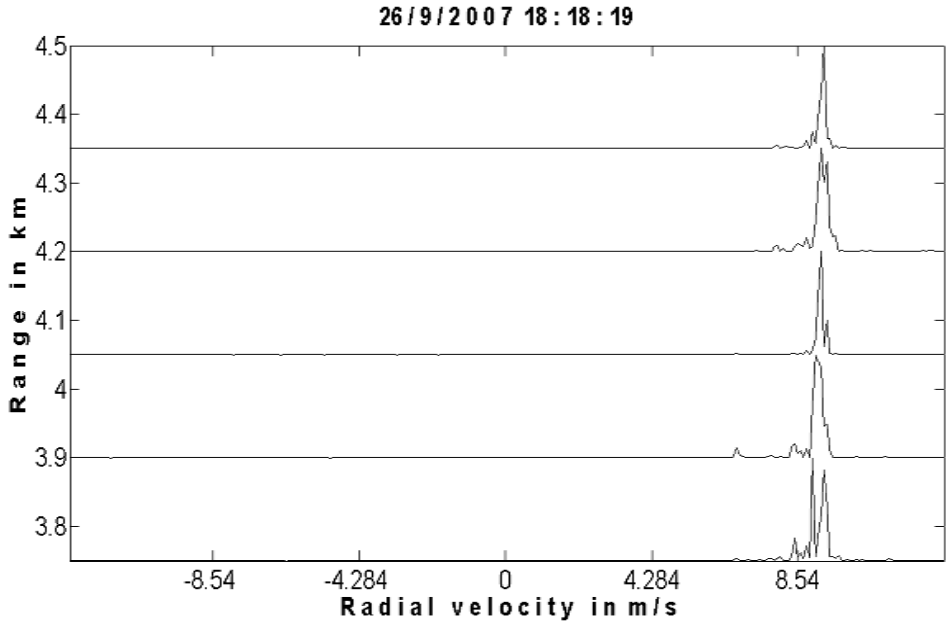

Fig. 5.2 (a) *WP Power spectra of few Range Bins before noise removal (Section of MST Radar data, Beam Direction: West 10^0)*

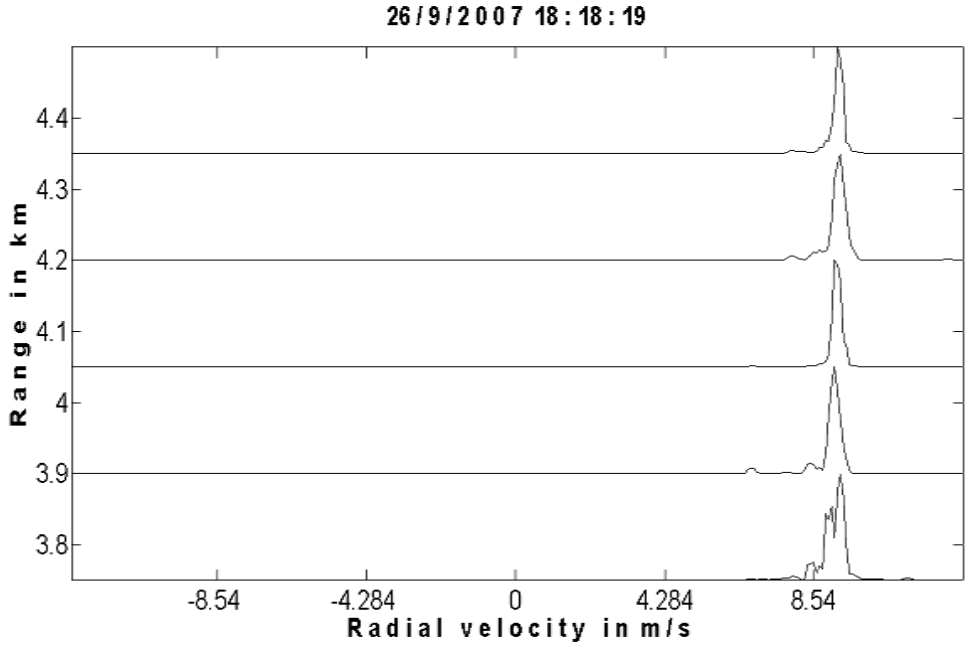

Fig. 5.2 (b) *Power spectra of the same Range Bins after noise removal (Section of MST Radar data, Beam Direction: West 10^0)*

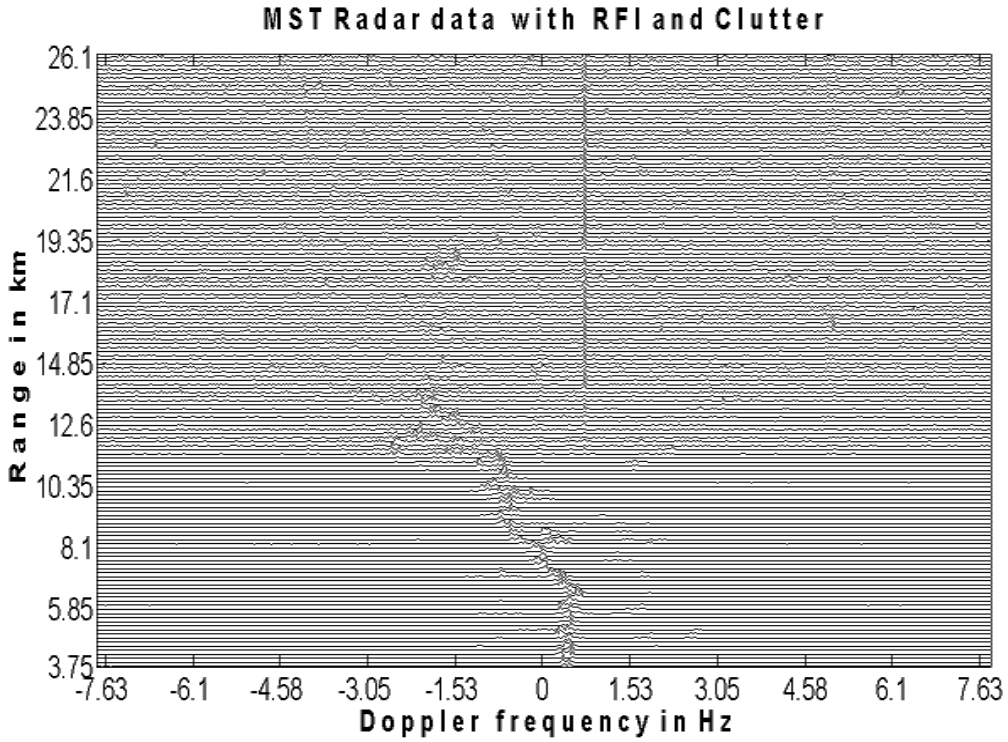

Fig.. 5.3 (a) MST Radar data (Beam Direction: West 10^0) with RFI and Clutter.

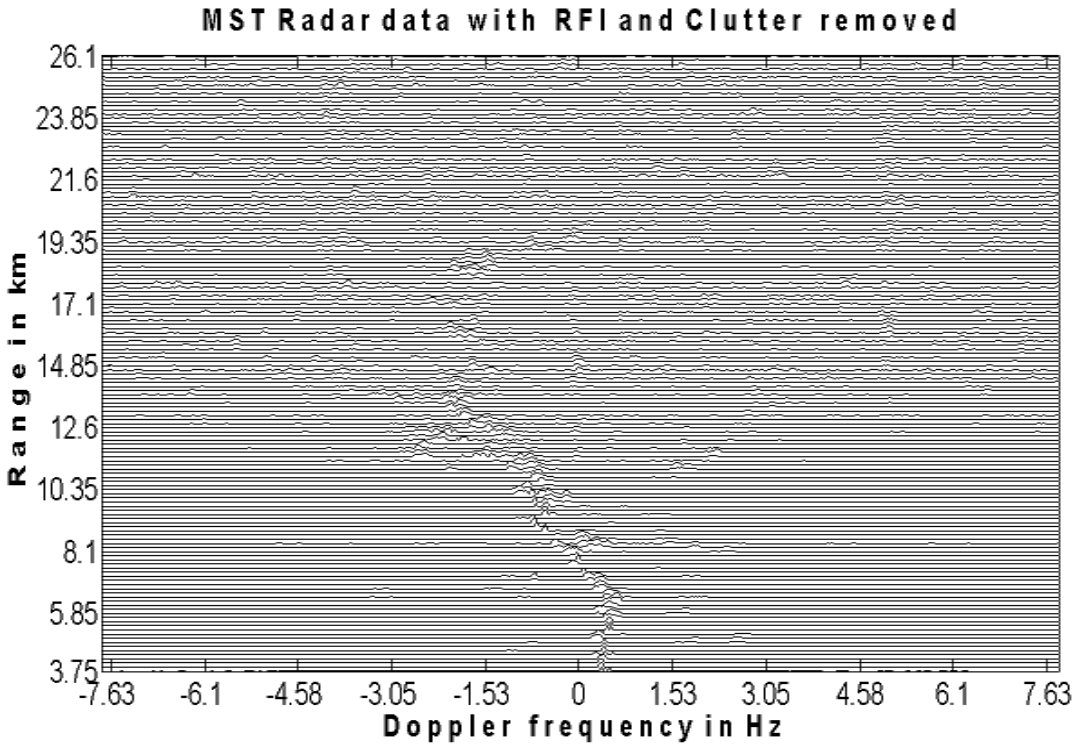

Fig. 5.3 (b). MST Radar data: (Beam Direction: West 10^0) Clutter and RFI removed.

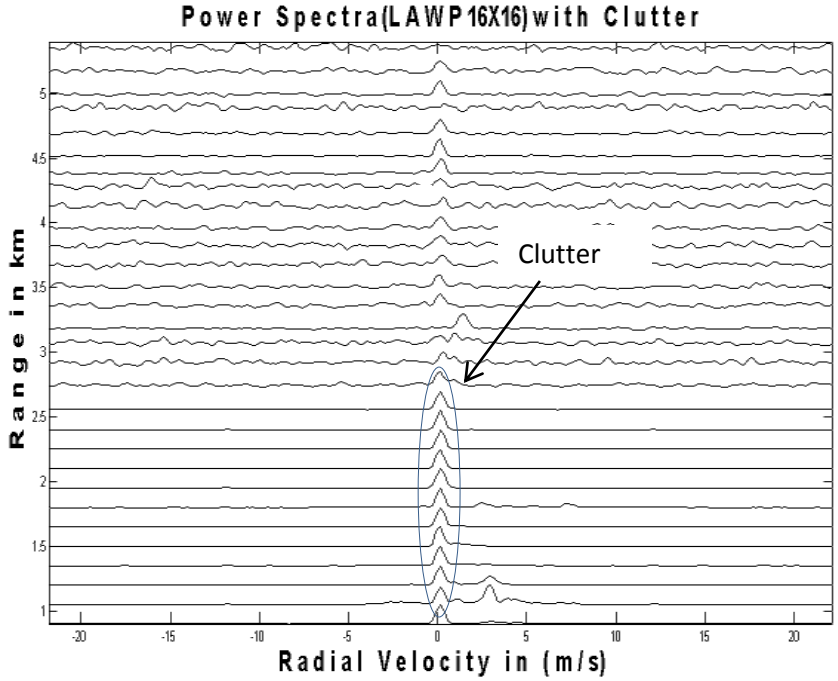

Fig. 5.4 (a) *Power spectra (LAWP beam Direction: Zenith) before clutter removal*

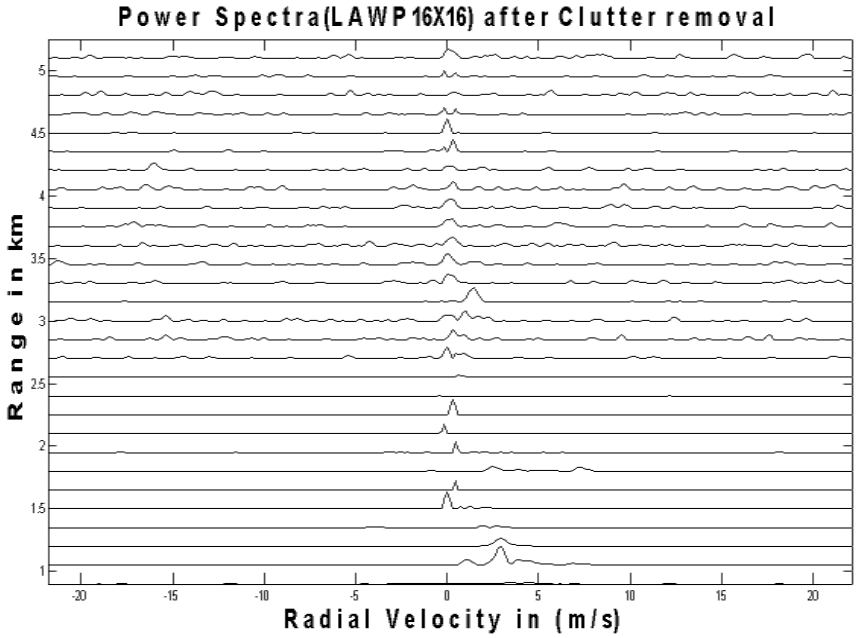

Fig. 5.4 (b) *Power spectra (LAWP beam Direction: Zenith) after clutter removal*

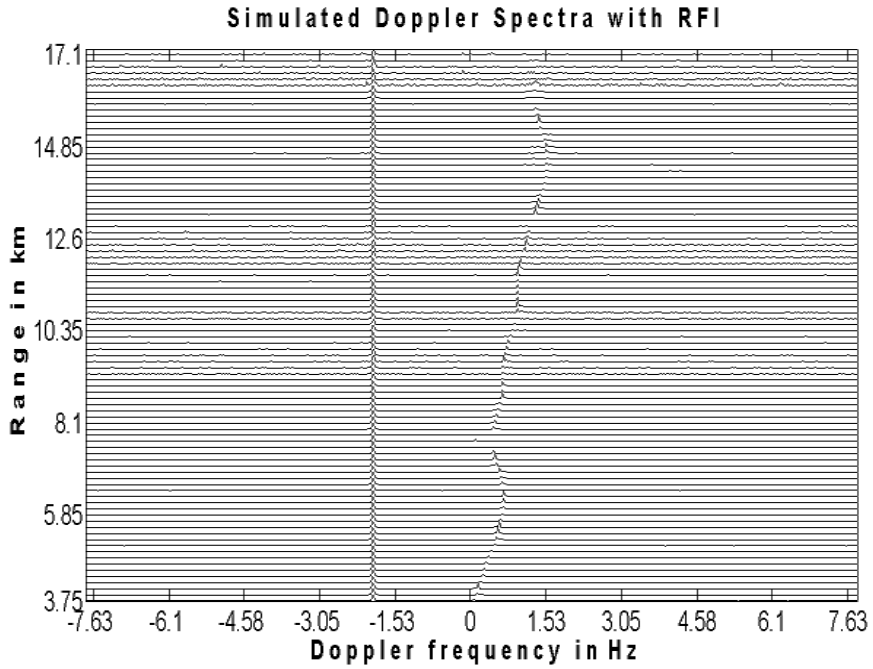

Fig. 5.5 (a) *Modeled Power spectra with RFI*

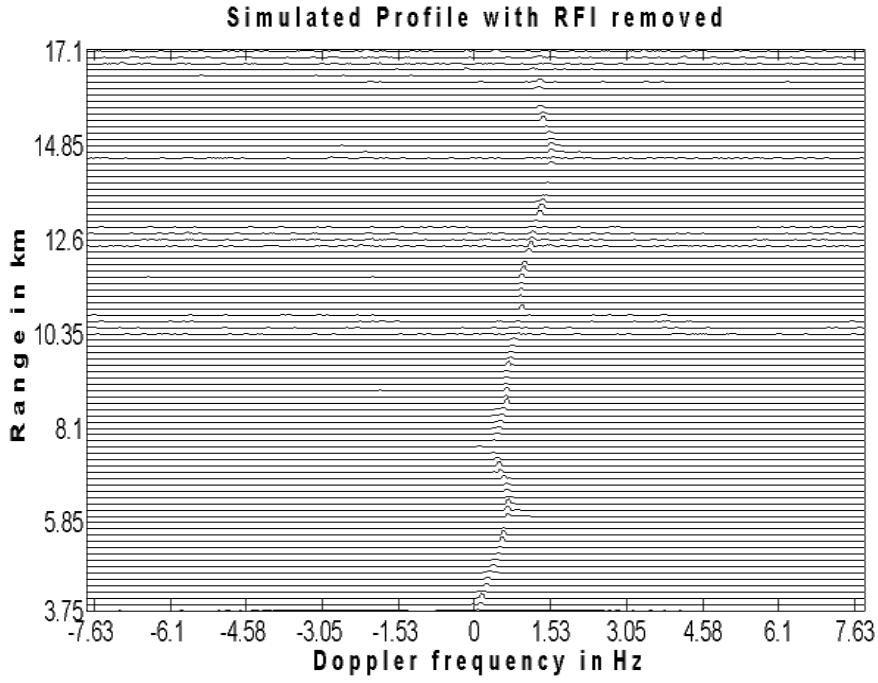

Fig. 5.5 (b) *Modeled Power spectra after RFI removal*

5.7 Summary

The need for pre-processing of Doppler power spectra and the procedure used are discussed in this chapter. Pre-processing mainly involves noise estimation and removal using Hildebrand algorithm, identification of clutter and RFI and its removal from the Doppler power spectra. The pre-processing method is applied to MST radar and LAWP radar and the results are presented. After preprocessing, the Doppler power spectra are subjected to the signal processing technique(s) for the extraction of the wind information. The wind profiling radars are often operated with more than 3 beams. Though the data received from additional beams are redundant, it facilitates improved feature extraction and data interpretation [79]. Averaging of the data from coplanar beams [80] and fuzzy logic [47] based techniques are some of the ways to improve the atmospheric feature extraction from the radars. Some of the leading methods of Doppler profile extraction and a new method developed during this research for wind profiling are presented in the next chapter 6.

Chapter 6

A Novel Multiparameter Cost Function Method for the Estimation of Doppler Profile

The main function of the wind profiler radar is to obtain *three dimensional (3-D)* wind velocity information. As discussed earlier, it is done by doing Doppler analysis of the backscattered echoes. The processing of the backscattered signal of one beam provides the *radial velocity (wind velocity component in the direction of the radar beam)* profile. From the information of three or more such beams the 3-D wind is computed using simple mathematical techniques. The information extraction from the Doppler power spectra of one beam is the important theme.

In this chapter, section 6.1 and 6.2 discuss the need for automated Doppler profiling and some of the leading methods of Doppler profile extraction respectively. Section 6.3 presents a newly developed novel method of profile tracing which was one of the main objectives of this thesis.

6.1 Tracing the Doppler Profile

It has seen that the Doppler power spectral data is *cleaned* by pre-processing. The pre-processing removes the noise and unwanted signals like Clutter and RFI. After this activity, all the stronger spectral components are expected to be from atmospheric targets. The strongest atmospheric target is assumed to give strongest spectral peak in the corresponding range bin. Doppler profile could be obtained by simply connecting the strongest. Fig. 6.1 shows a small section of the wind profiler data. There are multiple peaks and estimating the correct peak and including it in the Doppler profile is a skilled job. Conventionally, this job was done by a Human Expert. Modern radar metrology demands very frequent weather monitoring and WP radars generate a large amount of data for that purpose. There is a need of extracting wind information in *real time*. Therefore an automated profile extraction method is required. This research is directed towards the development of an *automated Doppler profile estimation algorithm*. A literature survey was done on the existing methods of Doppler profile estimation.

The following section presents some of the leading methods for the same.

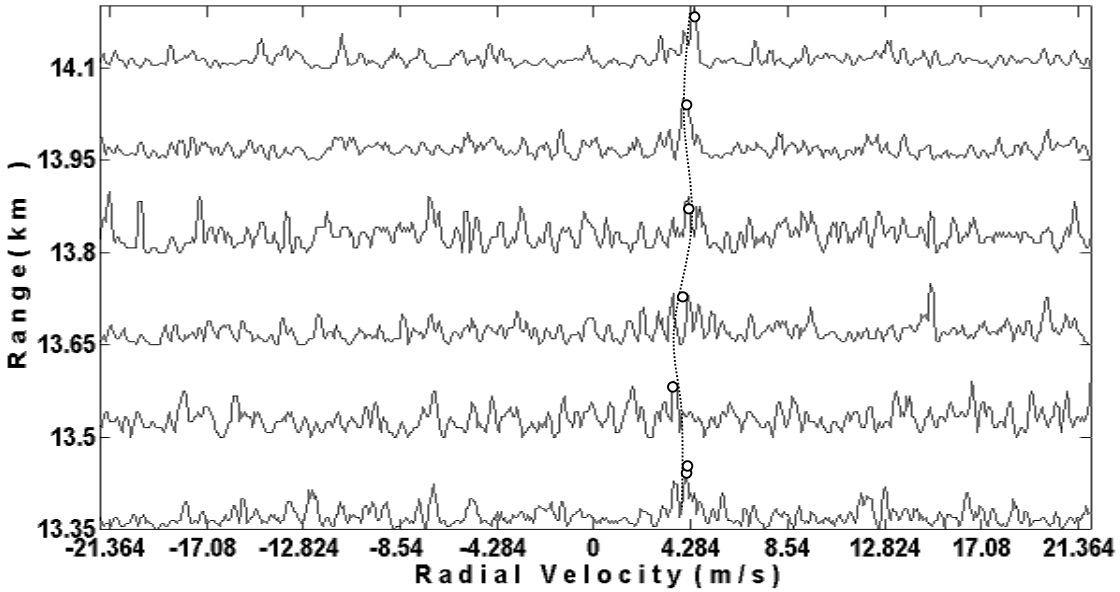

Fig. 6.1 *Tracing of a Doppler profile.*

6.2 Literature review of Doppler profile Estimation

In section 5.5, the mathematical formulae for the spectral moment computation are presented. Following facts are well-established in the previous chapter 5.

a) The zeroth moment is the summation of the amplitudes of the spectral components and is indicative of the *RF reflectivity* of the target.
b) The first moment gives the mean Doppler frequency. Therefore, it indicates the mean wind velocity.
c) The second central moment (variance) is a measure of the *Doppler spread* which automatically indicates the velocity spread and hence the wind turbulence.

This classical approach to Doppler profiling, which was formally introduced by Zrnić [5] is presented here and is followed as a basic method. The profile extraction is done by connecting the geometrical centers of the prominent Doppler components as shown in Fig. 6.1. This method performs reliably in case of a *Prominent Single Doppler Component*. However, this method fails in low SNR conditions or in the presence of strong non atmospheric spectral components. Due to this the profile tracing used to have discontinuities in the regions where

wind turbulence is more and hence Doppler could not be traced at larger heights. Subsequently many methods were developed to increase the range coverage and establish better height. Following approaches claimed consistent results and are in use till date by the researchers.

6.2.1 Adaptive moments estimation method

It is observed that in low SNR case, the estimation of Doppler component based on moments gives erratic results. This is because the first moment of the Doppler spectrum of adjacent range bins would vary by a large amount on either side! This problem was addressed by Anandan [41] by proposing *adaptive moment method*. This method proposed profile tracing from the lowest range bin where the SNR is high. High amplitude spectral components present in a pre-decided Doppler window of the subsequent range-bins are tagged as *prospective candidates.* One of the candidate peak is finalized as a member of the profile on the basis of SNR and wind shear criterion.

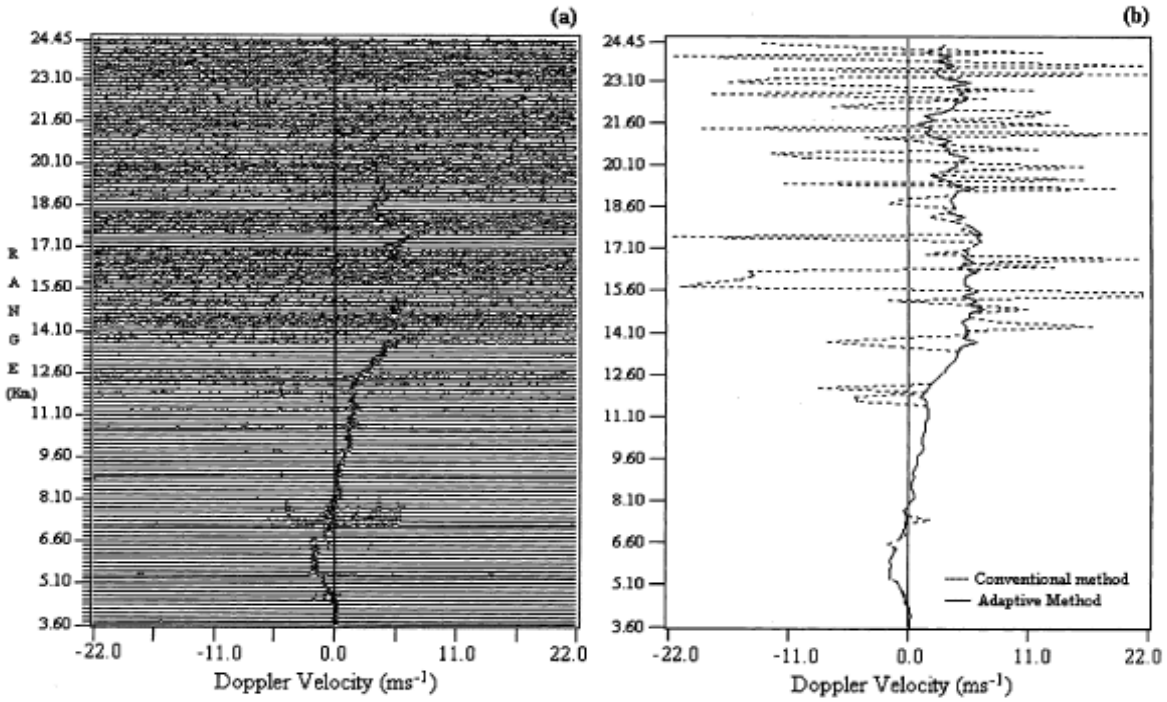

Fig.6.2 *Doppler power spectra of a Doppler profile of Indian MST radar (East beam tilt 10^0on 10-07-2002). It is seen that in Low SNR range bins the first moment profile (dotted line) shows erratic variations. Adaptive moment estimation takes a corrective action* ***Source [41].***

This method also suggests improvement in Doppler profile if the data from Symmetrical

beam is available. This method claims good results and is one of the leading methods of Doppler profiling currently in use. However, some of the parameters and decision processes are subjective and may require tuning depending on the radar data. As a result, the process needs to be customized for different radars and for different atmospheric conditions. This leads to the change of algorithm parameters. Thus factors like radar operating parameters and changing environmental conditions pose limitation for this method as a candidate as an ***automated algorithm.*** Fig. 6.2 [41] shows an illustration bringing out the strength of the ***adaptive moment estimation method.***

6.2.2 Profile Chain building

The concept of identifying prospective spectral components was also reported by Clothiaux [42] and has proposed *first guess feature based algorithm*. This method proposes connecting of the prospective candidates to form possible Doppler profile chains. The data from multiple Doppler power spectra of similar conditions is collected and subjected to *neural network learning* technique. Finally a continuous chain obtained by selecting most suitable branches is selected as the Doppler profile. Fig. 6.3 shows some data slides illustrating the method from reference [42]. The computation complexity of this method changes depending on the data type and number of possible profile chains. Hence the extent of computation becomes unpredictable. Also the method requires a large training data that is similar to the Doppler spectra under consideration.

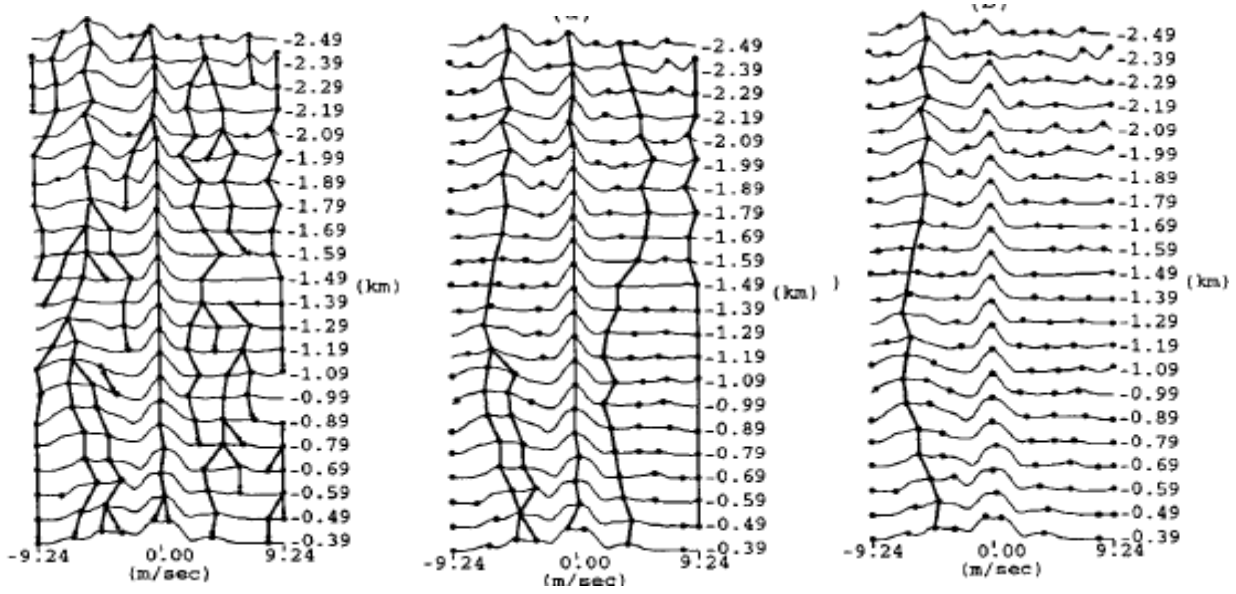

(a) *(b)* *(c)*

Fig.6.3 *Demonstration of 'first guess feature based algorithm' (a) identification of all the chains. (b) Removal of incomplete chains to have candidates for complete profiles (c) Selecting final profile based on the neural network technique* ***(Source [42])***

6.2.3 Fuzzy Logic based Doppler Profile Estimation

In the recent years Fuzzy logic (FL) methods have been used by many researchers and have claimed very accurate results. Fuzzy logic approach considers every spectral point in the data set of Doppler profile spectra. These points are evaluated for various features like spectral variances, feature slopes and curvature, asymmetry etc. A fuzzy logic approach examines some of these features and then concludes whether the spectral component is a *member of that particular feature* or not. As an example, a spectral component could be examined *whether it is a weather echo component or a clutter component or a RFI component.* The procedure for this is as follows:

A membership function is defined for each of these features and a value, usually between 0 and 1, is assigned for each feature. This assignment is done by defining a *membership function* having the range 0 to 1 (e.g. Gaussian function). These assigned values are combined to get a *membership value.* There are two approaches of getting the membership value.

First approach computes a weighted sum of these values. This value is subjected to a threshold to decide whether the component is included in the class under consideration [43][44]. The national Centre for Atmospheric Research (NCAR) uses this concept. The method 'NCAR Improved Moments Algorithm (NIMA) additionally uses other spectral cleaning techniques.

The other approach combines the membership function values and then subject it to another function (also called classification function or *soft thresholding function*) for the decision of whether the spectral point is included in the class under consideration [44][45][47]. The fuzzy logic methods are capable of classifying the spectral component into different classes like weather echoes, clutter RFI and so on. Due to this capability, it is possible to identify the components of different features simultaneously on the same Doppler power spectra. Fig. 6.4 shows an illustration indicating spectral components due to different features. However, for the optimal performance tuning of *confidence value threshold* is generally required. Also the parameters and the functions used in Fuzzy logic approaches are dependent on the nature of the signal, radar site and parameters etc. Allabaksh [47] has used the same method suggested by Bianco [45] and has reported that the change of parameters and membership function was necessary to obtain good results. As a result the method could not be treated as objective.

It is seen that the leading methods give very consistent performance of Doppler profile

extraction. However, they are computationally complex and require changes in the processing parameters or strategy depending on data type, radar site and operating parameters. Therefore these methods could not be considered as objective methods. It cannot be used for automated Doppler profiling.

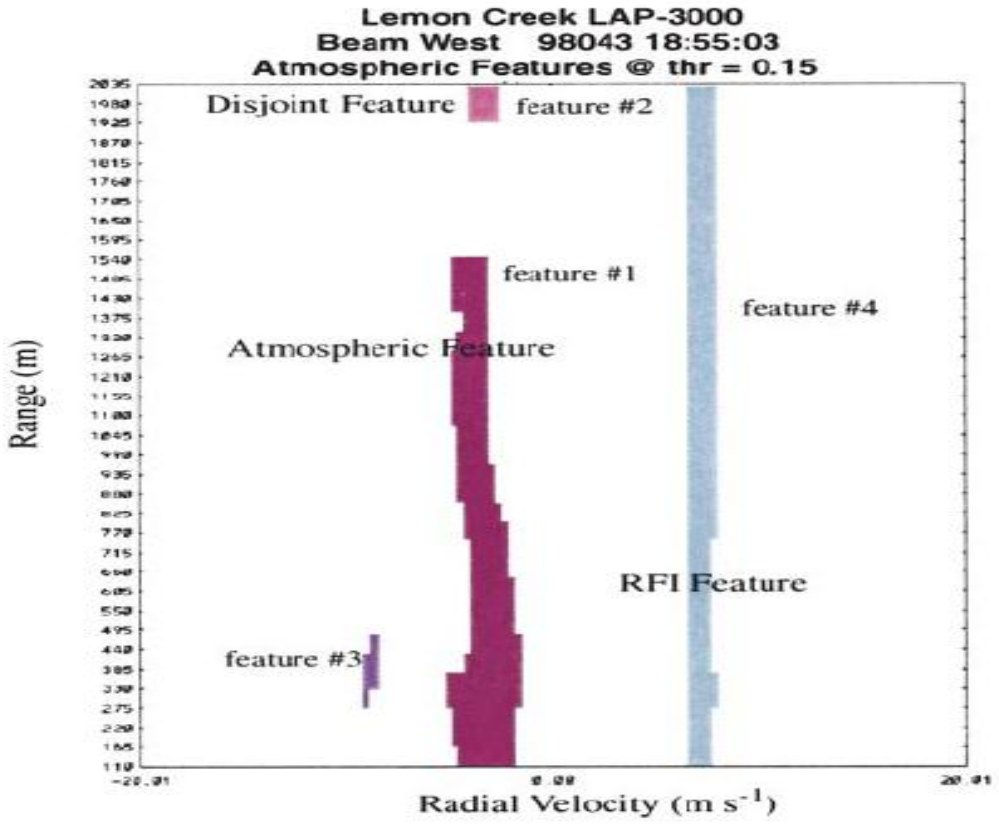

Fig.6.4 *Classification of spectral components based on 'first guess feature method* using Fuzzy logic *The diagram shows components due to weather echoes, RFI, and disturbances due to small isolated objects* ***(Source [43])***

6.3 Newly developed Multi Parameter Cost Function (MPCF) Method

As mentioned in earlier sections, the estimation of wind parameters is difficult due to bad SNR and the presence of echoes from non-atmospheric targets. The objective was to develop the algorithm that works in low SNR conditions; has moderate computational complexity and has consistent performance in most atmospheric conditions. It was realized that the new method should consider features like continuity, limited wind shear etc. A nonlinear function was designed to consider multiple factors and a new method was developed for the said purpose. This *multi-parameter cost* is the key innovation in the proposed method. This section presents

step-by-step procedure of the newly developed algorithm.

Step 1: Removal of unwanted components

The power spectrum is a standard *product* of the radar signal processing system that serves as an input for the Doppler profile tracing. Pre-processing actions are as discussed in chapter 4, namely noise power level estimation by 'Hildebrand Algorithm' [24], three point moving average for smoothing followed by clutter and RFI removal.

Step 2: Identifying *prospective spectral peaks* and formation of Possible Doppler Traces:

Identifying spectral peaks of atmospheric targets is the most critical task of this algorithm. The complete set of Doppler spectra is divided into groups of five range bins each. This method performs the task of profile tracing in individual groups starting from the lowest range group and proceeding sequentially to the next high range group. The method uses the concept of selecting five prospective peaks as proposed by Anandan [41]. After identification of the prospective peaks in all five range-bins, all possible Doppler profile traces are constructed as used by Clothiaux [42]. The proposed method uses the established concepts of selecting spectral components as prospective candidates and forming various possible traces. The main difference in the approach is limiting the length of the traces to five in single step. This number is arrived after multiple experiments on different types of data. The main advantage of this restriction is in having limited and predictable computational complexity. The procedure is as follows:

(i) Make groups of 5 range-bins starting from the lowest. In spectrum of each range-bin, identify five highest magnitude peaks that satisfy the SNR threshold. These peaks may be called *prospective peaks.*

(ii) Start from the lower group of range-bins. List all possible traces using these *prospective peaks*. Fig. 6.5 shows a group of 6 range-bins of East beam Doppler profile (18:12:0, 26/7/2007), where prospective peaks are identified and many Doppler traces can be constructed. In this example, the group consists of 5 range-bins starting from 13.5 km is shown. The highest range-bin of the lower group (at 13.35 km) is considered in trace building.

(iii) Identify all the possible traces where the condition of Doppler window is satisfied. This means that the prospective peak to be included in possible trace must be within the Doppler window. In Fig. 6.5 the path shown by the dotted line may not satisfy the Doppler window criterion. Therefore, it will be omitted from further processing.

The detailed explanation is given below:

There are maximum of five prospective peaks in each range bin and the links could be formed between any two peaks. These components are indicated as $f_{m,n}$, meaning m^{th} peak of n^{th} range-bin and $f_{p,n-1}$ meaning p^{th} peak of $n\text{-}1^{th}$ range-bin. The generalized expression of Doppler shear will be '$f_{m,n} - f_{p,n-1}$'; where the subscripts 'm' and 'p' are different numbers taking the value between 1 to 5.

For a case when a link between 3rd peak of 2nd range-bin and 1st peak of 3rd range-bin is considered, the values of *m*, *p* and *n* are 3, 1, 3 respectively. Similarly, the *differential shear* term in equation 6.2 is written as '$f_{m,n} - 2f_{p,n-1} + f_{q,n-2}$;' where *m*, *p*, and *q* are integers with values 1 to 5. The Doppler window criterion is applied to $f_{m,n-1}$, and $f_{p,n}$ and is given in equation 6.1. With this condition, the number of possible traces reduces to a couple of hundreds. This algorithm sets the limit to ± 4.4 ms^{-1} for the range bin size of 150m. The limit is sufficiently high to include all realistic wind shear values. This limit is changed proportional to the size of the range bin. This means that the radar operating for range resolution of 300 m will have wind shear value limit of ± 8.8 ms^{-1}, as shown in equation 6.1

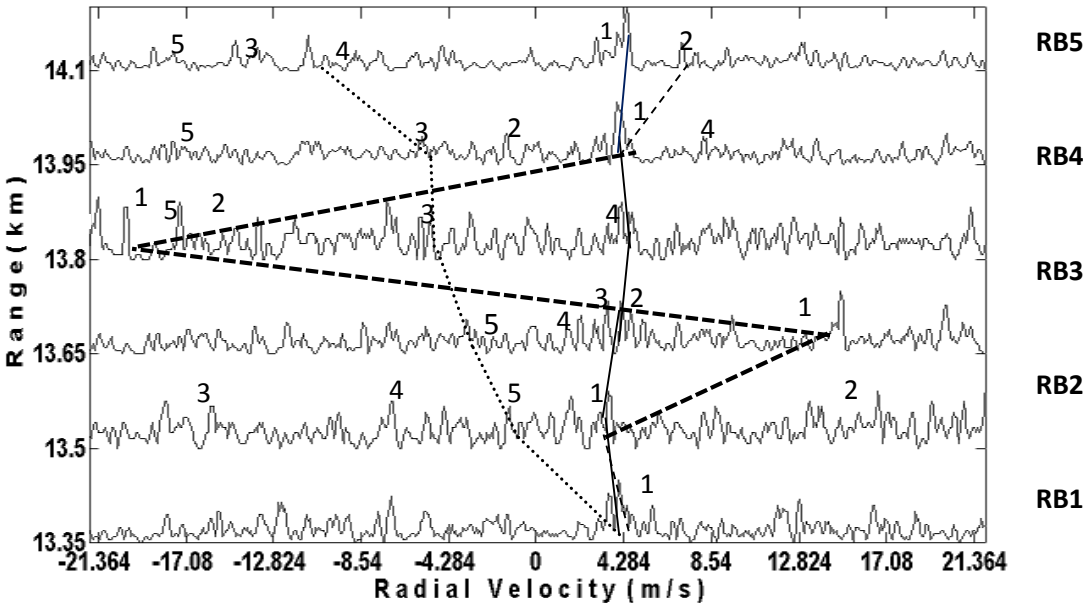

Fig.6.5 *Selections of 'Prospective Components' and profile tracing (Section of East beam 10^0)*

In case of the lowest range-bin group, there is no starting point and no Doppler frequency peak to initiate the traces. We assume a *proxy value* of '0 ms^{-1}' to initiate the traces. It may be

noted that it is not a realistic wind velocity. As a result, the shear criterion cannot be applied to this first link.

$$\left| f_{m,n} - f_{p,n-1} \right| \leq ((4.4 \div 0.15) \times RR) ms^{-1} \quad (6.1)$$

Where, RR is the range resolution in km.

Step 3: Assigning *cost* to the traces

After identifying all possible traces, a *cost* is assigned to each link. The cost function is designed with the objective to figure out whether the link is part of Doppler profile. We have shown three traces indicated by a solid line, dashed line and a dotted line in Fig. 6.5. These are some of the indicative traces. Link 2, 3 and 4 in the trace, indicated by the dashed line, does not satisfy the *Doppler window* criterion. This trace will not be included in further processing. The solid line traces show less wind shear for all the links. An experienced operator will choose this trace as a Doppler profile. On the other hand, the dashed trace having links with more wind shear is less likely to be selected as Doppler profile. The cost function is a mathematical formulation of this *human perception*. The activity of profile tracing prefers two qualities, - '*consistent high power components*' and '*low change in wind shear'.* The proposed mathematical model considers these features and calculates the cost functions consisting weighted sum of two terms. First term is a function of Relative Spectral Power (*RSP*) and the second term is a function of change in the wind shear (*x*). Relative spectral power is the ratio of the peak spectral power to *average noise power density* (indicated by Sn). The change in wind shear is defined with respect to the spectral components, $f_{q,n-2}$, $f_{p,n-1}$ and $f_{m,n}$ of 3 consecutive range-bins. The expression in the modulus sign of equation 6.2 gives differential wind shear. The complete cost function is given in equation 6.3. The first term in equation 6.3 deals with Relative Spectral Power and the second term represent the probability of occurrence of the differential wind shear. This probability is found by experimental data collection. The power spectral data of 5 cycles at different times was collected. Each cycle consists of 4 beams tilted by 10 degrees East, West, North and South. Each beam was operated with the parameter settings given in table 1. Approximately 2600 differential wind shear values were obtained for 130 range bins in this exercise. The cost assigned to differential wind shear should be matching to the envelope function. As seen from the Fig. 6.6, Rayleigh distribution function with 'σ =1' between abscissa 1 and 4 matches the best.

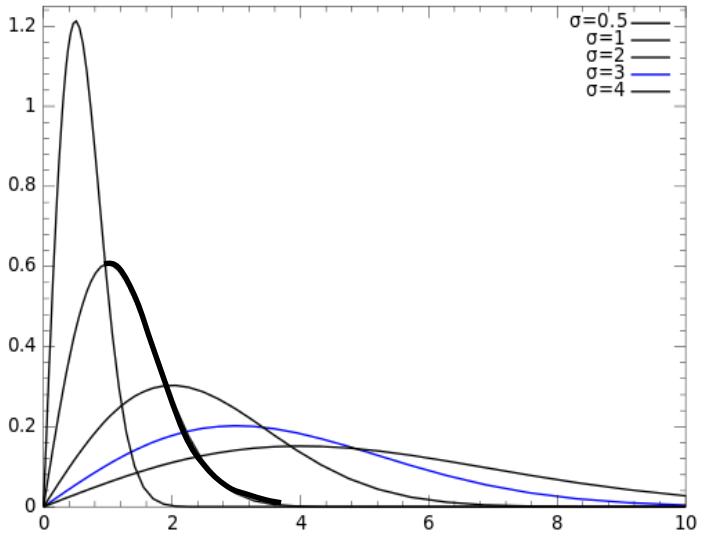

Fig.6.6 *Selected part of Rayleigh function as 'cost' for change in wind shear*

This matching is achieved by mapping the *3 unit spread* of Rayleigh function with the maximum *Differential shear* value. Fig. 6.7 shows that the maximum shear value is 2.2 ms^{-1} for the radar operation when the range resolution was 0.15 km. Therefore at arbitrary range resolution *RR* the maximum shear value will be given by RR × 2.2 ÷ 0.15. Thus the Differential Doppler wind shear value is normalized to (RR × 2.2 ÷ 0.15) and is matched to the desired section of Rayleigh distribution function by multiplying 3 as shown in Equation 6.2. Graph shown in Fig. 6.7 presents *frequency of occurrence*. Equation 6.3 incorporates the parameter '*x*' with appropriate shift in the expression of Rayleigh distribution function.

The term '$\left| f_{m,n} - 2f_{p,n-1} + f_{q,n-2} \right|$' in equation 6.2 is the magnitude of *differential wind shear* (*y*), where *m*, *p*, and *q* are integers corresponding to the peak numbers with values ranging from 1 to 5. The weights 0.4 and 0.6 were found out after rigorous experimentation wherein we carried out Doppler profile tracing exercise on approximately 2000 Power spectral data sets.

$$x = 3 \times \left| f_{m,n} - 2f_{p,n-1} + f_{q,n-2} \right| / ((2.2 \div 0.15) \times RR)\, ms^{-1} \tag{6.2}$$

where, '***x***' is the normalized and scaled deviation from constant wind shear.

$$C = (0.4 \times RSP) + 0.6 \times (x+1) \times e^{(-(x+1)^2/2)} \tag{6.3}$$

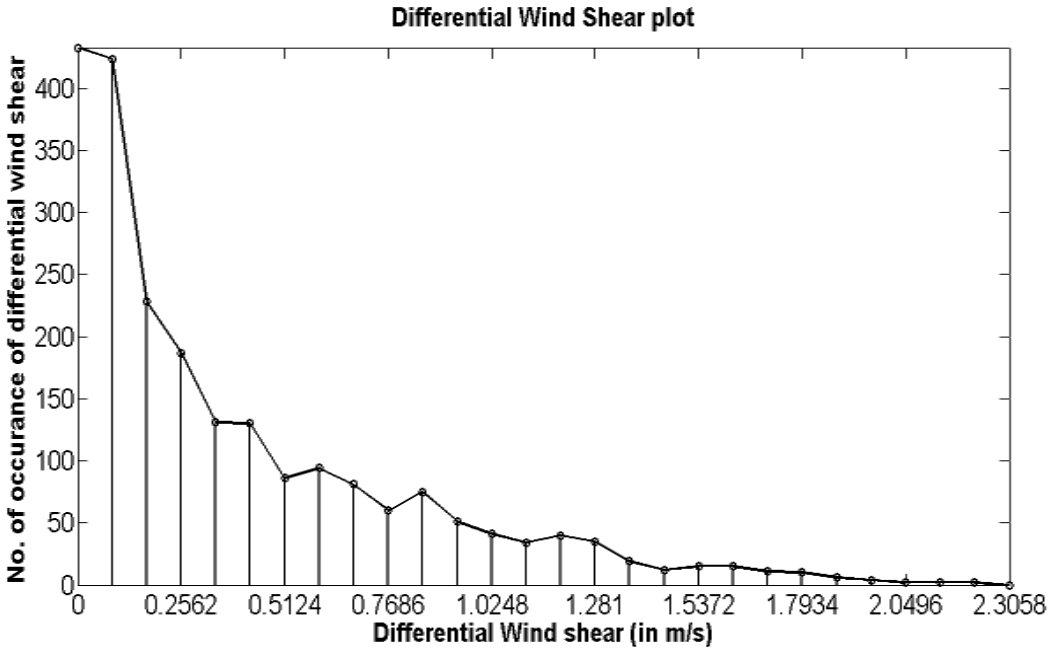

Fig.6.7 *Occurrence profile of the absolute value of differential wind shear*

Each link has 'RSP' values (corresponding to spectral component f_n) and the differential wind shear values (illustrated in Fig.6.8). Each trace has 5 links connecting the peaks in the range bins n and n-1 (n = 1 to 6). Cost is calculated for each link using Equation 6.3. The sum of the cost of all 5 links is the total cost associated with the trace. The trace with the maximum cost is finalized as Doppler trace for that group.

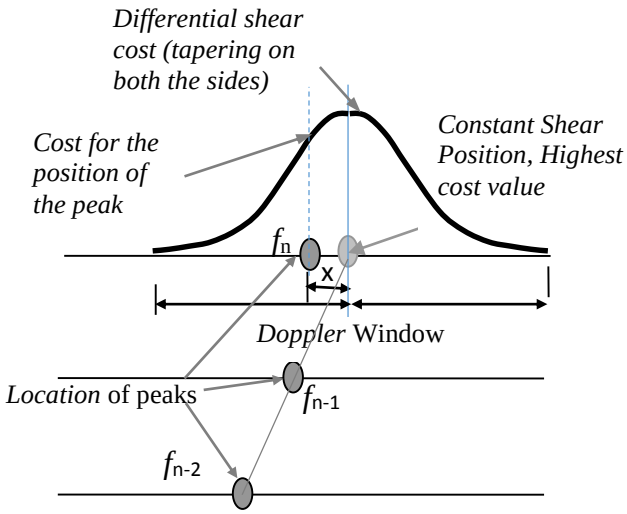

Fig 6.8 *Assigning cost to differential wind shear*

Step4: Sequential Formation of Connected Traces

Trace in the lowest Range-bin group is finalized by following step 1 to 3. The processing of the next higher range-bin group starts with step 1 of identifying the peaks. In step 2, the formation of traces starts with the *highest point* of the trace of the 'lower range-bin group'. This condition ensures the connectivity of the traces. Complete Doppler Profile is automatically obtained after completion of the highest 'Range-bin profile.

The profile could be traced to best possible heights with SNR threshold of 5 dB and Doppler window of ±20 % of the Doppler Bandwidth. It is occasionally possible to encounter a few range-bins that do not have a single 'prospective peak' satisfying SNR threshold. In such cases, the threshold is lowered to 0 dB and the range-bin is marked as 'suspect'. Power spectra of these range-bins are shown by lighter shade. The process of Doppler profile extraction terminates if all 5 range-bins of a group are marked as *suspect.* Fig. 6.9 shows the Doppler profile estimated by this method. It can be seen that the performance can be traced to low SNR ranges and it is comparable to the tracing by human expert. This method is also applied to the Lower Atmospheric Wind Profiler (LAWP) data without changing any of the weights. This radar has the antenna array of 16×16 elements and is operated at NARL. The same method is applied to another operational LAWP with antenna array of 8x8 elements.

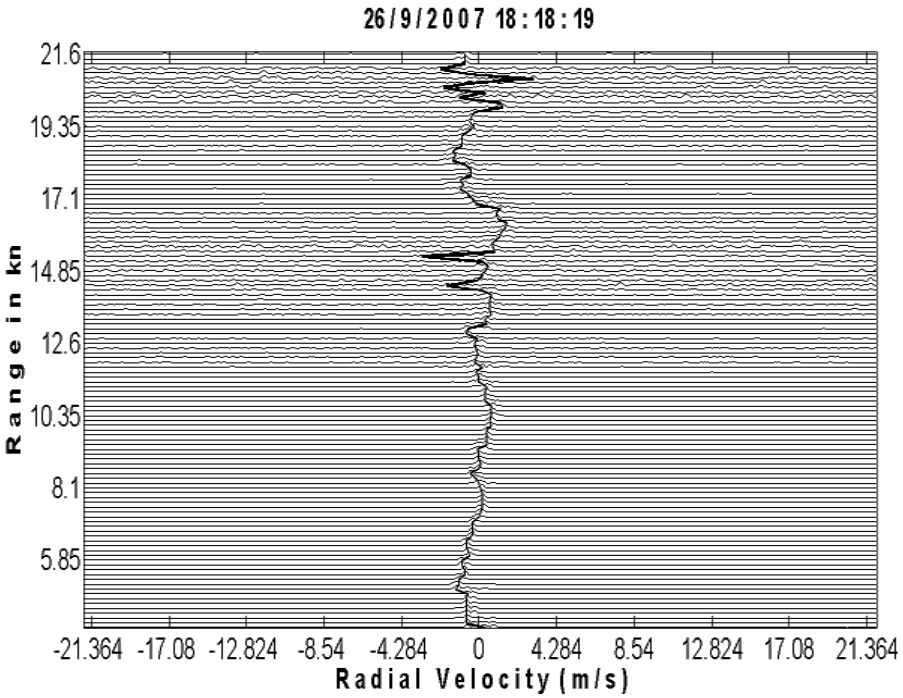

Fig.6.9 *Doppler profiling using Multi-parameter cost function method (Beam Direction: North 10^0)*

The results of LAWP 8x8 and LAWP 16×16 are shown in Fig. 6.10(a) and 6.10(b) respectively. The MPCF method also traces Doppler profile even in presence of strong precipitation echoes. A representative example is given in Fig.6.11 (a) and (b) respectively.

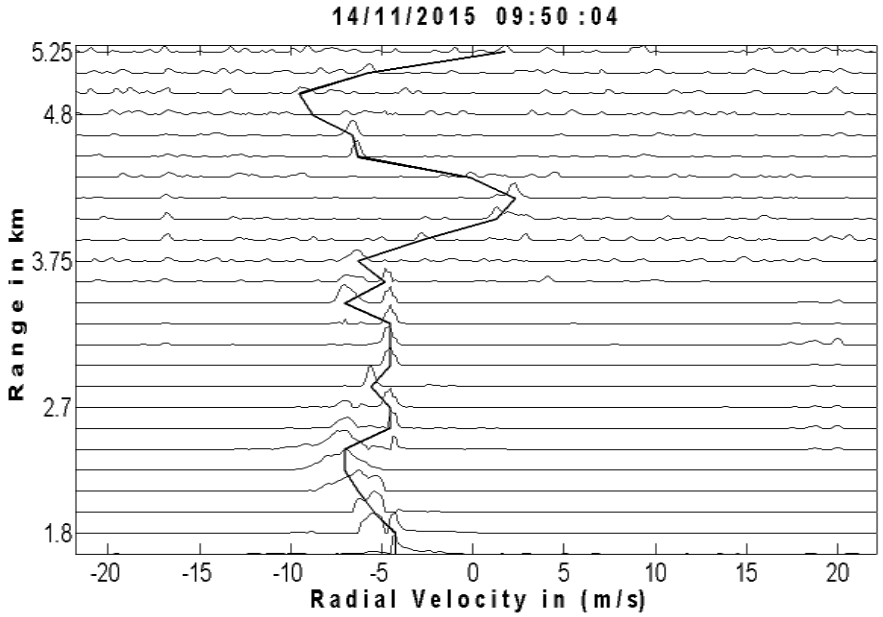

Fig. 6.10(a) *Doppler profile estimated using Multi-parameter cost function method for LAWP (8X8) (Beam Direction:14.2^0 down at North East)*

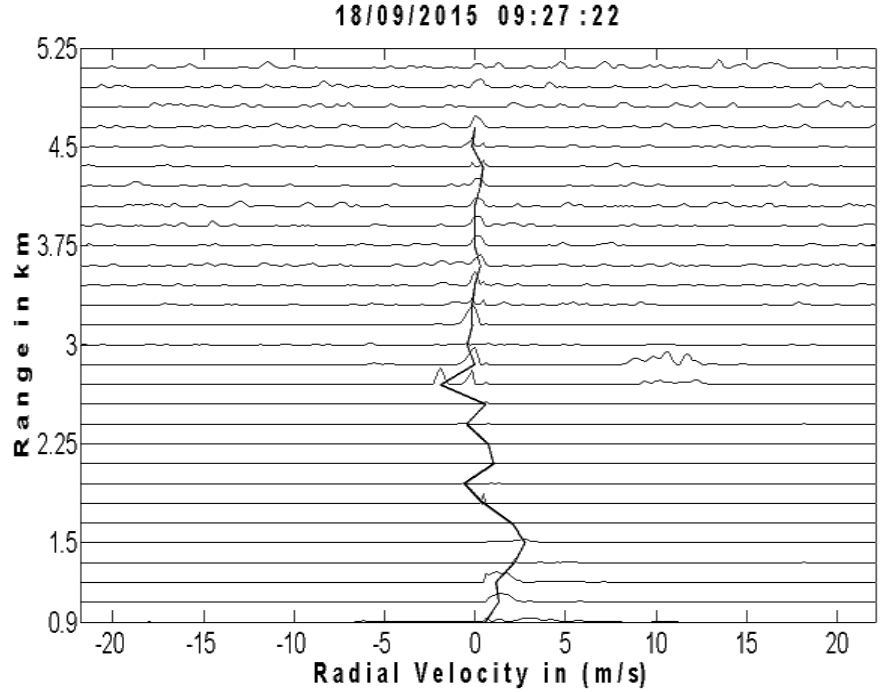

Fig. 6.10 (b) Doppler profile estimated using Multi-parameter cost function method for LAWP (16X16) (Beam Direction: Zenith)

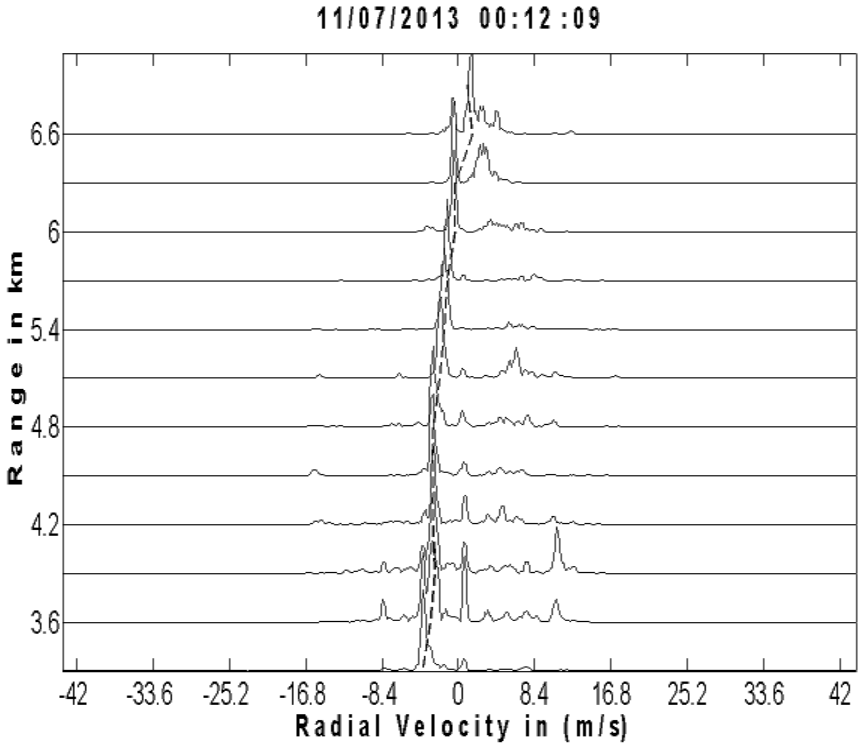

Fig.6.11(a) *Doppler Profile Estimation using the Multi-parameter cost function for precipitation data; Doppler profile shown in dotted line(Indian MSI radar data Beam Direction: South 10^0)*

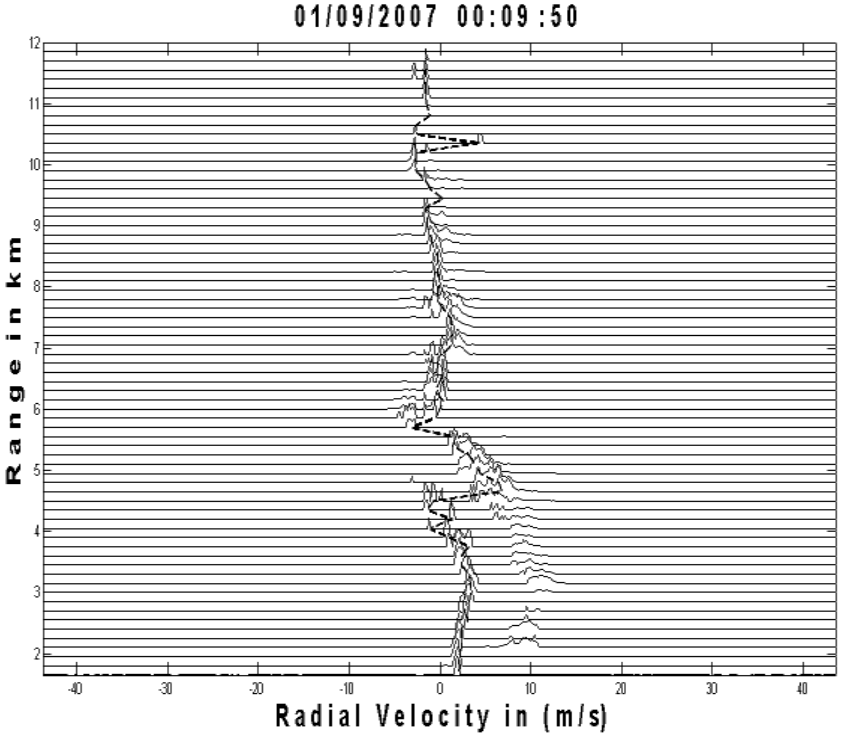

Fig.6.11 (b) *Doppler Profile Estimation using the Multi-parameter cost function for precipitation data; Doppler profile shown in dotted line (Indian MSI radar data Beam Direction: North 10^0)*

6.3.1 Profile improvement using symmetrical beam

Most of the radars operate in more than 3 beams. The main purpose of having additional beams is getting redundant reading which can be used for having more accurate estimate. It is known that the Doppler profile of symmetrical beam (East-West or North-South) is symmetrical around *Zero Doppler velocity*. This is because approaching wind observed by the east beam would appear receding beam in the west beam. Therefore symmetrical (with opposite sign) Doppler frequency components would be observed. Taking advantage of this fact, the tracing accuracy could be improved if the data of symmetrical beam is available. The MST radar at Gadanki has two zenith beams with orthogonal polarization. The Doppler Profile from these two beams (Z_x and Z_y) are expected to be identical. For practical purposes, the agreement between the data is defined as the Doppler frequency of the same range-bin is within 2 % of the Doppler Bandwidth. The accuracy of the Doppler profile could be improved by following strategy. The data is checked

(i) Case 1, The Doppler frequency in both the beams is '*in agreement*': Average Doppler frequency is assigned to that range bin.

(ii) Case 2, The Doppler frequencies are not in agreement: The same cost function is used to evaluate the corresponding part of the traces. The trace having higher *cost* is selected as the Doppler profile data. The Doppler profile improved using the Image beam Power spectral data is given in Fig. 6.12. It is seen that the abrupt deviations in the profile could be eliminated

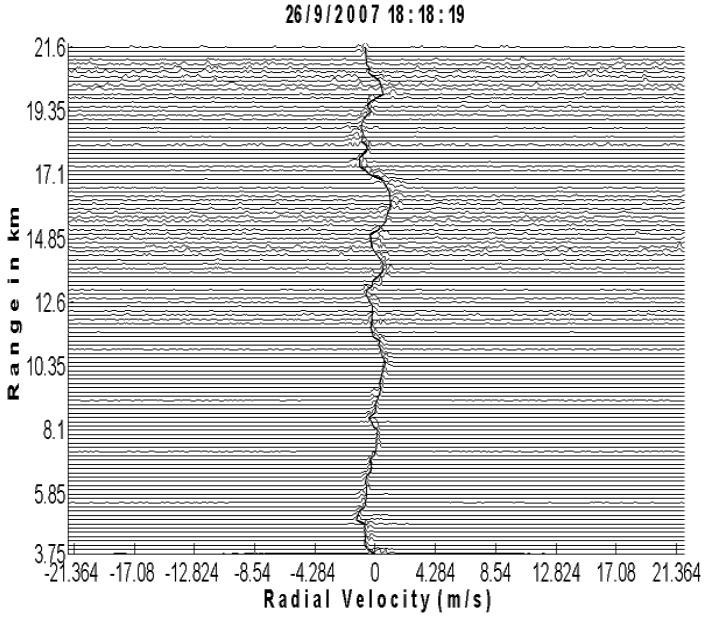

Fig.6.12 *Enhanced Doppler Profile Estimation using the Multi-parameter cost function (MPCF) with image beam data (Indian MST radar data, Beam Direction: North 10^0)*

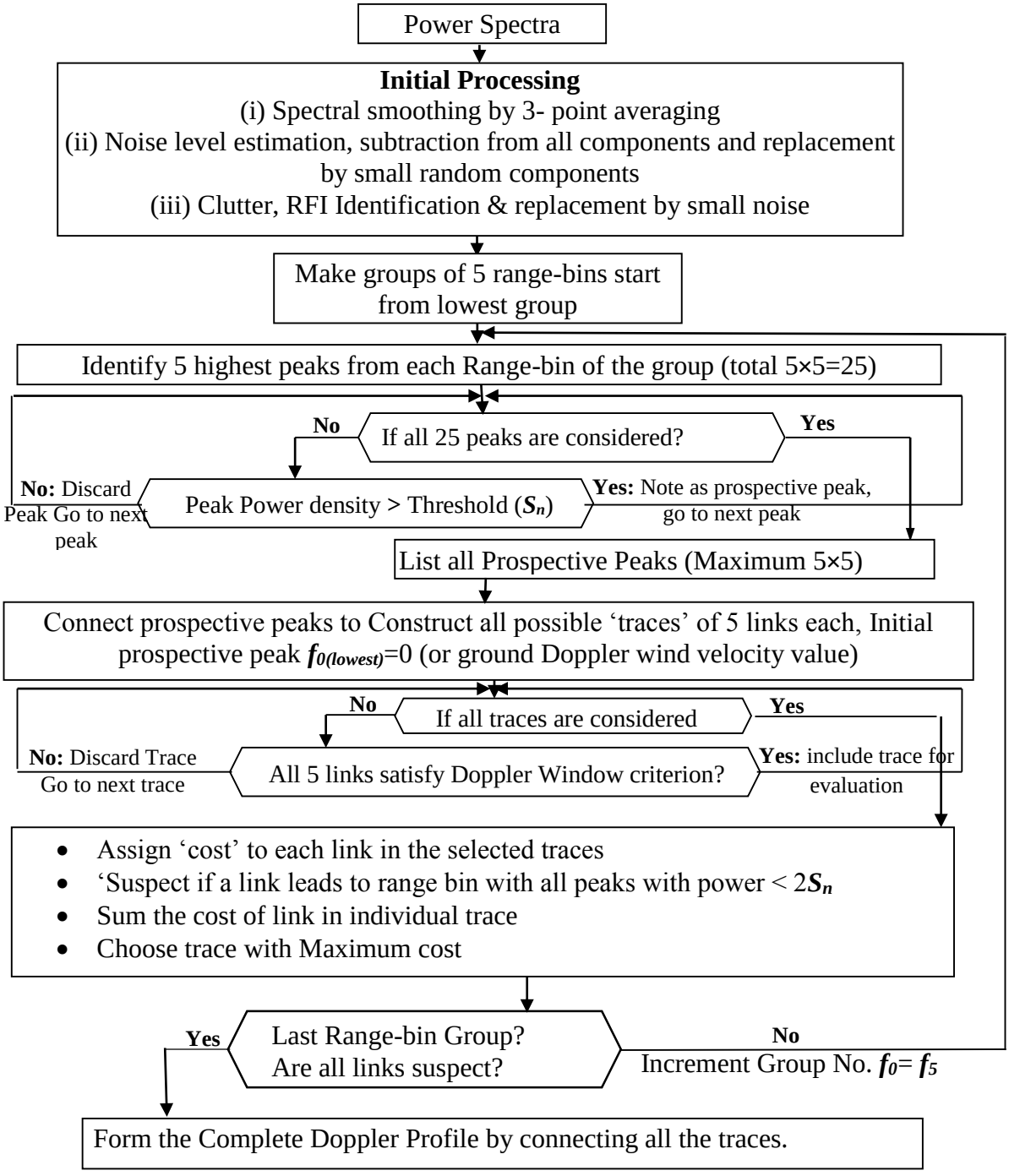

Fig.6.13 *Flow Chart of Doppler Profile estimation by "multi-parameter cost Function Method"*

It can be seen that the Doppler profile tracing using *Multi-Parameter Cost function* followed by corrections from the data of symmetrical beam gives performance comparable to that of human expert analysis. The complete flow chart for MPCF is shown in Fig. 6.13.

6.3.2 Performance comparison of Doppler Profile Estimation Methods

Performance of Doppler Profile estimation of the newly developed algorithm is compared with the established methods discussed in section 2 in this chapter. In order to compare the performance the Matlab program for the *adaptive moment estimation* [41] and *Fuzzy logic method* (proposed by Bianco [45]) were written. Fig 6.14 and Fig. 6.15 show the Doppler profile estimated by *adaptive moment estimation method* and *fuzzy logic method* respectively. These illustrations are representative examples. The same experiment was tried on about 30 data sets and the observations were similar

When Fig 6.12 is compared with Fig. 6.14 and Fig.6.15; it is seen from the above illustrations that the moment estimation method using multi-parameter cost function estimates the Doppler profile with accuracy comparable (if not better) to the established methods. Main advantage of this method is that it does not require tuning the parameters according to the environment, radar or human perception. Hence this post processing method has a potential of operating without the need of a human expert for analysis and tracing in real time.

6.3.3 Comparison of Computational Complexity

Gross estimation of computational load for these methods is as follows:

Considering set of Doppler power spectra of **N** range-bins and **M** Doppler components per range-bin; the estimate on the required computations is as follows:

The multi-parameter cost function requires **5N** sort operations, **50N** exponential function computations and 20 N additions and 20 N multiplications!

The adaptive moments method requires. M×N multiplications and 5K×N sort functions. Where, **K** is the number of iterations while deciding whether the candidate peak is the member of the estimated Doppler profile. The value of **K** is generally limited to below 50.

Fuzzy logic methods require 5×M× N exponential function computations, M× N Multiply and accumulate ***operations***.

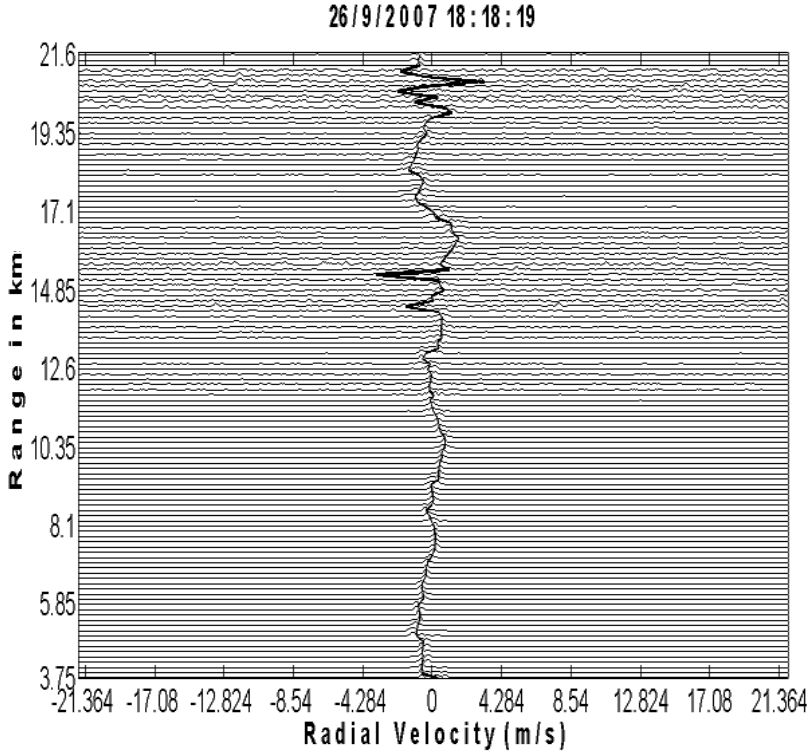

Fig.6.14 *Doppler Profile estimation by Adaptive Moments Estimation (Beam Direction: North10^0).*

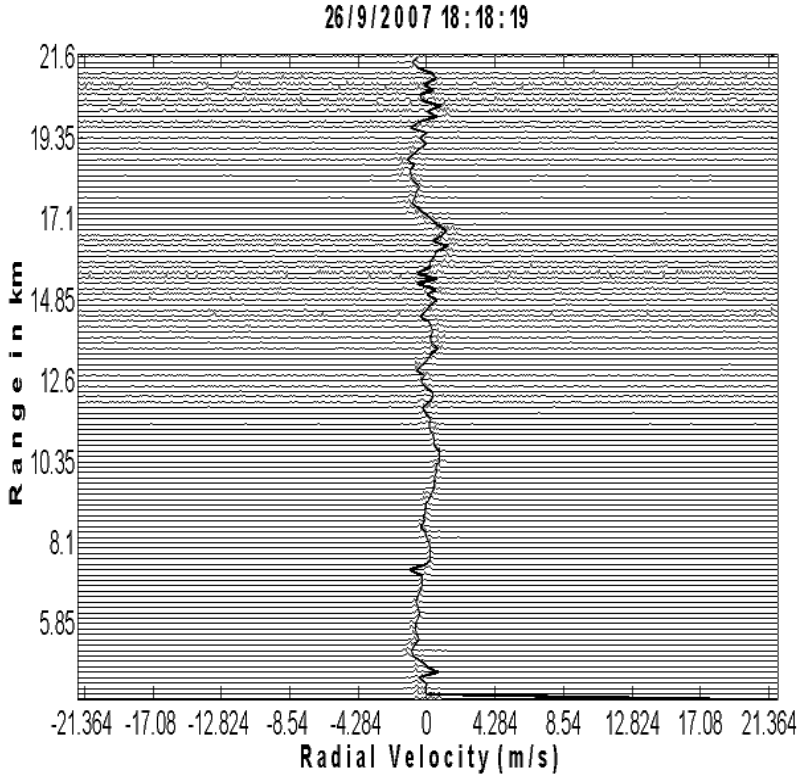

Fig.6.15 *Doppler Profile estimation by Fuzzy Logic method (Bianco approach) (Beam Direction: North10^0).*

Prima facie, it is seen that the *cost function method* requires less computations. Another experiment was conducted to arrive at relative computational complexity. The three programs were run on the same data set. These programs were run using Matlab (7.11) on a personal computer with clock speed of 1.6 GHz. The cost function method required 5.6 seconds; whereas the AME and FL methods clocked 8.8 seconds and 9.6 seconds, respectively. On this basis it could be concluded that the new 'cost function method' is expected to perform Doppler profile estimation in approximately 63% of time compared to AME and 58% of time compared with FL method. The same procedure was followed to get the scatter plots. The resulted scattering coefficients from the experiments are given in table 6.1. The results of AME and FL methods were obtained using programs written by the authors. Original programs with optimized parameters may give different results.

6.3.4 Experimental results: Verification of Doppler profiling with concurrent Radiosonde flight data

Estimation of wind velocity is also done by sending sensor electronics and Global Positioning System receiver along with a balloon. The balloon data is received by the ground based receiver and the wind velocities are estimated. This system is known as *GPS sonde*. This is an independent wind velocity estimation system. The MST Radar was operated simultaneously with GPS sonde flights. The GPS sonde flight offers the wind speed (WS) and wind direction data (WD) at every second. This reflects to a height resolution of 5 to 10 meters. This high range-resolution data was grouped and averaged in the sets corresponding to the radar range-resolution, 150 m in this case. From these WS and WD values of Zonal (U) and Meridional (V) wind speed corresponding to the radar ranges were computed. Fig. 6.16 (a) and (b) show the U and V wind profiles of MST radar using Cost Function method and from GPS sonde data respectively. The profile shows very good agreement. A series of experiments were conducted to compare the wind estimations using MST radar and GPS sonde. The scatter plots of the comparison for Zonal and Meridional winds are shown in Fig.6.17 (a) and (b) respectively. Similar experiment was conducted to validate the MPCF algorithm on the LAWP radar using GPS sonde. Fig. 6.18 (a) and (b) show the U and V wind profiles of LAWP (16×16) radar using Cost Function method and from GPS sonde data respectively and Fig. 6.19 (a) and (b) show the scatter plots of the comparison for Zonal and Meridional winds of LAWP (16×16)

radar. The GPS sonde flights were conducted on 10th, 11th, 14th and 15th of December 2015. The scatter plots were generated by combining the data of all the four flights. The correlation coefficient (R) for the zonal wind is 0.9250 and meridional wind is 0.9132 for wind profiler. For LAWP, the zonal wind is 0.9723and meridional wind is 0.9005. This proves that the wind velocity estimation by MPCF method shows excellent match with the GPS sonde data. The same data was compared with the wind estimations by other methods. Table 6.1 shows the correlation coefficient for various experiments. It is seen that the MPCF gives the best match.

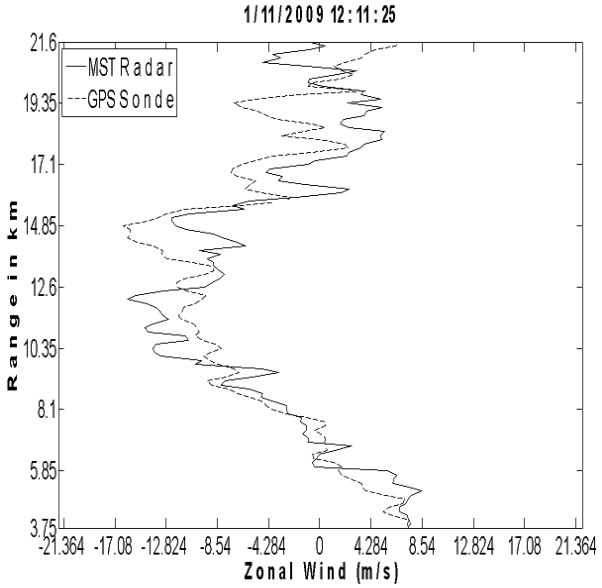

Fig.6.16 (a) *Zonal wind velocity comparison using GPS sonde and MST radar observations*

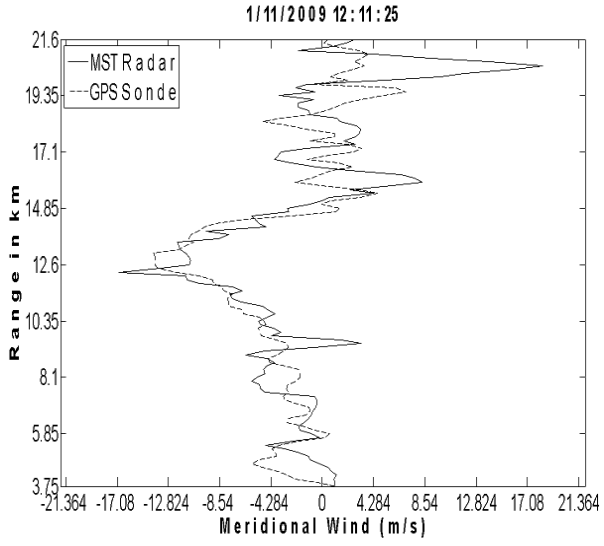

Fig.6.16 (b) *Meridional wind velocity comparison using GPS Sonde and MST radar observations*

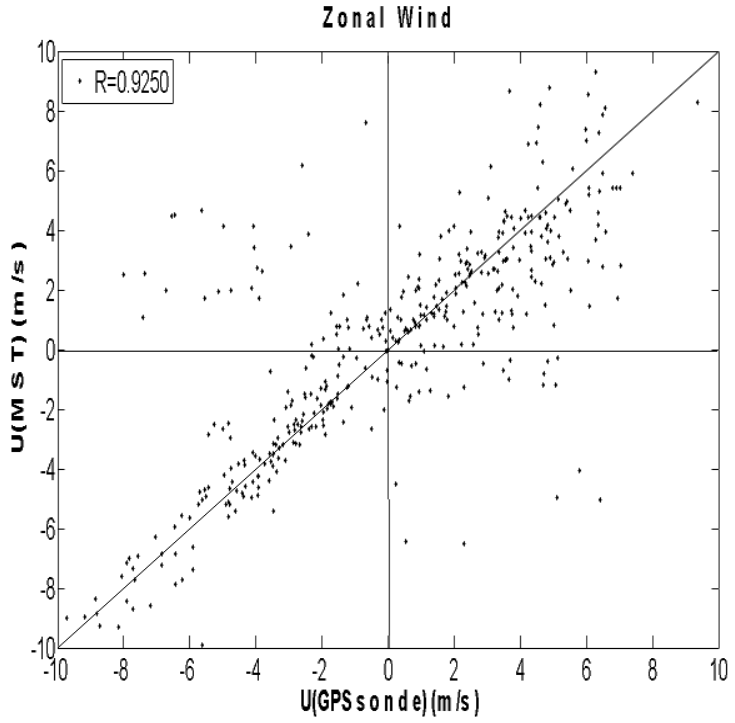

Fig.6.17 (a) *Scatter plot showing the comparison of Zonal (U) winds for GPS Sonde and MST radar. (10th, 11th, 14th and 15th December 2015)*

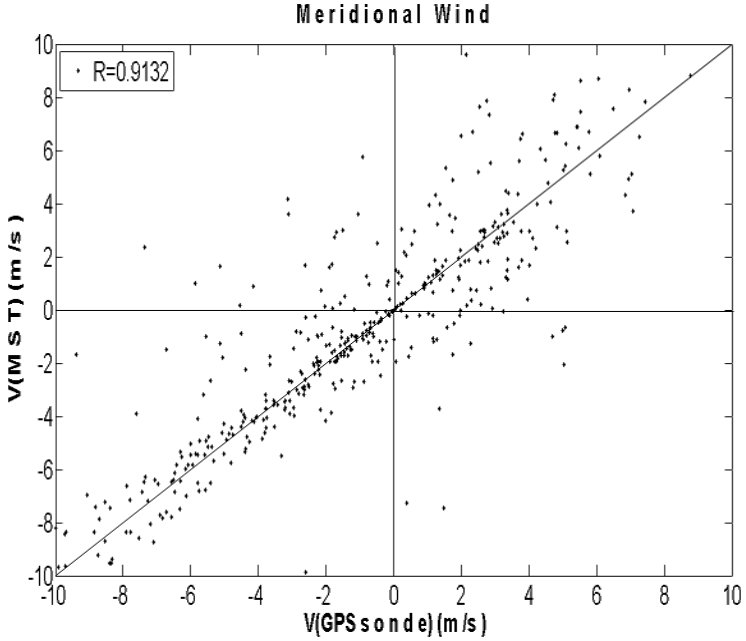

Fig.6.17 (b) *Scatter plot showing the comparison of meridional (V) winds for GPS Sonde and MST radar. (10th, 11th, 14th and 15th December 2015)*

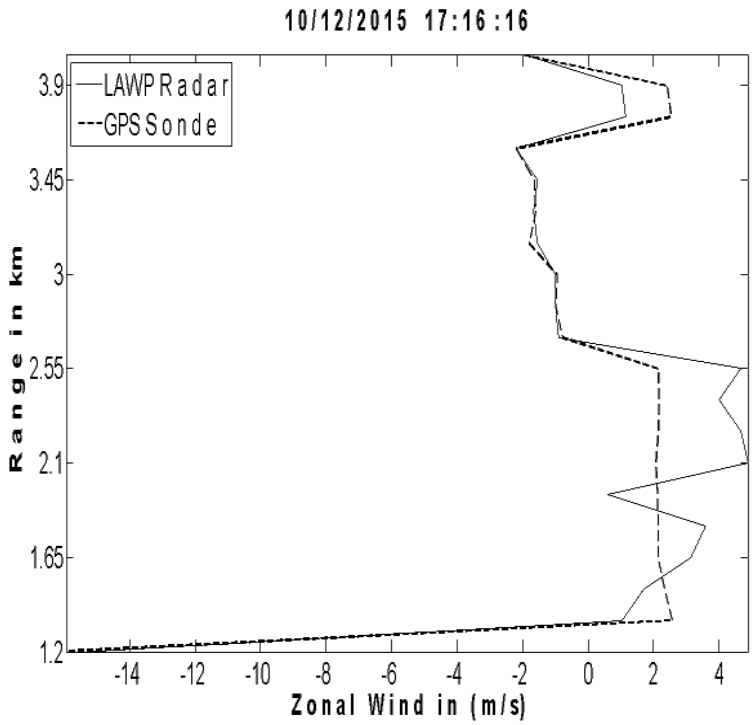

Fig 6.18 *(a) Zonal wind velocity comparison using GPS Sonde and LAWP (16 × 16) radar observations*

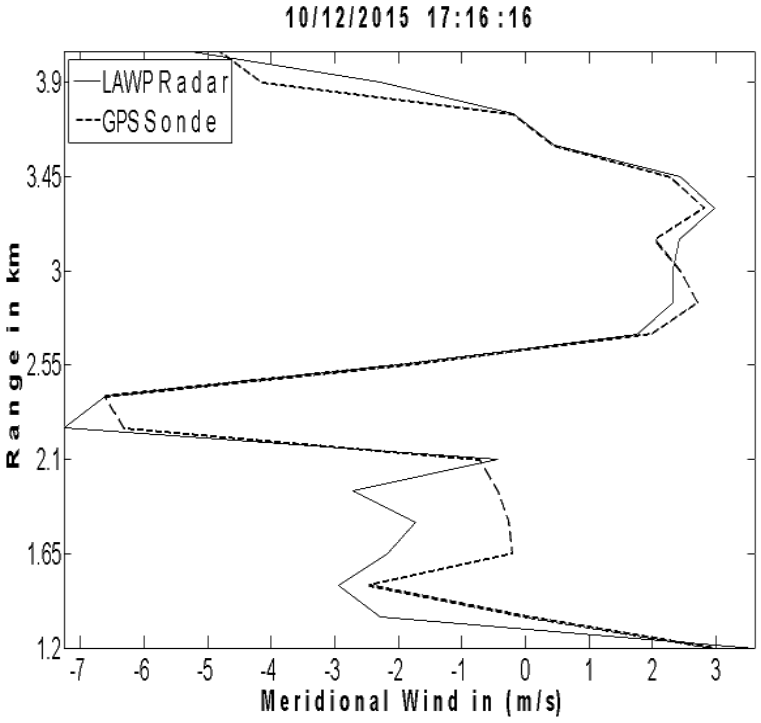

Fig 6.18 *(b) Meridional wind velocity comparison using GPS sonde and LAWP (16 × 16) radar observations*

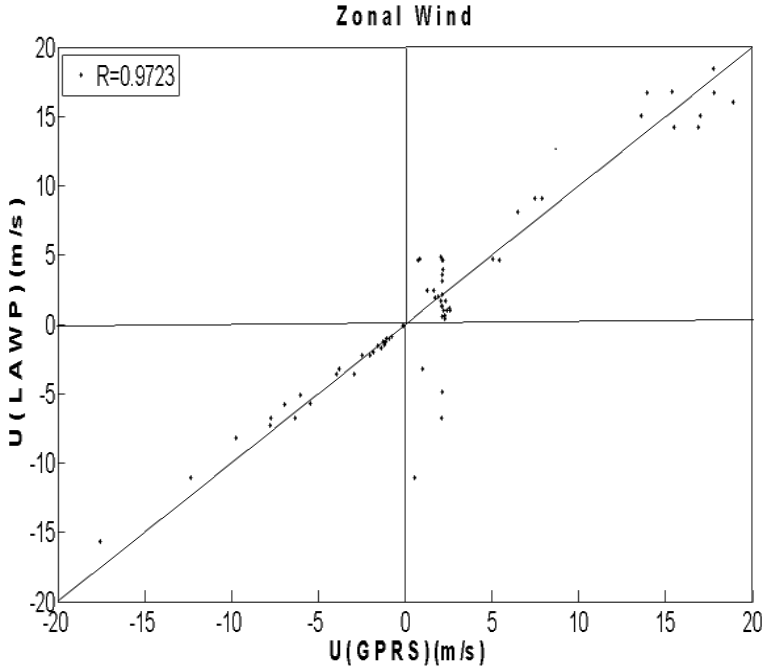

Fig.6.19 (a) *Scatter plot showing the comparison of Zonal (U) winds for GPS Sonde and LAWP (16 × 16) radar. (10^{th}, 12^{th}, 13^{th} and 15^{th} December 2015)*

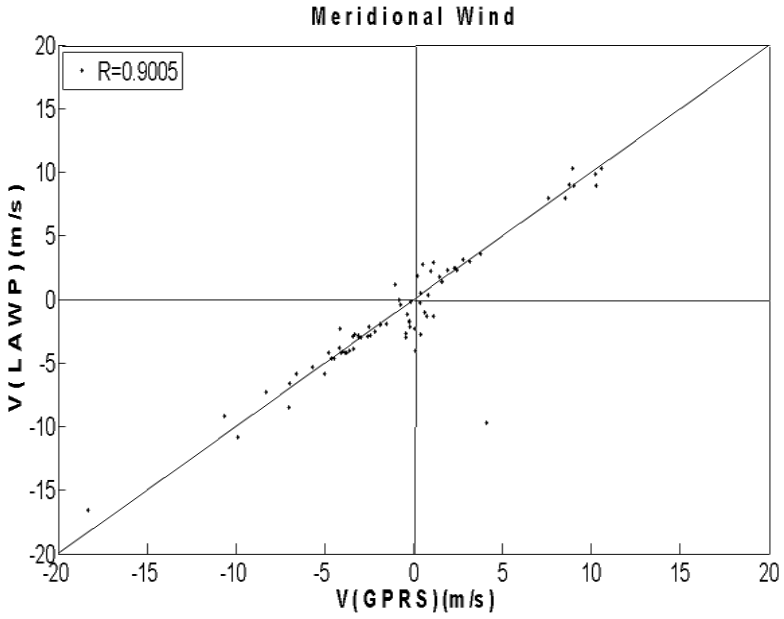

Fig.6.19 (b) *Scatter plot showing the comparison of meridional (V) winds for GPS Sonde and LAWP (16 × 16) radar. (10^{th}, 12^{th}, 13^{th} and 15^{th} December 2015)*

Table: 6.1 Comparison of wind velocity estimations by Scatter plots : GPS Sonde v/s wind profiling radar using different methods

Scatter Plot Correlation Coefficient (R)	MST radar (Zonal winds)	MST Radar (Meridional winds)	LawP 16 × 16 (Zonal winds)	LawP 16 × 16 (Meridional winds)
MPCF (single beam data)	0.8634	0.8379	0.9723	0.9005
MPCF (with image beam)	0.9250	0.9132	3-beam system No Image data	3-beam system No Image data
AME method*	0.7420	0.7159	0.6583	0.6843
FL Method*	0.8092	0.7821	0.6642	0.6853

***** *Programs for AME and FL methods were written by the authors using the descriptions given in the publications*

6.4 Doppler profile tracing in presence of interference and noise

Doppler power spectral data is subjected to pre-processing for the removal of noise, clutter and RFI. Therefore, the Doppler tracing is not done under the presence of clutter and RFI. However, in a few cases, the interference does not present itself in an orderly manner. Such components are not identifies as RFI and are not removes. Sometimes the signal power is low, the noise becomes comparable to the signal and the Relative Spectral Power (RSP) value is low. In both these cases, there is limitation in Doppler profile tracing. This limitation is seen as follows.

(i) *Presence of Interference*: The traced profile shows abrupt deviation in the Doppler profile. An example of the same is shown in Fig. 6.9 and 6.14. We have also seen that if the data from image beam is available and the there are no interference signals in the image beam, the Doppler profile tracing improves significantly (please refer Fig 6.12). The echoes from the precipitation are also interference for Doppler profile tracing. Occasionally the Doppler profile shows deviations due to the presence of precipitation echoes, as shown in fig. 6.11(b); whereas, in some cases, the MPCF shows accurate profile tracing even in presence of precipitation echoes, as shown in Fig 6.11 (a).

(ii) *Low signal strength*: At higher ranges, the signal strength is low and the SNR is low. This reflects as relatively low values of RSP in spectral domain. Therefore, there could be cases where all 5 range bins in a group do not have any peak having power more than $2\times S_N$. In such case, the MPCF algorithm terminates. This can be seen in Fig. 6.10 (b).

6.5 Summary

Wind profilers are used to obtain the 3D wind velocity information. Wind velocity profiles can be obtained by processing the backscattered signal. Two established methods called Adaptive Moment Estimation and Fuzzy Logic based method used for wind profiling, are discussed in section 2. These methods are computationally extensive. Hence, a comparatively simpler method is developed and presented in this thesis.

The Multi Parameter Cost Function (MPCF) method is a newly developed algorithm for tracing Doppler Profile. This algorithm was tested on Indian MST radar data. Data file details are are given in Appendix 4. The results have shown good agreement with other established methods of Doppler profile extraction such as *Adaptive Moment Estimation* (AME) and *Fuzzy Logic* (FL). The new algorithm was also successfully tested on two of the Lower atmospheric wind profilers located at Gadanki India namely LAWP (8×8) and LAWP (16×16). The application of the MPCF method from the MST to LAWP was seamless and did not require any change in parameters.

The performance of MPCF method is validated with another independent wind estimation method. The estimation of easterly and northerly winds by this method using Indian MST radar showed excellent agreement with the data obtained by concurrent GPS sonde flight as well.

It was also observed that this method require much less computations compared to the above mentioned existing methods. MPCF is a promising algorithm which can be used for automated data processing. The method does not require any parameter change depending on data type, weather conditions and locations. Therefore, it is claimed that this new algorithm presented is an *objective* method of Doppler profile estimation.

The MPCF algorithm shows a little degraded performance in presence of Noise and interference. MPCF provides the best possible effort approach by providing an improvement using the image beam data and having strategy of building traces in groups.

This step is followed by *Automatic classification* of the Doppler spectra based on the target type of the prominent echo. This requirement is also owing to the fact that there is large data generation and the data sets need to be classified in real time for further analysis. In order to cope up with the speed of data generation, the method must be able to perform automatically without human intervention. A simple spectral feature based classification algorithm is developed and tested successfully. This method is described in the next chapter 7.

Chapter 7

Spectral Feature based Classification of Doppler Power Spectra

Radar target classification has been a very well-studied topic and a good amount of literature is available for different types of radar. The target classification is generally based on the target structure [49]. The accuracy of the classification is often increased by considering multiple perspectives [50]. These techniques can broadly be classified as signature matching techniques. This approach was found useful for surface surveillance radars [51] [52]. Milanko presented a data base for such technique and also presented experimental results for acoustic ranging and detection systems [53][54]. Similar techniques have also been successful on Ground Penetrating radars (GPR) [55]. In addition to signature matching advanced techniques like extinction profile [81] and use of orthogonal pseudo-Zernike polynomials [82] improve the performance of radar target classification. However, atmospheric targets consist of randomly moving particles in motion similar to Brownian motion. Statistically these processes are non-stationary and therefore these targets do not show definite signature on Range-Doppler plane. Techniques using rough sets [83] having concepts similar to fuzzy logic have been found effective for the target classification of the weather radars.

In section 6.2 it was shown that the NIMA method is capable of identifying various features separately and classifying them according to their target type. This is demonstrated in Fig. 6.4 of chapter 6. This method is computationally intensive. It also requires fine tuning of membership functions and the thresholds according to the radar site and atmospheric conditions. Therefore, in spite of being very robust and consistent, the method may not be implemented as an automatic tool for classification. It is felt that an automatic classification algorithm should adopt a strategy based on the *Signature Correlation*. In other words an algorithm searching for a specific signal pattern on the Doppler spectra is expected to give performance as a tool for automated classification of the spectral data.

Chandrasekhar [56] presented a consolidated report of classification techniques on dual polarized weather targets. Hurricanes and water carrying targets have been more important targets for socio economic reasons. Various techniques have been used for identification,

classification and resolving different types of targets from radar data. Luke presented a technique to separate drizzle and precipitation [57] and Harasti used similar technique for resolving types of hurricanes [58]. Neural network techniques are popular for bulk meteoric classification using polarimetric radar [59][60]. Some of the observations of meteor types have been presented by Wannberg [61] and Krishna [62]. Following sections present a new spectral feature based technique to classify most types of the wind profiler targets.

7.1 Types of targets and their representation on the Doppler spectra.

Wind Profilers are mainly meant to analyze the clear echoes and derive 3-D wind speed from the backscatter. It was presented in Chapter 2 that these echoes are due to the change of RF refractive index. Additionally, the radar receives echoes from other phenomenon and objects present in the atmosphere. It may be noted that these echoes are not from man-made objects and are not strictly *unwanted*. These are echoes from other atmospheric phenomenon and are topic of study for the atmospheric scientists. It could be referred as bi-products of the WP radars. Five types of the phenomena are studied with the help of wind profiler data. They are as follows

(a) **Wind profile (clear air turbulence, CAT)**: The main product of the WP radars is Doppler profile or the radial velocity profile. We have seen in chapter 3 that the radio waves are scattered back due to the change in the refractive index. This occurs due to wind velocity change in small volume. Normal wind flow is always associated with turbulence. In other words, the air pockets in atmospheric layer have different velocities. This turbulence leads to the backscatter of radio waves. This phenomenon is known as Clear Air Turbulence (CAT) as there are no particle scatterers in the radar target.

(b) **Precipitation Echoes:** Rain or precipitation is a tropospheric phenomenon and the echoes are observed at the ranges up to 6 to 8 km. These echoes are due to particulate scatter due to the rain drops. They appear as strong spectral components in the positive half plane on the range Doppler plane. The Doppler shift also allows the study of rain drop velocities.

(c) **Meteoric Echoes:** These echoes are generally observed in upper troposphere to lower mesospheric ranges (from 10 to 50 km). Falling meteors encounter friction with air. The air is ionized due this friction. Due to the presence of the charges ions, the radio waves are reflected and this phenomenon gives strong backscattered echoes.

(d) **Ionospheric echoes:** Ionosphere contains ionized molecules and therefore the RF reflectivity of the ionospheric targets is very good. In spite of large distance, the ionospheric echoes show good signal strength. These echoes are seen at the ionospheric ranges (between 75 km to 200 km).

(e) **Mesospheric Echoes.** Wind turbulences lead to change in RF refractive index of the air. This phenomenon could occur in Mesosphere.

(f) **Echoes due to Ionospheric Turbulence:** It is occasionally observed that the due to strong solar activity or strong magnetic disturbance in ionosphere. This is reflected as multiple strong power spectral components spread over the complete Doppler band. This signature is similar to Clear air turbulent echoes observed in lower ranges.

It is also observed that sometimes discrete objects like flock of birds, dust, pollutants etc. contaminate the WP data. Such data sets are classified separately. Therefore this is included as 8^{th} type for classification.

7.2 Characteristic signatures on the Doppler spectra

The occurrences of this phenomenon are observed by identifying the characteristic features (or signature) in the *range-Doppler* plane. They are as follows:

(a) Wind profile, (CAT) echoes,

The main product of the WP radars is Doppler profile or the radial velocity profile. This is characterized by the following conditions. Power contained in the highest two peaks must be more than 3 times the power contained in the remaining peaks and standard deviation of the peaks must be less than 5 ms^{-1}; as given in expression (7.1).

$$\left(\sum_{i=1}^{2} P_i\right) \geq 3 \times \left(\sum_{i=3}^{7} P_i\right) \cap std\_dev < 5 \qquad (7.1)$$

If this condition is satisfied for more than 30% of the total range the data is classified as wind profile. The wind profile appears as one or two closely spaced prominent peaks. These conditions ensure that most of the backscattered power is concentrated in a peak or closely spaced components

(a) ***Precipitation Echoes***

Rain or precipitation is a tropospheric phenomenon and the echoes are observed at the ranges up to 8 km. In this case, falling raindrops is target. Their echoes would result in positive Doppler frequency as they approach the radar. The spectral components appear on the right half of the range-Doppler plane. The terminal velocities of falling rain drops are generally between 4 ms^{-1} to 12 ms^{-1}[84]. The precipitation echoes are identified using conditions give below.

$$if\ \{R(i) < 8\ \cap\ peakval(i,j) > 10 \times N(i)\ \ \cap\ 4 < velocity\ (i,j) < 12 \qquad (7.2)$$

Where, *R(i)* indicates the range of i^{th} range bin in *km*, and *peakval(i,j)* is the power of the j^{th} Doppler component of the i^{th} range bin. *N(i)* is the RMS noise level of i^{th} range bin and *velocity(i,j)* is the velocity of the falling rain drops in ms^{-1}. If this condition is true for more than 2000 meters, or more than 7 range bins in our case, the target is classified as precipitation echo.

(b) ***Ionospheric Echoes***

The Ionosphere is an atmospheric layer that contains the charged particles like electrons and ions. It surrounds the earth at altitudes between 80 km to more than 1000 km and is classified into D, E and F layers depending on the types of particles. During the day, the D and E layers become heavily ionized; thereby increasing the RF reflectivity of that layer. In spite of large distance, the ionospheric echoes show good signal strength on the MST radar Doppler power spectra. They present themselves as prominent peaks clustered together. The radial Doppler velocity spread of the ionospheric echoes is observed to be less than 44 ms^{-1}[85]. The following conditions are used to identify the ionospheric echoes.

$$If\ \{90 \geq R(i) > 60 \cap peakval(i,j) > 4 \times N(i) \cap std\_dev(i) < 44(ms^{-1})\} \qquad (7.4)$$

Where, *R(i)* is the range of i^{th} Range bin, *peakval(i,j)* is the amplitude for the i^{th} range bin j^{th} peak selected from power spectral component, *N(i)* is the RMS noise level of i^{th} range bin. If this condition is true for more than 300 meters or more than 2 range-bins in this case, the target is identified as ionospheric winds. The expression (7.4) shows the condition for D layer. For E and F layers the range condition changes to $150 \geq R(i) > 90$ and $R(i) > 150$, respectively.

(c) ***Meteoric Echoes***

Meteoric echoes are generally observed in upper troposphere and up to lower ionospheric ranges, (from 10 to 100 km). Falling of meteors creates ions due to the friction with air. This ionization gives strong backscattered echoes. These echoes appear at prominent peaks clustered together. These peaks are generally found in the positive Doppler velocities. Meteoric velocity's could be very high and may exceed the maximum Doppler velocities. As a result, the Doppler peaks of the meteoric echoes may fall in the negative Doppler region due to *fold-over*. The conditions used to identify the meteoric echoes are as follows:

$$if\ \{R(i) > 10 \cap peakval(i,j) > 10 \times N(i) \cap std\_dev < 17\} \quad (7.5)$$

Where, *R(i)* is the range of i^{th} range bin in *km*., *peakval(i,j)* is the amplitude for the i^{th} range bin j^{th} peak selected from power spectral component, *N(i)* is the RMS noise level of i^{th} range bin. *std_dev* standard deviation of the selected peaks in ms^{-1}. If this condition occurs for more than 300 meters or for more than 2 range bins in our case, the target is classified as meteoric echo.

(d) ***Mesospheric Echoes***

Occasionally wind turbulence occurs in Mesosphere. Due to this, wind profilers see moderately strong peaks spreading over complete Doppler frequency band. The signature is similar to the CAT signature with the difference only in the range at which it occurs (typically between 30 km to 70 km).

$$if\ \{80 > R(i) > 30 \cap std\_dev < 4 \cap peakval(i,j) > 1.5 \times N(i)\} \quad (7.6)$$

Where, *R(i)* is the range of i^{th} range bin in km and *std_dev* is the standard deviation of the peaks in ms^{-1}. The data is classified as mesospheric echo if the conditions are true for the range of 9 km. or more than 4 range bins in this case.

(e) ***Echoes due to Ionospheric Turbulence***

It is occasionally observed due to strong solar activity or strong magnetic disturbance in ionosphere. This is reflected as multiple strong power spectral components spread over the complete Doppler band. This signature is similar to Clear air turbulent echoes observed in lower ranges. The conditions used to identify the magnetic activity ionospheric echoes are as follow

$$If\ \{R(i) > 80 \cap peakval(i,j) > 100 \times N(i) \cap std\_dev > 7\ \} \quad (7.7)$$

Where, $R(i)$ is the range of i^{th} Range bin in km, $peakval(i,j)$ is the amplitude of the j^{th} spectral peak of the i^{th} range bin and $N(i)$ is the RMS noise level of i^{th} range bin. If this condition occurs for more than 2.4 km or for more than 2 range bins in this case, the target is classified as magnetic activity ionospheric echo.

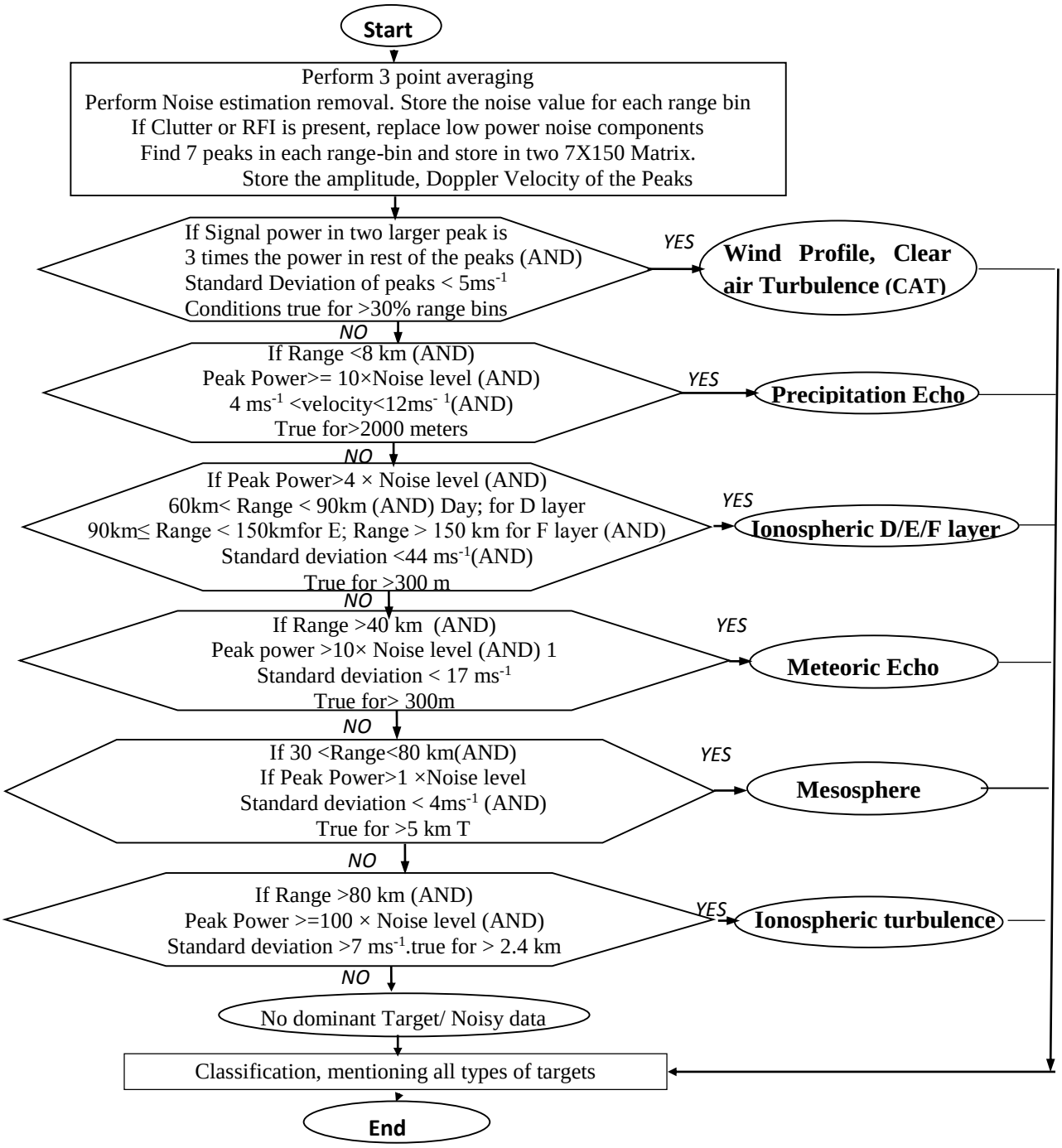

Fig.7.1 *Flow Chart demonstrating the SFBC classification algorithm*

7.3 Target feature identification and classifications

It may be noted that the spectral signatures for the six types of echoes are independent to each other. The characteristic feature for each type of echo was translated into mathematical conditions of the range and Doppler frequency. These conditions were checked by a simple *sequential search* algorithm, used for the classification. This approach is scalable in the sense that a new type of the echo could be included easily. Also the feature signature conditions could be fine-tuned if required. This method describes the target types in terms of atmospheric parameters. For the same atmospheric parameters, the radar Doppler data parameters change due to radar beam width and beam tilt [86]. Considering this fact the descriptor conditions or the limits and thresholds used in this method are kept accommodative to include the variations due to the radar beam. This method is independent of radar operating parameters. In this method, we are looking for concurrence probability, limits kept are hard but relaxed, which effectively forms the basis of fuzzy logic. A Matlab program capable of reading and classifying the data was written. The flow chart for the classification algorithm is given in Fig. 7.1.

7.4 Experimental results verification on classification using Indian MST radar data

The Classification algorithm was tried on approximately 20,000 sets of MST radar data. Data file details are given in Appendix 4. These sets were classified by conventional methods / human experts. The pre classified data was subjected to the *Spectral feature based classification* algorithm described in the chapter. The program classified all the data sets correctly. There was no *wrong identification* neither was there *missed identification* when ionospheric and meteoric data was analyzed. However, in case of precipitation cat and mesospheric echoes there were approximately 10 % missed identification. When these cases were observed manually it was found that the data was having poor SNR. This indicates that the classification algorithm has limitation of the performance when the SNR is low. The data sets having two or more features (e.g. CAT and Precipitation were classified into both the categories. A representative spectrum is shown in Fig. 7.2 to 7.9.

Presently the classification algorithm is capable of identifying the presence of 7 different types of atmospheric targets/ phenomenon. The detection and classification of various targets is done by a search of specific features defined in terms of certain thresholds and limits. This algorithm is computationally simple and has shown excellent results. This algorithm can be

used on any wind profiler without requiring change of parameters. The algorithm is implemented in Matlab. Due to computational simplicity it takes 1.5 seconds per frame to classify the data set. This is less than the data generation rate. Due to these features the algorithm could be used as an automated tool for *real time* WP data classification. Summary of result is given in table 7.1.

Table 7.1: Summary of the Results of classification algorithm on MST radar at Gadanki

Type of Atmospheric Phenomenon	No. of Data sets	Range of Vales of the Critical Parameters			Comments (%Auto/Human)
		Range	Peak power / Noise level	Radial Velocity/Std Dev	
Ionospheric(D)	3000	75 - 80 km	4	< 44 ms^{-1}	100% match
Ionospheric (E)	2000	80 - 110 km	4	< 44 ms^{-1}	100% match
Ionospheric (F)	3000	>110 km	4	< 44 ms^{-1}	100% match
Precipitation	3000	0- 8 km	10	4 - 20 ms^{-1}	90 % match
CAT/ Wind Echoes	3000	0 – 12 km	4	< 5 ms^{-1}	92 % match
Mesospheric Echo	3000	30-80km	1.5	< 4 ms^{-1}	91%match
Meteoric Echo	3000	>40 km	10	<17 ms^{-1}	100% match

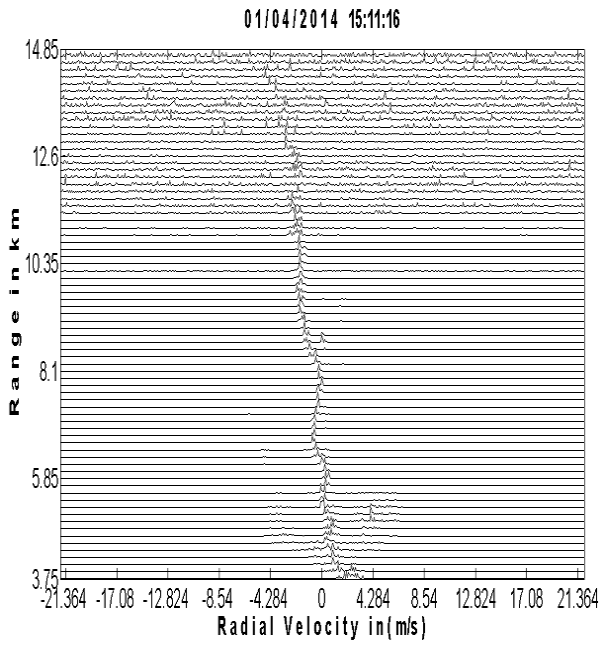

Fig.7.2 *Wind profile /CAT Echo (Beam Direction: West 10^0))*

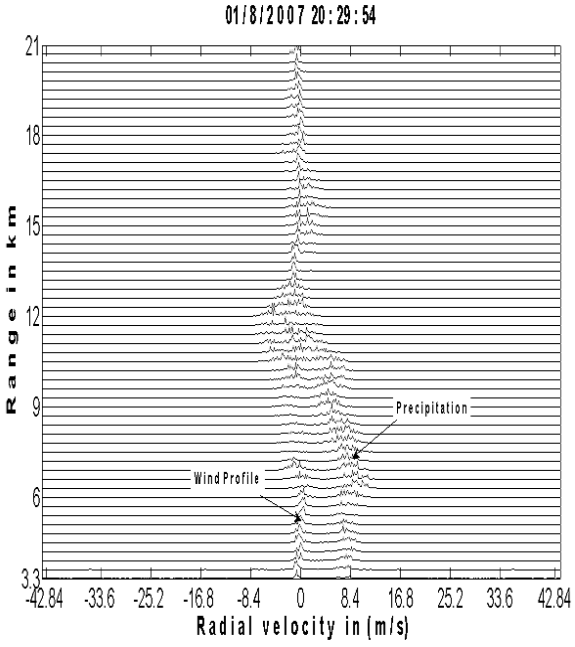

Fig.7.3 *Wind Profile with Precipitation Echo (Beam Direction: West 10^0))*

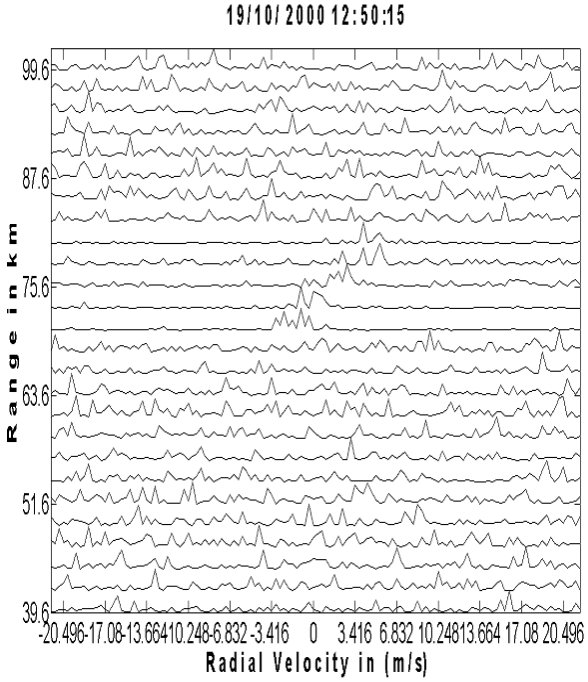

Fig. 7.4 *Ionospheric Echo (D) (Beam Direction: North 15^0)*

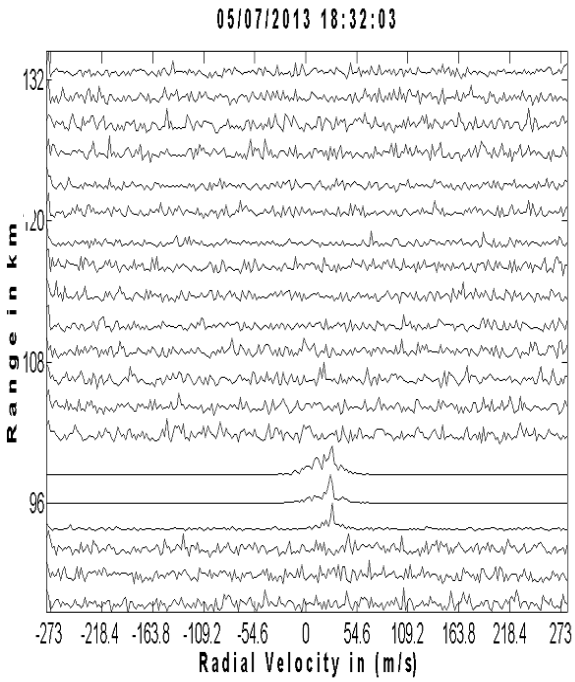

7.5 *Ionospheric Echo (E) (Beam Direction: North 15^0)*

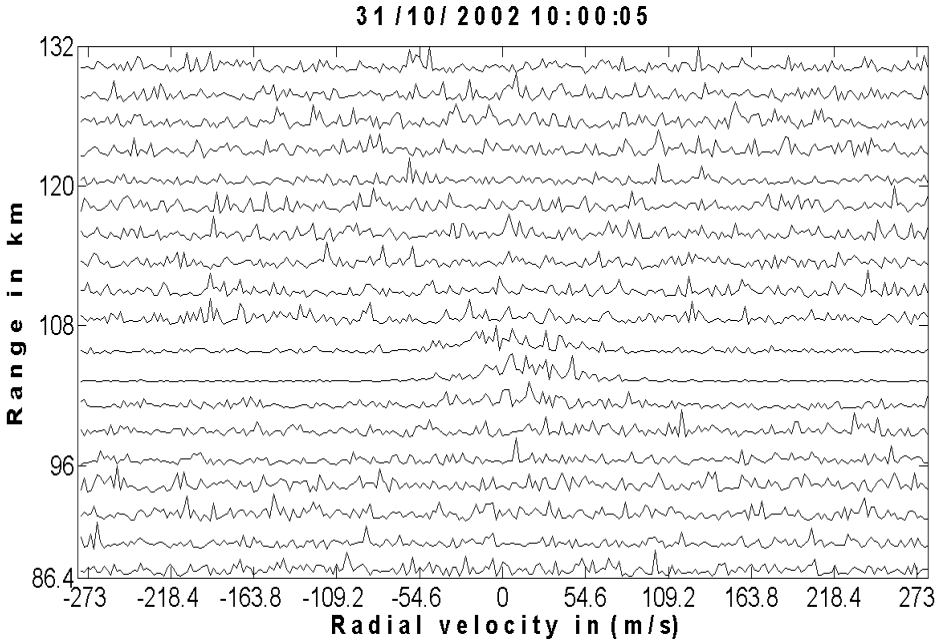

Fig. 7.6 Ionospheric Echo (F) *(Beam Direction: North 15^0)*

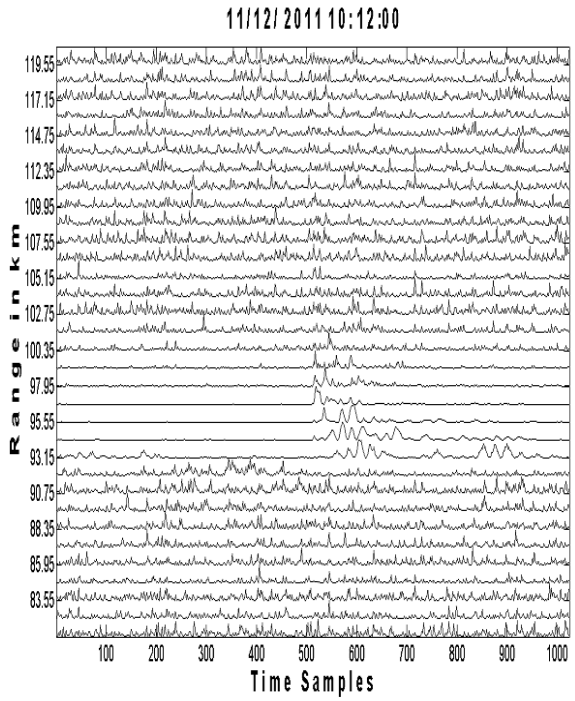

Fig. 7.7 *Meteoric Echo (Beam Direction: East 20^0)*

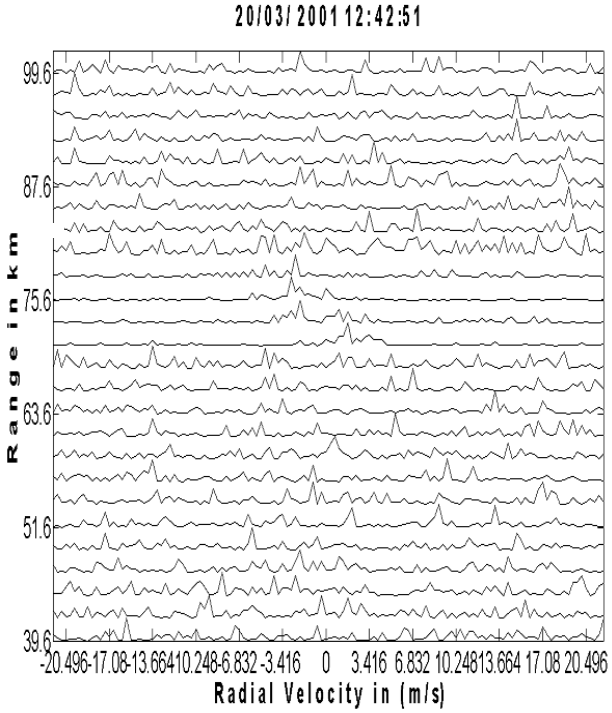

Fig. 7.8 *Mesosphere Echo (Beam Direction: East 10^0)*

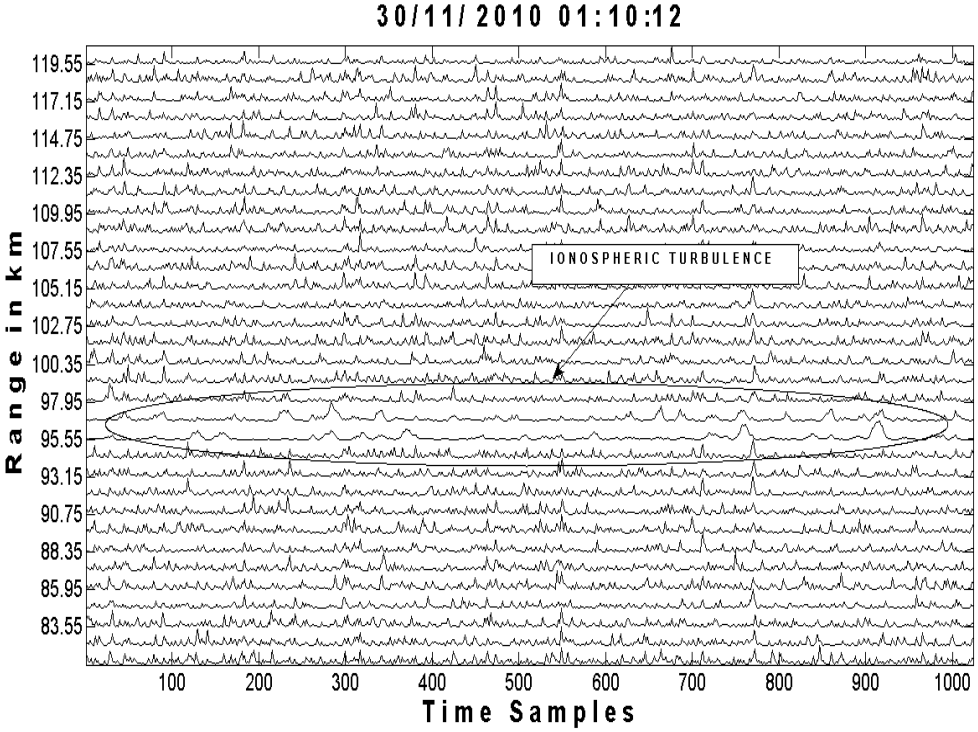

Fig. 7.9 *Ionospheric turbulence (Beam direction East 10^0)*

7.5 Classification in low SNR conditions and in the presence of Interference

The processing of WP Doppler spectra starts with preprocessing followed by the Doppler profile tracing. The classification of the data type is taken up after these two steps. Therefore the presence of noise and interfering signals is minimal when the Doppler power spectral data is subjected to the classification. However, there is always probability of the presence of interference signal and noise with power comparable to the signal. The classification algorithm presented in the earlier sections works on the presence of high power prominent peaks in the Doppler spectra. Due to the interference and noise with comparable strength, the selected of spectral peaks do not belong to the atmospheric echoes. As a result, the algorithm is not able to classify the data set into appropriate data type. This limitation is seen in the results presented in table 7.1. It is seen that the non-decisive classification percentage is 8 to 10% in case of CAT, precipitation and mesospheric echoes. It may be appreciated that such situation never arises in case of meteoric and ionospheric echoes. This is mainly because the echoes from these phenomena are high in signal strength and the interfering components are almost always of lower magnitude. However, the good part is that the classification algorithm does not lead to wrong classification.

7.6 Summary

Classification of wind profiler Doppler spectra is very much necessary to archive the data which helps the researchers to a great extent. The radar Doppler spectra are generally classified based on the atmospheric target or back scatter. It is done according to the spectral features associated to the target structure. Various algorithms are developed and is in use for different kind of radars. A spectral feature based radar target classification algorithm is developed and presented in this chapter. The algorithm is simple and easy to use. This classification algorithm is capable of identifying the presence of 7 different types of atmospheric targets/ phenomenon. The detection and classification of various targets is done by a search of specific features defined in terms of certain thresholds and limits. This algorithm showed successful classification of 100 % in 4 categories and around 90% in 3 categories. The lower accuracy of classification is mainly due to the presence of noise and interfering spectral components with power comparable signal. This algorithm is computationally simpler compared to other established algorithms and has shown very good results. These results indicate that the

algorithm is of great utility. This algorithm can be used on any wind profiler without requiring change of parameters. The algorithm is implemented in Matlab. Due to computational simplicity it takes 1.5 seconds per frame to classify the data set. Most of the classification algorithms operate in the transform domain; either wavelet transform or the Gabor transform. The time required for proposed method is 25% less compared to the wavelet based algorithm which required approximately 7.5 seconds. Also, the implementation time is much lesser than the data generation rate of 16 to 32 seconds. Due to these features the algorithm could be used as an automated classification algorithm for WP data.

Next chapter revisits contributions and evaluates their significance.

Chapter 8

Research Contributions and Discussions

This chapter revisits the research carried out and consolidate the contributions and evaluate the significance and relevance to the research objectives. A discussion on results and the limitations are also included.

8.1 Modeling and Simulation of Doppler Spectra

The research work started with the study on the operation of the wind profiler radar. The efforts were directed towards understanding the theory behind the radar backscatter, radar operation, signal processing schemes and mathematical representation of the received signal. It is also realized that the Doppler power spectra is the most important standard product of the Wind Profiler and the research to extract the wind information is carried out taking this product as the primary data set.

Clear air Doppler radars normally operate in *monostatic mode i.e.*, the transmitting and the receiving antenna are the same. Phase coded RF energy is transmitted. The echo signals are detected by correlating with the replica of the transmitted signal. The *Bragg-Scatter* type of echo has the same texture of refractive index turbulence throughout the radar beam volume. Therefore it does not have variations in the backscattered power which is mathematically represented by Fraunhofer approximation of the two way backscatter expression. Backscatter due to refractive index discontinuities show specular reflections, aspect sensitivity and velocity biases in the wind measurements. The modelling of this type of scatterers need Fresnel approximation or the quadratic term of the two way backscatter expressions. The apriori knowledge on the statistical nature of the Doppler spectra can be used to model the same. [87]

The radars are used to observe the back scattered signal from the atmospheric targets and estimate the dynamics of the atmosphere. The backscattered signal is coherently sampled and FFT is computed for the Doppler analysis to get the velocity information of the target. Use of appropriate window on the time domain data helps in improving SNR. With this background,

the radar signals can be viewed as a discrete representation of the backscattered signal on the range-Doppler plane. This 2-D representation is subjected to spectral moment estimation followed by consensus averaging. This data is used to determine the structure of the target.

Modeling of Doppler spectra makes it possible to create *customized data*. Knowing the structure of atmospheric targets, one can *create* Doppler power spectra corresponding to any type of weather condition! In practice, operating radars are not expected to have power spectral data of all possible weather conditions. The modeled data can be conveniently used in such situations to evaluate the signal processing algorithms initially.

Atmospheric backscatter signals from VHF/UHF bands generally have Additive White Gaussian noise. The additive WGN term ***n(k)*** is included in the model by using the Matlab function AWGN. However, the simulation algorithm allows the user to select noise of any probability distribution. The power of the signal is the squared sum of the real and imaginary parts of the signal components (given in equation 3.5).

To begin with, a Matlab program to simulate the Doppler power spectra was written. This program mathematically emulate the processing steps of the WP radar. This exercise provided insight to the processes involved and could generate Doppler power spectra for various atmospheric conditions with added noise of required statistical feature. This facilitated generation of radar like data even for the conditions which occur rarely at the radar site.

This simulation program turn out to be a very useful tool to create data sets of all the weather conditions. And hence it can be used as initial *test data* to evaluate all the post processing algorithms for Wind Profilers.

8.2 Modeling, Simulation and Removal of Clutter and RFI signal

Real radar signals are often contaminated with clutter, RFI and other man-made signals. The Matlab program is modified to model clutter and RFI of various specifications. In practical applications, these disturbing signals need to be removed.

Clutter is the most unwanted signal in the Wind Profilers. Clutter consists of echoes from nearby stationary and slow moving objects like trees, hills, sea etc. It appears on the Doppler power spectra as a low frequency spectral component symmetrically placed around 0

Hz. These signals are modelled by adding extra components at low Doppler frequencies corresponding to velocities below 2.5ms^{-1}.

System generated power frequency disturbances such as leakage, electrical noise and other interfering sources are categorized as Radio Frequency Interference RFI. RFI is generally a single frequency disturbance spanning over short time. This appears as a sharp spectral component in 8-10 or more range bins. RFI occurs at same Doppler bin at all the affected range bins. Hence this type of unwanted signal presents itself as a set of sharp peaks placed in a vertical line. This disturbance is modelled by adding another frequency component in the Doppler spectra. From the simulated results, it is verified that the modeled data perceived same as the real radar data.

In this manner, the characteristic features of RFI and clutter are determined. It is possible to simulate the contaminated Doppler power spectra for various testing purpose. However, this capability is most useful to identify and remove the Clutter and RFI components. This is an important step in the pre-processing of the Doppler power spectra. The pre-processing algorithm is briefly described in the following text.

Various noise estimation methods are studied and the classical method suggested by Hildebrand et al. is still found consistent. Matlab program is written for the noise estimation of atmospheric radar Doppler spectra using Hildebrand method based on following reasonable assumptions.

1. Weather echo spectrum is Gaussian but colored. (non-uniform frequency contents)
2. The noise spectrum is Gaussian but white. (uniform frequency content)

The Doppler spectrum corresponding to each range-bin is subjected to smoothing before noise removal. The widely adapted spectral processing technique namely three point averaging is used in this thesis for Doppler Spectra smoothing. Once the noise is estimated, it is removed by subtraction from the smoothened Doppler spectrum.

Knowing the characteristics of the RFI and Clutter present in the atmospheric Doppler spectra, the algorithm is developed to remove the Clutter and RFI from the data without affecting the weather signal (chapter 3). The performance of this algorithm is tested exhaustively using the simulated data, MST radar data and different LAWP radar data for the Clutter and RFI removal.

8.3 Newly developed Multi-Parameter Cost Function method: A Novel approach for wind profiling

The main function of the Wind Profiler is to extract wind velocity information at various atmospheric layers. Many researchers have worked in this area and fair amount of literature is available.

This literature was studied and a new computationally simple algorithm is developed in this thesis. The power spectrum is a standard *product* of the radar signal processing system that serves as an input for the Doppler profile tracing. Pre-processing of the power spectra is carried out by noise power estimation using *Hildebrand* Algorithm to clean the Doppler spectra (Discussed in Chapter4). The MPCF [88], Doppler profile tracing algorithm followed a different approach to estimate the wind profile (Chapter 6).

Identifying spectral peaks of atmospheric echo is the most important task of this algorithm. The complete set of Doppler spectra is divided into groups of five range bins each. This method performs the task of profile tracing in individual groups starting from the lowest range group and proceeding sequentially to the next high range group. After identification of the prospective peaks in all five range-bins, all possible Doppler profile traces are constructed. The procedure is summarized as below:

(i) Make groups of 5 range-bins starting from the lowest. In spectrum of each range-bin, identify five highest magnitude peaks that satisfy the SNR threshold. These peaks are called *prospective peaks.*

(ii) Start from the lower group of range-bins. List all possible traces using these *prospective peaks* in each range bin.

(iii) Identify all the possible traces where the condition of Doppler window is satisfied.

After identifying all possible traces, a *cost* is computed to each link. The cost function is designed with the objective to determine whether the link forms part of Doppler profile. The cost function is a mathematical model of *human perception to decide whether a link belongs to the profile*. The profile tracing look for two factors, - '*consistent high power components*' and '*low change in wind shear'.* A cost function is computed as the weighted sum of two terms based on Relative Spectral Power (*RSP*) and a function of change in the wind shear.

Each link has 'RSP' values (corresponding to spectral component) and the differential wind shear values. Each trace has 5 links connecting the peaks in the range bins. Cost is calculated

for each link using Equation 6.3. The sum of the cost of all 5 links is the total cost associated with the trace. The trace with the maximum cost is finalized as Doppler trace for that group. The processing of the next higher range-bin group starts with step 1 identifying the peaks. In step 2, the formation of traces starts with the *highest point* of the trace of the 'lower range-bin group'. This condition ensures the connectivity of the traces. Complete Doppler Profile is automatically obtained after completion of the highest 'Range-bin profile. The tracing accuracy is found improved if the data of symmetrical beams are available.

The performance of the new Multi Parameter Cost Function (MPCF) algorithm is compared with two of the well-established techniques, namely the Adaptive moment estimation method and the Fuzzy logic based profile extraction method. The performance by the MPCF algorithm is found better in some cases and comparable in most of the cases. **The key feature of the MPCF method is its computational simplicity and good performance even in low SNR conditions.**

The MPCF algorithm is computationally simpler than available alternatives and does not require any change of parameters when migrated from one radar to another. This is a significant advantage as all other methods of Doppler profile extraction require algorithm parameter change when migrated to different radar. Another advantage of the MPCF algorithm is that it performs better than other two algorithms in low SNR conditions. MPCF works reliably well when the RSP of signal components is more than 3dB. However, when the spectral power of the strongest atmospheric components are within 200% (less than 3dB) of the noise power, consistently for 5 consecutive range bins, the algorithm terminate the process of Doppler profile tracing. However, if the low RSP condition is for less than 5 range bins the process continues marking the estimations in the noisy range bins as *suspects*. The limitation of the MPCF is reflected only in the case when the signal is overpowered by the non-atmospheric components for a band of more than 5 range bins. The computational complexity is less by approximately 60 to 70 percent. This leads to lesser computation time by the same margin. The results obtained by the MPCF algorithm are also validated with the wind data obtained by the GPS Sonde observations. The matching results with different radar data sets proved that the MPCF algorithm provides a valid profiling tool. Hence this algorithm is presented as a strong tool to be used for automatic processing of the wind profiler spectra.

8.4 Atmospheric Target Classification of Wind Profiler Spectra

Another important requirement of Wind Profilers is classification of the data according to the target present. Many methods are developed to classify the Doppler spectra based on the echoing targets. Techniques using rough sets having concepts similar to fuzzy logic have been found effective for the target classification of the weather radars. In section 6.2 it is shown that the NIMA method is capable of identifying various features separately and classifying them according to their target type. However this method is computationally intensive. It also requires fine tuning of membership functions and the thresholds according to the radar site and atmospheric conditions. Therefore, in spite of being very robust and consistent, this method may not be implemented as an automatic tool for classification. It is felt that an automatic classification algorithm should adopt a strategy based on the *Signature Correlation*. A new Spectral Feature Based Classification algorithm is developed to classify most types of the atmospheric targets. The spectral characteristics of Clear Air Turbulence (CAT), Precipitation echoes, Meteoric echoes, Ionospheric echoes, Mesospheric echoes and Echoes due to Ionospheric Turbulence are defined. This spectral characteristic feature of each type of echo are translated into its equivalent mathematical conditions in terms of range and Doppler frequency. These conditions were checked by a simple *sequential search* algorithm to classify the Doppler spectra. For the same atmospheric echo, the radar Doppler data parameters change due to Radar beam width and beam tilt. The limits and thresholds to define the spectral features of various echoes are decided by considering the variations of the radar beam as well. This method of target classification is independent of radar operating parameters.

A Matlab program was developed for automatic classification of the Doppler power spectra without human intervention (Chapter 7). This is a very effective tool for automatic segregation of the wind profiler Doppler spectra. This algorithm classifies the data from atmospheric phenomenon like ionospheric echoes, precipitation echoes etc. This algorithm has a limitation when the data has low SNR and strong interference signals. Approximately 8-10% of the datasets are not classified in such cases. This limitation could be overcome by introducing more accurate feature definitions of the various atmospheric targets.

8.5 Limitations of the research

The research conducted during the doctoral study was implemented on the Doppler power spectral data sets of three different radars. They are Indian MST Radars, LAWP radars

and Radio Sonde. The techniques were found useful, computationally simple and fast to implement so as to cope up with radar data generation speed.

However, the profile tracing algorithm (MPCF) shows limited performance in Low SNR conditions or in presence of interfering signals. The program terminates when it encounters noisy spectra in 5 consecutive range bins. Similarly the classification algorithm becomes indecisive in very low SNR conditions or in the presence of strong interfering signals.

The algorithms developed during this research are specific to the wind profiling radars. These techniques require the data headers giving the information of radar operating parameter. The system requires manual data entry if the data header is not available. They cannot be used for other types of atmospheric ranging instruments like Doppler weather radars and Lidars. Another limitation with these systems is its use in extreme weather conditions like hurricanes and heavy precipitation (more than 7.5 mm/hr). Under such severe conditions the Doppler profile estimation has to be done manually.

Chapter 9

Conclusion and Future Scope

The motivation of this research work was to develop various signal processing algorithms for modeling, automatic processing and classification of the wind profiler spectral data. Modern wind profiler radars are generally operated for long hours and generate a large volume of data. It is required to process the data in near-real-time. Therefore, the processing algorithms need to be faster and computationally efficient. Also, the algorithms should be data independent and parameter independent. The research was carried out with this objective. During the course of this research work, study of the wind profiling radar operation is done. The algorithms are developed addressing real data processing requirements. In this doctoral research the techniques for modeling and the simulation of the WP data are developed and the complete processing of the Wind profiler Doppler power spectra is addressed. The processing of the WP data is done in three steps.

They are (a) Preprocessing (b) Doppler profile tracing (c) classification.

The concluding remarks on the research done are summarized below.

9.1 Conclusions

a) A versatile software tool to model and simulate the Doppler Power spectra is developed. The established method of Sum of Sinusoids to generate the Doppler spectra is used in this thesis. This procedure allows the user to select the Doppler velocity and the Doppler velocity spread the required. The amplitude and the pattern of the amplitude envelope can also be chosen. Thus this technique offers complete flexibility in modeling the spectra to the user. With knowledge of the atmospheric process dynamics, the user can create the Doppler spectra of almost any observable weather phenomenon. The modeling exercise resulted in a powerful tool to create a set of Doppler spectra corresponding to various atmospheric conditions.

b) Pre-processing algorithm: Algorithms are developed and implemented to estimate the noise content and identify the RFI and Clutter components present in the spectral data. This information is used to automatically remove the noise and unwanted signals like RFI and

Clutter cleaning the Doppler power spectra. The algorithm implemented removed the unwanted signal components with known pattern from the WP Doppler Spectra successfully. Some less probable interference components may survive the preprocessing.

c) A novel Doppler profile estimation method using Multi parameter Cost Function (MPCF) is developed, evaluated and validated in this thesis. The MPCF algorithm is based on the concepts established by the earlier researchers. The innovation in this method is the use of a cost function developed considering also the 'differential wind shear' criterion. The cost function is derived using weighted sum of Relative Spectral Power and the 'differential wind shear'. This algorithm shows Doppler profile tracing comparable to the leading techniques for the profile extraction such as AME and Fuzzy Logic methods. The performance of the MPCF is also validated using the correlation with the GPS Sonde data. However, the MPCF method shows limited performance in very low SNR. Computational simplicity is the main feature of MPCF method. Due to this computational simplicity the method is capable of tracing the Doppler profile in 7 seconds on Matlab. This time is much faster than the data generation time. Also the MPCF algorithm could be migrated to any wind profiling radar operating in pulse Doppler mode. This is due to MPCF's ability to adapt to the radar parameters. These features of the MPCF qualify it to be an algorithm for automated processing of the wind profiler data.

d) Spectral Feature Based Target Classification (SFBC) algorithm has been developed for the Wind Profiler Doppler spectral data. The SFBC algorithm is computationally efficient and has shown excellent performance in classifying the WP data. The algorithm is computationally simple and performs the classification in 2-5 seconds when implemented using Matlab. Due to this the classification program could be implemented on an operational radar and the data classification can be done as the data is generated. In other words, the programs can be adapted into real time operations of Indian MST radar or any other wind profilers. These programs are objective in the sense they do not require any modifications when migrated from one radar to another.

9.2 Future Scope

Main motive of the research work was to develop algorithms to implement the Wind Profiler signal processing in real time. It is established that all the three steps in the signal processing can be implemented in less than 14 seconds. Therefore the processing using this

algorithm is possible to be implemented in an automated process in real time. Hence the immediate future scope would be to implement the algorithms on the wind profiling radar in real time.

1) Integration of the pre-processing algorithm with MPCF algorithms. The Matlab code written to implement the algorithm could be optimized and translated to C programs. This would give further improvement in processing speed. The software programs could be implemented on a wind profiling radar / MST radar. This process requires interfacing the programs on the MST radar computer and matching the data exchange protocols and formats.

2) After processing the data, the sa+me needs to be subjected to classification using SFBC algorithm. This algorithm is capable of performing the operations and classifying them according to the target type. After the classification, the data could be systematically archived in appropriate format.

3) For modeling and classification, broad characteristics of various atmospheric phenomena are defined and their spectral signatures are developed. This can be further extended to develop more detailed characteristic features. This kind of detailed study would enable us to establish the relation between structures of atmospheric targets. This knowledge about the structure of atmospheric targets would lead to more accurate classification of localized atmospheric targets.

4) The processing algorithms could be implemented on atmospheric radars operating on similar principles; namely the Sodar and Cloud radar.

5) MPCF algorithm, can be further improved to have better performance in noisy conditions too. Similarly the SFBC algorithm can also be augmented with additional discriminatory conditions to improve the performance. The new techniques can be applied to transformed domain like wavelets.

6) The MPCF algorithm can further be extended to study the wind turbulence from the frequency spread of the Doppler components.

Thus this research has established a systematized base for atmospheric climate studies and prediction using radar meteorology.

Appendix-1

Data format of Indian MST Radar

New MST and LAWP Header variables (128 bytes)

```
short int    magicnumber; // 1 Operation mode of the system  new entry
short int    baudlength;        // 2 Baud length of transmission New entry
short int    nrgb;              // 3 No.of range bins
short int    nfft;              // 4 No.of FFT points
short int    ncoh;              // 5 No.of Coherent integrations
short int    nicoh;             // 6 No.of Incoherent integrations
short int    ipp;               // 7 Inter pulse period
short int    pwd;               // 8 Pulse width in micro seconds
short int    cflg;              // 9 Code flag
short int    nwin;              // 10 No.of observation windows
short int    w1start;           // 11 Window1 start
short int    w1len;             // 12 Window1 length
short int    w2start;           // 13 Window2 start
short int    w2len;             // 14 Window2 length
short int    year;              // 15 Year
short int    month;                   // 16  Month
short int    day;               // 17  Day
short int    hour;              // 18  Hour
short int    min;               // 19  Minute
short int    sec;               // 20  Seconds
short int    nbeams;                  // 21 No of beams in a beam scan cycle
short int    beam;              // 22 Beam position (current)
(new data –YXX.  Y – beam position 1-east, 2- west, 3 -North, 4 –South; XX – beam
angle)
short int    scancycle;         // 23 Number of the beam scan cycle in progress
short int    attn;              // 24 Receiver attn.level
short int    w3start;           // 25 3rd window of observation new entry
short int    w3len;             // 26 3rd window length  new entry
short int    simrange1;         // 27 Simulated signal range New Entry
short int    txpower;           // 28 TX power
short int    winfn;             // 29 Window fn. used for FFT
```

short int	noofpulses;	// 30 No of pulses in transmission new entry
short int	dtype;	// 31 Data type
short int	pulsedelay[9];	//32 Pulse delay from starting
short int	stc_win;	//41 STC window length
short int	pulsedelay10;	//42 Tenth pulse delay
short int	pulsedelay11;	//43 Eleventh pulse delay
short int	simrange2;	// 44 Simulated signal-2 range New Entry
short int	stc_win_start;	//45 STC window start
short int	noOfFreq;	// 46.No of frequencies used in tx in sequence ofIPP(for FDI)
float	txIFFreq[4];	// 50.IF values used in Transmission
short int	operationMode;	// Whether DBS/SDI etc.
short int	adptiveRefRange;	//51 Adaptive refernce range
short int	adaptiveRefLevel;	//52 % of the maximum
BYTE	commentCode;	//53 comments of 256 type can be stored
char	comment[13];	// User defined comments on the experiment

DATA Formats

Power Spectrum (Data type – Float)

Data header (128 bytes)
Range bin 1 : No. FFT Points
Range bin 2 : No. FFT Points
:
:
:
Last Range bin: No. of FFT points

No. FFT Points :

0	$+\delta f$	.....	$\pm f_{max/2}$	.....	$-\delta f$

Total volume of data in a frame =

(No. of FFT points * No of range bins * 4) bytes

Raw data - Ttime series (Data type – Integer)

Data header (128 bytes)
FFT Sample 1
:
:
:
:
FFT Sample N

FFT sample

I_1 Q_1	I_2Q_2	..	..	..	..	I_N Q_N

N - No. of FFT points

Ir & Qr is the data for the r^{th} range bin

Total volume of data in one frame =

(No. of range bin * No. of FFT points * 2) bytes

Complex power spectrum (Data type – Float)

Data header (128 bytes)
Range bin 1 complex FFT Points
Range bin 1 complex FFT Points
:
:
:
Range bin n complex FFT Points

Complex FFT points

I_1 Q_1	I_2Q_2	..	..	..	..	I_N Q_N

N - No. of FFT points

I_N & Q_N is the data for the N^{th} FFT point

Total volume of data in one frame =

(No. of range bin *No. of FFT points * 4 * 2) bytes

Moments (Data type – Float)

Data header (128 bytes)
Range bin 1 – SNR, Power, Doppler, Doppler width, Noise
Range bin 2 – SNR, Power, Doppler, Doppler width, Noise
:
:
:
Range bin n – SNR, Power, Doppler, Doppler width, Noise

Total volume of data in one frame = (No. of range bin * 5 * 4) bytes

UVW (Data type – Float)

Data Header (128 bytes)
Range bin 1 – U (Zonal), V (Meridonal), W (Vertical)
Range bin 2 – U (Zonal), V (Meridonal), W (Vertical)
:
:
:
Range bin n – U (Zonal), V (Meridonal), W (Vertical)

Total volume of data in one frame = (No. of range bin * 3 * 4) bytes.

Appendix-2

Procedure for reading the MST Radar Data File and Plotting in 2D Format

1. Read the header.
2. Assign values from the header to the following parameters. Ignore all other parameters.
    a. No. of range bins (NRB)
    b. No. of FFT points (NFFT)
    c. No. of coherent integrations (NCOH)
    d. No. of incoherent integrations (NICOH)
    e. Inter Pulse Period (IPP)
    f. Pulse width of transmission (PWD)
    g. Code Flag (CFLG) (1 for Coded Transmission; 0 for Uncoded)
    h. Observation Window Start (W1Start)
    i. Observation Window Length (W1Len)
    j. Year
    k. Month
    l. Day
    m. Hour
    n. Minute
    o. Second
    p. No. of beams (NBEAMS)
    q. Beam direction (BEAM)
    r. Data Type (DTYPE) (1 for Raw Data; 2 for Power Spectrum; 3 for Moments; 4 Power Spectrum + Moments; 5. UVW; 6; Complex Spectrum)

3. Compute no. of data points = NRB × NFFT .
4. Compute Range resolution (meter) =
    a. (if CFLAG = 0) 150 × PWD
    b. (if CFLAG = 1) 150
5. Read the float type data points into a matrix - one row for each range bin.
6. Organize each range bin data by “FFTshift”.
7. Make a copy of this matrix. Use this copy for further modifications required for plotting. Do not alter the original data. Keep it for signal processing later.
8. Now find the maximum value in each range bin and divide all the data points of that range bin with its maximum value. Now all the data points will be in the range 0-1.
9. Now add a constant to each point of a range bin which is= (range bin no.-1) so that it is zero for the first range bin and (NRB-1) for the last range bin.
10. Now plot this data.
11. Now to set the values on the range and Doppler shift axes:
    a. Lowest range in meter = W1Start × 150
    b. Now to get a particular range add (rangebin no. × range resolution to the value in 11a.
    c. Compute maximum unambiguous Doppler shift as ±1/(2×NCOH × IPP).
    d. Positive Doppler shift denotes target approaching. Negative target receding.
    e. Divide twice the value in 11c. by NFFT to get Doppler resolution.

f. Assign the Doppler shift values from left to right.
g. Identify the zero Doppler shift point in each range bin.
h. Replace the zero Doppler shift point with an average of the points on positive and negative side.

12. Write the ASCII data in the format required for the Plotting program and then plot.
13. If End Of File reached - exit; else Repeat procedure for next frame of data.

Appendix-3

Table: 1 Operating parameters of various Radars at NARL, India (location: 13.4^0N, 79. .17^0E) used in this thesis

Parameter	**(a) MST Radar**	**(b) LAWP (8X8)**	**(c) LAWP (16X16)**
Transmission Frequency	53 MHz	1280 MHz	1280 MHz
Peak power	2.5 MW	0.3 KW	1.2 KW
Operation mode	DBS, 6 Beams, N10, E10, S10, W10, Z_x, Z_y.	DBS, 3 Beams, Zenith, and 14.2^0 down at NE, SW.	DBS, 3 Beams. (11^0, 15^0), (101^0, 15^0), (0^0, 0^0).
Baud Rate	1 µs.	1 µs.	1 µs.
Coherent Integration	64 (Time domain averaging)	32 (Time domain averaging)	32 (Time domain averaging)
FFT points	512	512	512
Doppler Resolution	0.0305 Hz	1.22 Hz	1.22 Hz
Sampling Start (after Tx)	24 µs	5 µs	5 µs
No. of range bins	150	35	30
Starting range	3.6 Km	0.75 Km	0.75 Km
Range Resolution	150 m	150 m	150 m
Maximum radial velocity	±22.11 ms^{-1}	±30 ms^{-1}	±30 ms^{-1}
Radial velocity resolution	0.08636 ms^{-1}	0.1464 ms^{-1}	0.1464 ms^{-1}

Appendix-4
Data sets used for testing the Algorithms
(Description of the data files and the data formats)

1. Classified as wind echoes with RFI

	File name:12JA2015.d21	File name:15Ju2015.d7	File name:01no2007.d7
Specifications	**Data type: RFI present only**	**Data type: RFI with echo**	**Data type: Normal echo**
Baud length(in μs)	1	1	1
No. of RBs	150	150	150
No. of FFT points	512	512	512
No. of ncoh	64	64	64
No. of Incoh	1	1	1
Inter pulse period(in μs)	1000	1000	1000
Pulse width(in μs)	16	16	16
Code flag	Coded	coded	Coded
No. of beams	6	8	6
Scan cycle	1,2,3,4,5,6	1,2,3,4,5,6,7,8	1,2,3,4,5,6
Rx. attenuation	0 dB	0 dB	0 dB
Data type	Spectrum	spectrum	Spectrum
No. of observation window	1	1	1
Window start	24	24	24
Window length	150	150	150
Data file name	12JA2015.d21	15JU2015.d7	01NO2007.d7
File size	3.6MB	9.6MB	3.6MB

2.

	File name:26se2007.d76	**File name:01AP2009.d6**	**File name:01de2009.d2**
Specifications	**Data type: Wind echo**	**Data type: Wind echo**	**Data type: Wind echo**
Baud length(in μs)	1	1	1
No. of RBs	150	150	150
No. of FFT points	512	512	512
No. of ncoh	64	64	64
No. of Incoh	1	1	1
Inter pulse period(in μs)	1000	1000	1000
Pulse width(in μs)	16	16	16
Code flag	Coded	coded	Coded
No. of beams	6	8	6
Scan cycle	1,2,3,4,5,6	1,2,3,4,5,6,7,8	1,2,3,4,5,6
Rx. attenuation	0 dB	0 dB	0 dB
Data type	Spectrum	spectrum	Spectrum
No. of observation window	1	1	1
Window start	24	24	24
Window length	150	150	150
Data file name	26se2007.d76	01AP2009.d6	01DE2009.d2
File size	3.6MB	9.6MB	3.6MB

3.

	File name:28MY2009.d1	**File name:08FE2006.d1**	**File name:01de2007.d1**
Specifications	**Data type: Wind echo**	**Data type: RFI +Normal echo**	**Data type: Normal echo + clutter**
Baud length(in µs)	1	1	1
No. of RBs	100	150	150
No. of FFT points	512	512	512
No. of ncoh	64	64	64
No. of Incoh	1	1	1
Inter pulse period(in µs)	1000	1000	1000
Pulse width(in µs)	16	16	16
Code flag	Coded	coded	Coded
No. of beams	5	8	6
Scan cycle	1,2,3,4,5	1,2,3,4,5,6,7,8	1,2,3,4,5,6
Rx. attenuation	0 dB	0 dB	0 dB
Data type	Spectrum	spectrum	Spectrum
No. of observation window	1	1	1
Window start	24	24	24
Window length	100	150	150
Data file name	28MY2009.d1	08FE2006.d1	01DE2007.d1
File size	1 MB	7.2MB	7.2MB

4.

	File name:24JL2013.d4	**File name:05JL2013.d6**	**File name: 11JL2013.d1**
Specifications	**Data type: CAT echo**	**Data type: Ionospheric echo**	**Data type: Precipitation**
Baud length(in μs)	1	16	2
No. of RBs	100	270	80
No. of FFT points	512	256	512
No. of ncoh	64	1	128
No. of Incoh	1	8	1
Inter pulse period(in μs)	1000	5000	250
Pulse width(in μs)	16	16	2
Code flag	Coded	coded	Coded
No. of beams	6	4	4
Scan cycle	1,2,3,4,5,6	1,2,3,4	1,2,3,4
Rx. attenuation	0 dB	0 dB	0 dB
Data type	Spectrum	spectrum	Spectrum
No. of observation window	1	1	1
Window start	24	560	10
Window length	100	4320	160
Data file name	28MY2009.d1	05JL2013.d6	11JL2013.d1
File size	100 MB	2.1MB	100 MB

5.

	File name:11DE2011.r1	**File name:12DE2011.r1**	**File name: 13DE2011.r1**
Specifications	**Data type: Meteoric echo**	**Data type: Meteoric echo**	**Data type: Meteoric echo**
Baud length(in μs)	8	8	8
No. of RBs	34	34	34
No. of FFT points	1024	1024	1024
No. of ncoh	4	4	4
No. of Incoh	1	1	1
Inter pulse period (in μs)	1000	1000	1000
Pulse width(in μs)	8	8	8
Code flag	Uncoded	Uncoded	Uncoded
No. of beams	4	4	4
Scan cycle	1,2,3,4	1,2,3,4	1,2,3,4
Rx. attenuation	0 dB	0 dB	0 dB
Data type	raw	raw	raw
No. of observation window	1	1	1
Window start	533	533	533
Window length	272	272	272
Data file name	11de2011.r1	11de2011.r1	11de2011.r1
File size	1088 MB	1088 MB	1088 MB

References

[1] D. Atlas, "Advances in radar meteorology," *Advances in Geophysics*, vol. 10**,** pp. 318-478, 1964.

[2] R. F. Woodman, and A. Guillen, "Radar observations of winds and turbulence in the stratosphere and mesosphere," *Journal of Atmospheric Science*, vol. 31, pp. 493-505, 1974.

[3] Dusan S. Zrnic, "Simulation of Weather like Doppler Spectra and Signals," *Journal of Applied Meteorology*, vol.14, pp. 619-620, 1975.

[4] J. Röttger, J. Klostermeyer, P. Czechowsky, R. Ruster, G. Schmidt, "Remote sensing of the atmosphere by VHF radar experiments," *Naturwissenschaften*, vol. 65, pp. 285–296, 1978.

[5] D.S. Zrnic', "Estimation of spectral moments for weather echoes," *IEEE Transactions on Geoscience Electronics*, vol. GE-17, no. 4, pp. 113-128, 1979.

[6] Toru Sato and R.F.Woodman, "Spectral parameter estimation of CAT radar echoes in the presence of fading clutter," *Radio Science*, vol. 17, pp. 817-826, 1982.

[7] R.G. Strauch., D.A. Merritt, K.P. Moran, K.B. Earnshaw and D Van de Kamp, "The Colorado wind profiling network," *Journal of Atmospheric and Oceanic Technology*, vol. 1, pp. 37-49, 1984.

[8] R. J. Doviak and D. S. Zrnic', "Echoes from the precipitation- free turbulent troposphere," *Doppler Radar and Weather Observations, 2nd ed.*, Orlando, FL: Academic, 1984, Ch. 11, Sec. 6, pp. 406-410.

[9] R. F.Woodman, "Spectral Moment Estimation in MST Radars," *Radio Science*, vol. 20, no. 6, pp. 1185-1195, 1985.

[10] W.L. Ecklund, D. A. Carter and B.B. Balsley, "A UHF wind profiler for the boundary layer: Brief description and initial results," *Journal of Atmospheric and Oceanic Technology*, vol.5, pp. 432-441, 1988.

[11] S. F.Clifford, J.C. Kaimal, R.J. Lataitis, and R.G. Strauch, "Ground-Based Remote Profiling in Atmospheric Studies: An Overview," *Proceedings of the IEEE*, vol. 82, pp. 313-355, 1994.

[12] E. Boyer, P. Larzabal, C. Adnet and M. Petitdidier, "Parametric spectral moment estimation for wind profiling radar," *IEEE Transactions on Geosciences and Remote Sensing*, vol. 41, no. 8, pp. 1859-1868, 2003.

[13] R. Dombrowsky, "*Complementary Use of Modern Doppler Radars and Profilers in the Upper Air Network, Operational Use of Wind Profiler Data in United States Weather Forecasting*," CIM O/OPAG-UPPER-AIR-/ET-RSUAT&T-1 Doc.4.1.(1), World Meteorological Organization (WMO), Geneva, Switzerland, 2005.

[14] S. Fukao, T. Sato, T. Tsuda, S. Kato, K. Wakasugi and T. Makihira, "The MU radar with an active phased array system 1: Antenna and power amplifiers," *Radio Science*, vol. 20, no. 6, pp. 1155-1168. 1985. (On line on 7th Dec 2012, doi 10.1029/RS020i006p01155).

[15] S. Fukao, T. Tsuda, T. Sato, S. Kato, and T. Makihira, "The MU radar with an active phased array system 2: In-house equipment," *Radio Science*, vol. 20, no. 6, pp. 1169-1176. 1985. (On line on 7th Dec 2012, doi 10.1029/RS020i006p01169).

[16] P. B. Rao, A. R. Jain, P. Kishore, P. Balamuralidhar, S. H. Damle, and G. Viswanathan, "Indian MST radar 1. System description and sample vector wind measurements in ST mode," *Radio Science*, vol: 30, no.4, pp. 1125-1138, 1995.

[17] E. E. Gossard, "The fine structure of elevated refractive layers: implications for over-the-horizon propagation and radar sounding systems," *Radio Science*, vol. 19, pp. 1523-1533, 1984.

[18] B.R. Bean, J. D. Horn, A. M. Ozanich, "Climatic Charts And Data Of The Radio Refractive Index For The United States And The World," *National Bureau of Standards Monograph 22*, US Govt. Printing Office, Washington, pp. 178.

[19] V.A. Tatarski, *"Wave Propagation in Turbulent Medium,"* New York, Mc Graw Hill, 1961.

[20] P.B. Chilson, A. Muschinski and G. Schmidt, "First observations of Kevin-Helmholtz Billows in an upper level jet using VHF frequency domain interferometry*," Radio Science*, vol. 32, pp. 1149-1160, 1997.

[21] Vaisala Inc, "*Wind Profiling, History, Principles and Applications*," Technical Note, 2003.

[22] P. Srinivasulu, P. Yasodha, P. Kamaraj, T. N. Rao, A. Jayaraman, S. N. Reddy and S. Satyanarayana, "1280-MHz Active Array Radar Wind Profiler for Lower Atmosphere: System Description and Data Validation," *Journal of Atmospheric and Oceanic Technology*, vol. 29, no. 10, pp. 1455-1470, 2012.

[23] C. M. Hall, J. Röttger, K. Kuyeng, F. Sigernes, S. Claes and J. L. Chau. "Tropopause altitude detection at 78°N, 16°E, 2008: First results of the refurbished SOUSY radar," *Radio Science*, vol. 44, no. 5, doi:, 2009. (doi: 10.1029/2009RS004144)

[24] P. H. Hilderbrand, and R.S. Sekhon, "Objective Determination of Noise Level in Doppler Spectra," *Journal of Applied Meteorology*, vol.13, pp. 808-811, 1974.

[25] Monique Petitdidier, Amadou Sy, Axel Garrouste and Jean Delcourt, "Statistical characteristics of the noise power spectral density in UHF and VHF wind profilers", *Radio Science*, vol. 32, no.3, pp. 1229-1247, 1997.

[26] Igor R.Ivic and Sebastián M. Torres1, "Online Determination of Noise Level in Weather Radars," *The Sixth International Conference on Radar Meteorology and Hydrology*, vol. ERAD-2010 (S2) http://www.erad2010.org/ Sibiu.htm; ext. abstr.

[27] Igor R. Ivić, Christopher Curtis, Sebastián M. Torres, "Radial-Based Noise Power Estimation for Weather Radars," *Journal of Atmospheric and Oceanic Technology*, vol. 30, no. 12, pp. 2737-2753, 2013.

[28] J.R. Jordan, R. J. Lataitis and. D. A. Carter , "Removing ground and intermittent clutter contamination from wind profiler signal using wavelet transform*," Journal of Atmospheric and Oceanic Technology*, vol. 14, pp. 1280 –1297, 1997.

[29] Anthony C. Riddle, Leslie M. Hartten, David A. Carter, Paul E. Johnston, and Christopher R. Williams, "A Minimum Threshold for Wind Profiler Signal-to-Noise Ratios," *Journal of Atmospheric and Oceanic Technology*, vol. 29, pp. 889-895, 2012.

[30] Volker Lehmann "Improved intermittent Clutter Filtering for Wind Profiler Radar." DR.RER.NAT. Dissertation, University of Bayreuth, 2009.

[31] Volker Lehmann, “Optimal Gabor-Frame-Expansion-Based Intermittent-Clutter-Filtering Method for Radar Wind Profiler,” *Journal of Atmospheric and Oceanic Technology*, vol. 29, no. 2, pp. 141-158, 2012.
[32] Volker Lehmann, G. Teschke, “Wavelet based methods for improved wind profiler signal processing,” *Annales Geophysicae* , vol. 19, pp. 825-836, 2001.
[33] Shaik Allabakash, P Yasodha, S V Reddy, P Srinivasulu, “Wavelet transform-based methods for removal of ground clutter and denoising the radar wind profiler data,” *IET Signal Processing*, vol. 9, no. 5, pp. 440–448, 2015.
[34] V. K. Anandan, D.B.V. Jagannatham, “An Autonomous Interference Detection and Filtering Approach Applied to Wind Profilers,” *IEEE Transactions on Geoscience and Remote sensing*, vol. 51,no. 1, pp. 520-526, 2013.
[35] Tian-You Yu, Xiao Xiao and Yadong Wang, “Statistical Quality of Spectral Polarimetric Variables for Weather Radar,” *Journal of Atmospheric and Oceanic Technology*, vol. 29, no. 9, pp. 1221-1235, 2012.
[36] K. D. Le, R. D. Palmer, B. L. Cheong, T.-Y. Yu, G. Zhang and S. M. Torres. “Reducing the effects of noise on atmospheric imaging radars using multilag correlation," *Radio Science*, vol. 45, no. 1, RS1008, 2010. (doi: 10.1029/2008RS003989)
[37] Isom Bradley, Robert Palmer, Redmond Kelley, John Meier, David Bodine, Mark Yeary, Boon-Leng Cheong, Yan Zhang, Tian-You Yu and Michael I. Biggerstaff, “The Atmospheric Imaging Radar: Simultaneous Volumetric Observations Using a Phased Array Weather Radar,” *Journal of Atmospheric and Oceanic Technology*, vol. 30,no. 4,pp: 655-675, 2013.
[38] Tridon Frdériéc, Alessandro Battaglia, PavlosKollias, Edward Luke, Christopher R. Williams, “Signal Postprocessing and Reflectivity Calibration of the Atmospheric Radiation Measurement Program 915-MHz Wind Profilers,”. *Journal of Atmospheric and Oceanic Technology*, vol. 30, no. 6, pp. 1038-1054, 2013.
[39] *Vaisala Inc, Using Wind Profiler Data for Air Quality Applications*, Application Note, 2010.
[40] K. R. Tuckley, “Feature Extraction Techniques for the Echoes From Distributed Radar Targets.” PhD Thesis, Indian Institute of Technology, Bombay, India, 2009.
[41] V. K. Anandan, P. Balmuralidhar, P.B. Rao, A.R. Jain, and C. J. Pan, “Adaptive Moments Estimation Techniques Applied to MST Radar Echoes,” *Journal of Atmospheric and Oceanic Technology,* vol. 22, pp. 396-408, 2005.
[42] E.E. Clothiaux, R.S. Penc, D. W. Thomson , T. P. Ackerman, and S. R. Williams, “A First-Guess Feature-Based Algorithm for Estimating Wind Speed in Clear-Air Doppler Radar Spectra,” *Journal of Atmospheric and Oceanic Technology*, vol. 11, pp. 888-907, 1994.
[43] C. S. Morse, R. K. Goodrich and L. B. Cornman, “The NIMA Method for Improved Moment Estimation from Doppler Spectra,” *Journal of Atmospheric and Oceanic Technology*, vol. 19: pp.274-295, 2002.
[44] L. B. Cornman, Robert, K. Goodrich, Corinne S, Morse, and Warner L. Ecklund, “A Fuzzy Logic Method for Improved Moment Estimation from Doppler Spectra,” *Journal of Atmospheric and Oceanic Technology*, vol- 15, pp. 1287-1305, 1998.
[45] Laura Bianco, and J. M.Wilczak, “Convective boundary layer Depth: Improved Measurement by Doppler Radar wind Profiler Using Fuzzy Logic Methods,” *Journal of Atmospheric and Oceanic Technology,* vol. 19, pp.1745-1758, 2002.

[46] C. Gaffard, L Bianco, V. Klaus, and M. Matabuena, “Evaluation of moments calculated from wind profiler spectra: A comparison between five different processing techniques”, *Meteorologicle Zeitschrift*, vol. 15, no.1, pp. 73-85, 2006.
[47] S. Allabakash, P. Yashoda, L. Bianco, S. Venkatrammana Reddy, and P.Srinivasulu, “Improved Moment Estimation for VHF Activephased array Radar Using Fuzzy Logic Method,” *Journal of Atmosphric and Oceanic Technology*, vol 32, pp 1004-1014, 2015.
[48] L.J. Battan, *Radar Observation of the Atmosphere*, The University of Chicago Press, Chicago, 1973.
[49] Paul B Silverstein., O. Scott Sands and Fred D. Garber,: Radar Target Classification and Interpretation by Means of Structural Descriptions of Backscatter Signals, *IEEE AES Systems Magazine*, pp. 3-7, 1991.
[50] M. Vespe., C.J. Baker and H.D. Griffiths, “Radar target classification using multiple Perspectives”, *IET Radar Sonar & Navigation*, vol. 1, no. 4, pp. 300-307, 2007.
[51] Allistair Moses, Matthew J. Rutherford and Kimon P. Valavanis, “Radar-Based Detection and Identification for Miniature Air Vehicles,” *IEEE International Conference on Control Applications (CCA),* pp. 933-940, 2011
[52] Milenko S. Andrić, Zeljko Durovic and Bojan Zrnić, “Ground Surveillance Radar Target Classification based on Fuzzy Logic Approach,” *EUROCON 2005*, pp. 22-24, 2005
[53] Milenko S. Andrić, Boban P. Bondžulić, and Bojan M. Zrnić, “The Database of Radar Echoes from Various Targets with Spectral Analysis,” *10th Symposium on Neural Network Applications in Electrical Engineering*, pp. 187-190, 2010.
[54] Milenko Andrić, Boban Bondžulić, Bojan Zrnić, Aleksandra Kari, and Goran Dikić, “Acoustic Experimental Data Analysis of Moving Targets Echoes Observed by Doppler Radars,” *Journal of Mechanical Engineering*,” vol. 58, no. 6, pp. 386-393, 2012.
[55] Hui-Lin Zhou, Mao Tian and Xiao-Li Chen, “Time-Frequency Representations for Classification of Ground Penetrating Radar Echo Signal,” *Proceedings of International Symposium on Intelligent Signal Processing and Communication Systems*, pp. 597-600, 2005.
[56] V. Chandrasekar, Keränen, S. Lim, and D. Moisseev, “Recent advances in classification of observations from dual polarization weather radars,” *Atmospheric Research*, vol. 119, pp. 97–111, doi:10.1016/j.atmosres.2011.08.014, 2013
[57] Edward P. Luke and Pavlos Kollias, “Separating Cloud and Drizzle Radar Moments during Precipitation Onset Using Doppler Spectra”, *Journal of Atmospheric and Oceanic Technology*, vol: 30, no. 8, pp. 1656-1671, 2013.
[58] Paul R. Harasti, “An Expanded VVP Technique to Resolve Primary and Environmental Circulations in Hurricanes,” *Journal of Atmospheric and Oceanic Technology*, vol. 31, no. 2, pp. 249-271, 2014.
[59] Y.P. Ostrovsky and F.J. Yanovsky, “Use of Neural Network for Turbulence and Precipitation Classification Procedure,” *11 Int. Conf. on Mathematical Methods in Electromagnetic Theory Ukrain*, pp. 161-163, 2006.
[60] M. Straka, D. S. Zrnić, and A. V. Ryzhkov, “Bulk hydrometeor classification and quantification using polarimetric radar data: synthesis of relations,” *J. Appl. Meteor.*, vol. 39, pp.1341-1372, 2000.
[61] A. Pellinen-Wannberg, “The EISCAT meteor-head method– a review and recent observations,” *Atmospheric Chemistry. Physics*, vol.4, pp. 649–655, 2004.

[62] Krishna B., Muralia, S. Varadarajan and V. Rajanikanth, “Meteor Detection during 2011-Leonid Meteor Shower using Indian MST Radar,” *International Journal of innovative in Engineering and Technology*, vol. 3, pp. 115-120, 2013.

[63] Merrill l Skolnik, “An Introduction to Radar”, *Introduction to Radar Systems, 3rd ed.*, Tata McGraw Hill Education Private Limited, Ch. 1, Sec. 1.2, pp. 3-7, 2010.

[64] P. K. James, “A review of radar observations of the troposphere in clear air conditions,” *Radio Science*, vol. 15, pp. 151-175, 1980.

[65] H. Sauvageot and G. Despaux, “The clear-air coastal vespertine radar bands,” *Bulletin of the American Meteorological Society*, vol.77, pp. 673-681, 1995.

[66] K.S. Gage and B. B. Balsley, “Recent advances in Doppler radar probing of the clear atmosphere,” *Atmospheric Technology*, vol.13, pp. 3-18, 1981.

[67] M. Shinriki, H. Takase, R. Sato, H. Susaki, “Multi-range-resolution radar using sideband spectrum energy,” *IEEE Proceedings on Radar, Sonar and Navigation*, vol. 153, no. 5, pp. 396-402, 2006.

[68] J.W. Wilson, T. M. Weckwerth, J. Vivekanandan, R. M. Wakimoto and R. W. Russell, “Boundary layer clear-air radar echoes: origin of echoes and accuracy of derived winds, *“Journal of Atmospheric and Oceanic Technology*, vol. 11, pp. 1184-1206, 1994.

[69] G.L. Achtemeier, “The use of insects as tracers for "clear-air" boundary-layer studies by Doppler radar,” *Journal of Atmospheric and Oceanic Technology*, vol. 8, pp.746-765, 1991.

[70] A. Muschinski, “Local and global statistics of clear air Doppler radar signals,” *Radio Science,* vol. 39, RS 1008, 2004 [Doi:10.1029/2003RS002908].

[71] R.F. Woodman, and Y.H. Chu, “Aspect sensitivity measurements of VHF backscatter made with the Chung-Li radar: Plausible Mechanisms,” *Radio Science,* vol. 24, pp. 113-125, 1989.

[72] R.M. Worthington R.D. Palmer, and S. Fukao, “An investigation of tilted aspect sensitive scatterers in the lower atmosphere using the MU and Aberystwyth VHF radars,” *Radio Science*, vol. 34, pp. 413-426, 1999.

[73] R.M. Worthington, A. Muschinski and B.B. Balsley, “Bias in mean vertical wind measured by VHF radars: Significance of radar location relative to mountains,” *J. Atmospheric Sciences,* vol. 58, pp. 707-723, 2001.

[74] Reddy, G.H, Y. Venkatarami Reddy, and S.N. Reddy, “The Effect of ß in Kaiser Window on the SNR of MST Radar Signals,” *Asian Journal of Scientific Research*, vol. 1, pp. 203-212, 2008.

[75] Gan,T., M.K.Yamamoto, H.Hashiguchi, H. Okamoto, and M.Yamamoto, “Error estimation of spectral parameters for high-resolution wind and turbulence measurements by wind profiler radars,” *Radio Science,* vol. 49, pp. 1214-1231, 2014.

[76] Wen-Chau Lee, Xiaowen Tang and Ben J.-D. Jou, “Distance Velocity–Azimuth Display (DVAD)—New Interpretation and Analysis of Doppler Velocity,” *Monthly Weather Review*, vol. 142, no. 2, pp.:573-589, 2014.

[77] P. Srinivasulu, P. Yashoda, P. Kamaraj, T. N. Rao , and A. Jayaraman, “1280-MHz Active Array Radar Wind Profiler for Lower Atmosphere: system Description and Data Validation ,” *Journal of Atmospheric and Oceanic Technology*, vol. 29, pp. 1445-1470, 2012.

[78] P. Srinivasulu, P. Yashoda, and A. Jayaraman, "Simplified Active Array L-Band Radar for Atmospheric Wind Profiling: Initial Results," *Journal of Atmospheric and Oceanic Technology*, vol. 28, pp. 1436-1447, 2010.
[79] A. Adachi, T. Kobayashi, K. S. Gage, D. A. Carter, L. M. Hartten, W. L. Clark, and M. Fukuda, "Evaluation of three-beam and four-beam profiler wind measurement techniques using a five-beam wind profiler and collocated meteorological tower," *J Atmos. Ocean Tech.*, vol. 22, pp. 1167-1180, 2005.
[80] R. Schafer, S. K. Avery, K. S. Gage, P. E. Johnston, and D. A. Carter, "Improving Wind Profiler–Measured Winds Using Coplanar Spectral Averaging," *J Atmos. Ocean Tech*, vol. 21, pp. 1671-1678, 2004.
[81] Pedram Ghamisi, Roberto Souza, Jon Atli Benediktsson, Xiao Xiang Zhu, Letícia Rittner and Roberto A. Lotufo, "Extinction Profiles for the Classification of Remote Sensing Data," *IEEE Transactions on Geoscience and Remote Sensing*, vol. 54, no. 10, pp. 5631-5645, 2016
[82] Carmine Clement, Antonio De Maio, and John Sorghan, "A Novel Algorithm for Radar Classification Based on Doppler Characteristics Exploiting Orthogonal Pseudo-Zernike Polynomials," *IEEE Transactions on Aerospace and Electronic Systems*, vol. 51, no. 1, pp. 417-430, 2015
[83] Dale E Nelson., "High Range Resolution Radar Target Classification: A Rough Set Approach*,"* Degree Doctor of Philosophy, The Ohio University, 2001.
[84] G.B. Foote, P.S. Toit, "Terminal Velocity of Raindrops Aloft", *Journal of applied Meteorology*, vol. 8, pp. 249-253, 1969.
[85] David Woodbridge, "Ionospheric Winds", Journal of Geophysical Research, vol. 67, no.11, pp. 4221-4231, 1962.
[86] Meng-Yuan Chen and Yen -Hsyang Chu, "Beam broadening effect on Doppler spectral width of wind profiler," *Radio Science*, vol. 46, RS5013, 2011. (doi:10.1029/2011RS004704, 2011).
[87] J. Smagorinsky, "Global Atmosphere Modeling and Numerical Simulation of Climate" in W. N. Mess(ed.), Weather and Climate Modifications, John Wiley and Sons, New York, pp. 633-686, 1974
[88] Swati Sinha, T.V. Chandrasekhar Sarma, Mary Lourde, R, "Estimation of Doppler profile using Multi-parameter Cost Function method ," IEEE transactions on geoscience and remote sensing, vol. 55, no. 2, pp. 932-942, 2017.

List of Publications from this Research

Journal Publications

1. Swati Sinha, T.V. Chandrasekhar Sarma, Mary Lourde, R, "Estimation of Doppler profile using Multi-parameter Cost Function method ", *IEEE transactions on geoscience and remote sensing*, vol. 55, no. 2, pp. 932-942, 2017**.**
2. Swati Sinha, T.V. Chandrasekhar Sarma, Mary Lourde R., "Removal of RFI and Clutter in Atmospheric Radar Spectra", *International Journal of Applied Engineering Resear*ch, vol. 11, no. 24, pp. 11864-11870, 2016.

.

1. **Swati Sinha**, T.V. Chandrasekhar Sarma, Mary Lourde R., "Doppler Feature based classification of wind profiler data", ***Journal of Physics: Conference Series,*** vol. 787, pp.20-28, 2017.

All are Scopus Indexed Journals.

- ***Conferences Publications***

1. Swati Sinha, T. V. Chandrasekhar Sarma, Mary Lourde. R, "Doppler profile Estimation of MST radar data using Multi-parameter Cost Function method", *IEEE International Conference on Radar, Antenna, Microwave, Electronics and Telecommunications*, Indonesia, pp. 50-54. 2015.
2. Swati Sinha, T. V. Chandrasekhar Sarma, Mary Lourde. R, "Simulation of Clutter &RFI in Wind Profiler Power Spectra*", (Extended Abstract) 2nd Union Radio-Scientifique Internationale (URSI) Regional conference on Radio Science, Delhi, pp.52*. 2015.
3. Swati Sinha, T.V. Chandrasekhar Sarma, Mary Lourde. R, "An Efficient Method of RFI and Clutter Removal in Wind Profiler Spectra", presented at *2016 IEEE 59th International Midwest Symposium on circuits and Systems, Abu Dhabi, pp.241-244*
4. Swati Sinha, T.V. Chandrasekhar Sarma, Mary Lourde. R, "Doppler Feature based Classification of wind profiler data", presented at *2016 International Conference on communication, Image and Signal Processing, Dubai.*
5. Swati Sinha, T. V. Chandrasekhar Sarma, Mary Lourde. R, "*Classification of Wind Profiler Power Spectra by Signature Matching using Wavelet Transform*", presented at *3rd Union Radio-Scientifique Internationale (URSI) Regional conference on Radio Science, Gadanki, Tirupati*. March 2017.
6. Swati Sinha, T. V. Chandrasekhar Sarma, Mary Lourde. R, "*Doppler Profile Estimation Using Gaussian Wavelets*", presented at *3rd Union Radio-Scientifique Internationale (URSI) Regional conference on Radio Science, Gadanki, Tirupat*i. March 2017.

Brief Biography of the Candidate:

Swati Sinha has obtained B. Tech degree in Engineering (ECE) from NEHU, India (1995) Masters (ECE) from Mumbai University, (2005). She has worked in industry on embedded system development. She has also been a faculty of Electronics and Telecommunication Engineering in Mumbai University for 12 years. Her current area of research is Signal processing techniques. Currently associated as a research scholar in BITS Pilani Dubai Campus.

Brief Biography of the Supervisor:

Mary Lourde. R has obtained B.Tech in Electrical Engineering from Kerela University, India in 1983 and M. Tech in Electronics from Cochin University of Science & Technology, India in 1987. She is awarded the Ph.D. Degree in Electrical Engineering from Indian Institute of Science, Bangalore, India for the thesis "Design and Analysis of Digital Controllers for high performance Sensorless PMSM Servo drives" in 1998. She worked as a faculty at CUSAT since 1990. Presently with Birla Institute of Technology & Science Dubai Campus, BPDC working as Associate Professor in EEE. Her current area of research includes Signal Processing and its applications, VLSI Desgin and Power Electronics & Drives. She is a MIEEE, LMIETE, LMISTE.

Brief Biography of the Co-Supervisor:

T. V. Chandrasekhar Sarma has obtained B.Tech. (ECE), M.Tech. (Commn. Engg.) and Ph.D.(Design and development of radio acoustic sounding system) respectively from Sri Venkateswara University College of Engineering, Tirupati, IIT Bombay, Mumbai and Kyoto University, Kyoto, Japan. He worked as a Scientific Officer at Society for Applied Microwave Electronics Engineering and Research (SAMEER), IIT Bombay Campus, Mumbai on the design, development, qualification and installation of MST Radar subsystems. He joined National Atmospheric Research Laboratory, Dept. of Space, Govt. of India, Gadanki, AP in the year 1994. His current research interests are development of atmospheric sensing techniques and flight instrumentation.
Dr. Sarma is a fellow of IETE, senior member of IEEE and member of Optical Society of America, American Geophysical Union and Acoustical Society of India.